

# Radiant Heating and Cooling System for Achieving Net Zero Carbon Building

ゼロ・カーボンビル実現を目指した放射冷暖房システムに関する研究

February, 2024

Kan SHINDO  
新藤 幹

# Radiant Heating and Cooling System for Achieving Net Zero Carbon Building

ゼロ・カーボンビル実現を目指した放射冷暖房システムに関する研究

February, 2024

Waseda University Graduate School of Creative Science and Engineering

Department of Architecture, Research on Architectural Environment

Kan SHINDO

新藤 幹

## **Table of Contents**

## **Terminology**

# Radiant Heating and Cooling System for Achieving Net Zero Carbon Building

ゼロ・カーボンビル実現を目指した放射冷暖房システムに関する研究

## 1. Introduction

1.1	Background and Objective	2
1.2	Building Decarbonization and Zero Carbon Building	4
1.3	Outline of This Study	14
	References	15

## 2. Design and control of radiant heating and cooling systems in Japan: Results from expert interviews

2.1	Introduction	20
2.2	Methods	22
2.3	Results from the installation survey of radiant systems in Japan	23
2.4	Results from expert interviews	25
2.5	Discussion	31
2.6	Conclusions	32
	References	33

## 3. Application of a slit ceiling on thermally activated building system in a daylight-harvesting office space

3.1	Introduction	38
3.2	Literature review of radiant cooling capacity enhancement under direct solar radiation	38
3.3	Methods	41
3.4	Results	48
3.5	Discussion and conclusions	57
	References	58

## 4. Resilient cooling comparison of an all-air system and a radiant system

4.1	Introduction	62
4.2	Methods	63
4.3	Results and Discussion	67
4.4	Conclusions	70
	References	71

**5. A comparative study of the whole life carbon of an all-air system and a radiant system in Denmark**

5.1	Introduction	74
5.2	Methods	74
5.3	Results	83
5.4	Discussion	90
5.5	Conclusions	93
	References	94

**6. A full-scale study of the upfront and operational carbon of an all-air system and a radiant system in Japan**

6.1	Introduction	98
6.2	Methods	102
6.3	Results and Discussions	111
6.4	Conclusions	114
	References	114

**7. Conclusions** 118

## Terminology

**Building decarbonization:** The process of removing and reducing greenhouse gases.

**Carbon emission factor (carbon intensity):** carbon emissions per unit of production and consumption in various business activities. In the case of electricity, the amount of carbon dioxide emitted to produce 1 kWh of electricity at an electric power plant.

**Dedicated outdoor air system (DOAS):** The heating, ventilation, and air-conditioning system that uses separate equipment to condition all the outdoor air brought into a building for ventilation and delivers it to each zone, either directly or in conjunction with local HVAC equipment serving those same zones.

**Direct solar load (DSL):** The proportion of the solar heat gain that is removed by a radiant system before it can contribute to the thermal absorption processes that are due to the room and furniture thermal mass.

**Dynamic simulation:** The annual calculation based on heat balance simulation.

**Embodied carbon:** The total greenhouse gas emissions arising from the manufacturing, transportation, installation, maintenance, and disposal of an asset (i.e., building).

**Environmental product declaration (EPD):** Quantifies environmental information on the life cycle of a product to enable comparisons between products fulfilling the same function.

**Global warming potential (GWP):** An index developed to provide a simplified means of describing the relative ability of a chemical compound to affect radiative forcing, if emitted to the atmosphere, over its lifetime in the atmosphere, and thereby to affect the global climate.

**Greenhouse gas emission (GHG):** Greenhouse gases are those gaseous constituents of the atmosphere, both natural and anthropogenic, that absorb and emit radiation at specific wavelengths within the spectrum of terrestrial radiation emitted by the Earth's surface, the atmosphere itself and by clouds.

**Heat extraction rate by radiant systems:** Heat removal per unit time by the radiant system

**Heat removal by radiant systems:** Cumulative heat removal

**Heatwave weather year (HWY):** Meteorological data assuming for heatwave events. The heatwaves were characterized by its intensity (maximum temperature), duration (length of heatwave), and severity (combined evaluation of temperature and duration, i.e., degree days).

**Life cycle assessment (LCA):** The process of evaluating a component, product, assembly, building, etc. and its development from the moment of extraction of raw materials, transportation, processing, manufacturing, use, recyclability, and disposal and assigning a value or assessment of its cumulative and ultimate social, environmental and economic costs, benefits, and impacts.

**Life-cycle carbon emissions (LCCO<sub>2</sub>):** Total carbon emissions related to a development over its entire life cycle including construction, operation, renewal, repair, and demolition.

**Net zero carbon building (ZCB):** Zero-carbon buildings are highly energy-efficient and resilient buildings that either use renewable energy directly or rely on a source of energy supply that can be fully decarbonized, such as electricity or district energy. The zero-carbon concept include both operational and embodied emissions.

**Net zero energy building (ZEB):** The net zero energy buildings (ZEB) are defined as buildings that aim to achieve annual primary energy consumption balance of zero while maintaining operations by saving energy as well as producing energy through the introduction of recyclable resources.

**Operational carbon:** The total greenhouse gas emissions associated with the operation of an asset (i.e., building) during the use stage of the asset.

**Primary energy factor (PEF):** The primary energy factor represents the ratio of primary energy input to the final energy output in each energy conversion or supply process. In other words, it quantifies how much primary energy (coal, natural gas, oil, nuclear, and renewable resources) is required to produce a unit of final energy that is delivered to end-users (electricity, heat, etc.).

**Radiant ceiling panel system (RCP):** Suspended, usually aluminum or metal panels distant under the ceiling with fluid temperature relatively close to room temperature.

**Radiant heating and cooling system:** The systems that use water (air) as the heat carrier and where the heat exchange within the conditioned space is more than 50% radiant.

**Radiant surface heat flow:** Cumulative sum of convection, short-wave radiation, and long-wave radiation heat transfer at the surface of the radiation system

**Radiant surface heat flux:** Sum of convection, short-wave radiation, and long-wave radiation heat transfer per unit time at the surface of the radiation system

**Resilient cooling:** Resilient Cooling is used to denote low energy and low carbon cooling solutions that strengthen the ability of individuals and our community to withstand, and also prevent, thermal and other impacts of changes in global and local climates.

**Thermally active building system (TABS):** The systems which are operated at heat carrier temperature very close to room temperature and take advantage of the thermal storage capacity of the building structure.

**Typical meteorological year (TMY):** A typical meteorological year is a set of meteorological data with data values for every hour in a year for a given geographical location.

**Upfront carbon:** The total greenhouse gas emissions associated with building material manufacturing and construction.

**Whole life carbon:** The total greenhouse gas emissions, including operational carbon emissions and embodied carbon emissions over the life cycle of an asset (i.e., building).



**Chapter 1:**  
**Introduction**

## 1.1 Background and Objective

Since the industrial revolution, buildings have been constructed using mass-produced building materials such as concrete, steel and plastic and consuming fossil fuels. They have also consumed large amounts of electricity and gas for heating, cooling, ventilation, lighting, and mechanical equipment to keep occupants comfortable. In recent years, extreme weather disasters caused by global warming and climate change have resulted in more frequent heatwaves, floods and other events that have severely affected buildings. There is an urgent need to building decarbonization to address climate change and transition away from dependence on fossil fuels.

The International Energy Agency (IEA) and Energy in Buildings and Communities Program (EBC) Annex 80: Resilient cooling of Buildings [1] also indicated that the world is facing a rapid increase of air conditioning of buildings for cooling by multiple factors, such as urbanization and densification, climate change and elevated thermal comfort expectation. Therefore, there is a need to develop new building design criteria that drive building decarbonization, while considering the risks of overheating inside buildings.

As a response to the building decarbonization and the comfort of indoor environments, net zero energy buildings (ZEB) [2] have been promoted. To fully achieve net zero energy buildings, energy consumption must be drastically reduced, and renewable energy resources should be generated. The ZEB Guidelines [3] classified buildings as ZEB oriented, ZEB ready, Nearly ZEB, or net ZEB. The ZEB guidelines also emphasized that it is very important to design buildings based on the following seven main policies. Each of them was classified as passive design, active design, and energy management.

### **Zero Energy Building (ZEB) design method**

#### **Passive design**

1. Appropriate surrounding environment: Appropriate building layout, architectural planning, and exterior planning
2. Reduction of heat load: Enhanced insulation levels of the building envelope, reduction of internal heat gain (light, people, equipment, etc.)
3. Use of natural energy: daylight use, natural ventilation
4. Suitable indoor environment: indoor thermal, air quality, and light environment

#### **Active design**

5. Higher efficiency of equipment and systems: Higher efficiency of air conditioning, ventilation, heat source, lighting, and hot water supply equipment, etc.
6. Installation of renewable energy sources: solar power, wind power, etc.

#### **Energy management**

7. Energy management: BEMS (Building Energy Management System), life cycle energy management, visualization, etc.

The concept of ZEB is to reduce operational energy and carbon emissions. In contrast, according to the IEA, the concept of a zero carbon building ready (ZCB) is highly energy-efficient and resilient buildings that either use renewable energy directly or rely on a source of energy supply that can be fully decarbonized, such as electricity or district energy [4]. The zero carbon concept include both operational and embodied emissions. Based on these concepts, the ZCB design method was summarized as follows.

**Zero Carbon Building (ZCB) design method**

1. Resilient buildings: suitable indoor environment in response to natural disasters, such as heatwaves.
2. Reducing operational carbon: combined ZEB design method and grid-efficient building
3. Reducing embodied carbon: low carbon building materials, low global warming potential (GWP) refrigerant

Low energy transformation initiative (LETI) embodied carbon primer described how to contribute zero carbon building in UK [5]. In response to climate change, reducing carbon emissions from operational energy consumption was focused on traditionally. However, buildings become more energy efficient, and the grid electricity generation system has been decarbonized, operational carbon of the new ZEB or ZEB ready buildings has significantly reduced. This means that embodied carbon can represent a high ratio of the whole life carbon, see Figure 1-1. To reduce embodied carbon, it is significant to reduce the carbon emissions of all materials used in building structures, building facades, and building services (including heating, ventilation, and air-conditioning). Based on the above, selecting a heating and cooling system that emits less whole life carbon emissions from the building is very important.

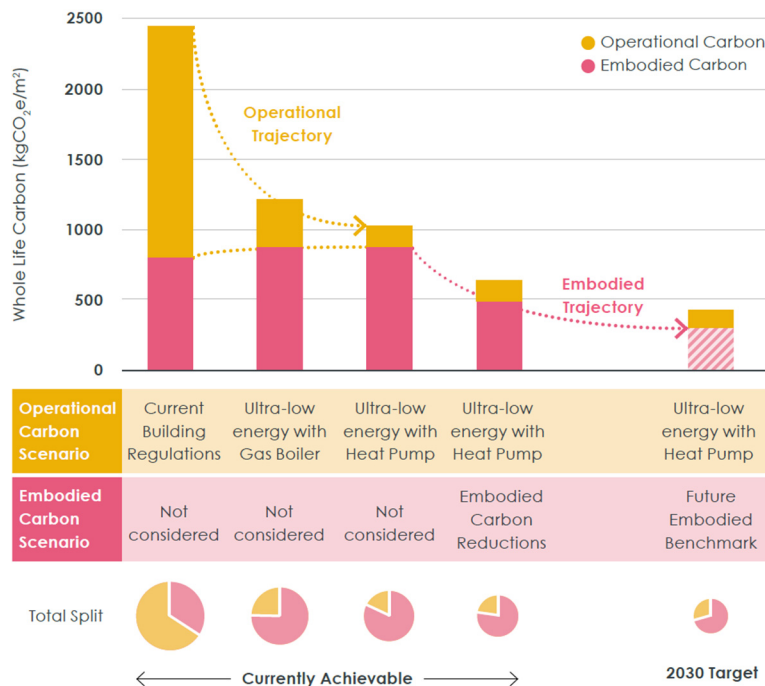


Figure 1-1. Trajectories of operational and embodied carbon from LETI embodied carbon primer [5]

Radiant systems are energy-efficient and resource-effective heating and cooling solutions for buildings [6]. If installing the radiant system becomes energy efficiency and results in a smaller heat source of heating and cooling systems, both operational and embodied carbon of the radiant system could be reduced. Another feature of a thermally active building system (TABS), one type of a radiant cooling system, is that it does not require a suspended ceiling, which reduces upfront carbon by reducing the floor height. Given these features, the installation of radiant systems in the building has the potential to contribute to the reduction of whole life carbon.

The final goal of this study is to verify the possibilities and limitations of using radiant heating and cooling systems for achieving zero carbon building. It was hypothesized that radiant systems would perform better than all-air systems in terms of indoor thermal environment and carbon emissions of the building.

## **1.2 Building Decarbonization and Zero Carbon Building**

### 1.2.1 Definition and terminology

Climate change is a severe problem, with natural disasters causing extensive damage to buildings and cities [7,8]. Temperatures in the last five years have been the hottest recorded since 1850, and global carbon emissions had increased by 6% in 2021, the highest level in history [9]. Global greenhouse gas (GHG) emissions should be reduced to prevent further acceleration of global warming. Supply chain emissions should be calculated to detect carbon emissions related to each business and effectively reduce carbon emissions. Supply chain emissions are the total emissions related to business activities, not only the emissions of a business itself. They refer to GHG emissions generated from the entire process of activities, including raw material production, manufacturing, transport, sales, and disposal, as defined by the Greenhouse Gas Protocol [10]. GHG emissions are classified into the following three categories [10]:

Scope 1: Direct GHG emissions, on-site fuel (gas) use, and refrigerant leakage

Scope 2: Indirect GHG emissions and purchased electricity from the grid

Scope 3: Other Indirect GHG emissions, material extraction, waste disposal, transport, and numerous others

Table 1-1 shows the percentages of global energy and process emissions from buildings in 2021, including the embodied carbon emissions from new building construction [11]. The building sector accounted for approximately 33% of global carbon emissions, with 8.4%, 18.5%, and 6.4% being direct (Scope 1), indirect (Scope 2) and building construction (Scope 3) emissions. The percentage of indirect emissions (Scope 2 and 3) was higher than that of direct emissions (Scope 1). GHG emissions not only originate from direct emissions but also from indirect emissions from the source of electricity in grids and phases outside of operation, both of which generate large amounts of global emissions.

Table 1-1. Global energy and process emissions from buildings, including embodied carbon emissions from new building construction, IEA, 2021 [11]

Scope	Category	Percentage of global energy and process emissions [%]
1	Residential (direct)	5.7
2	Residential (indirect)	10.9
1	Non-residential (direct)	2.7
2	Non-residential (indirect)	7.6
3	Building construction	6.4
-	Total of building sector	33.3

Figure 1-2 shows the classification of the life cycle of a building according to EN15978:2011 [12] and ISO21930:2017 [13]. It comprises several stages, namely A1–A3: products, A4–A5: construction, B1–B7: use, C1–C4: end of life, and D: benefits and loads beyond the system boundary (reuse, recovery, and recycling potential). The World Business Council for Sustainable Development (WBCSD) [14] and ASHRAE Task Force for Building Decarbonization (TFBD) [15] have provided definitions of the scope of life cycle assessments (LCAs) based on EN15978:2011 classification. According to their definition, whole life carbon emissions are the total GHG emissions, including operational and embodied carbon emissions, over the life cycle of buildings. Embodied carbon emissions are the total GHG emissions based on the manufacturing, transportation, maintenance, and disposal of buildings. Operational carbon emissions are the total GHG emissions related to the operation of a building during the use stage. The Whole Life Carbon Network (WLCN) [16] has also provided a definition of the scope of LCAs, including those for buildings and infrastructure, based on EN15978:2011 and PAS2080-carbon management in infrastructure [17]. Except for B8 (other operational processes) and B9 (users’ utilization of infrastructure), the classification of LCA is the same for EN15978:2011.

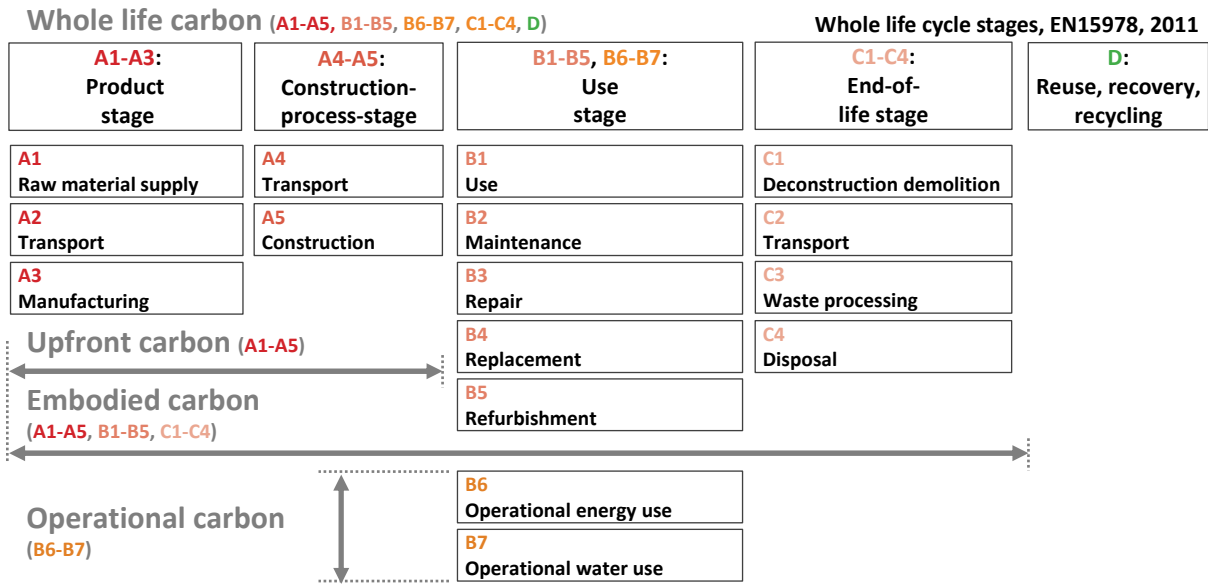


Figure 1-2. Building life cycle stage from EN15978:2011 [12]

The IEA EBC Annex 57 evaluated the embodied energy and carbon for building construction [18]. An analysis of 80 case studies showed various inconsistencies in the current methodologies, which inhibited the comparison of results and made it challenging to develop embodied energy and carbon reduction strategies. The most critical part of estimating embodied carbon is the transparency of the carbon intensity databases at each life-cycle stage, as highlighted in Annex 57. Environmental Product Declarations (EPDs) specify the Global Warming Potential (GWP) of each product and follow the steps of formulation, certification, and publication. Using EPDs with specified input rules enables an easy comparison of embodied carbon emissions for buildings and consequently improves the reliability of results. EPDs provide information regarding the GWP, ozone depletion potential, and other harmful environmental effects in compliance with EN15804 [19] and ISO 14025 [20]. The number of EPDs related to building frames and interior materials is increasing; however, there is a limited number of EPDs related to the mechanical, electrical, and plumbing (MEP) properties of buildings. In general, there is a lack of MEP embodied carbon studies [18].

1.2.2 Building regulations of embodied carbon and whole life carbon

In recent years, required or voluntary building regulations related to carbon emissions have been implemented in some European countries (e.g., Denmark). In March 2021, with parliamentary approval, the Danish government published regulations and requirements for whole life carbon (Chapter 11) in addition to the existing building regulation BR18 [21]. A requirement for new buildings of 1,000 m<sup>2</sup> or larger has been set to 12 kgCO<sub>2</sub>-eq/m<sup>2</sup>/year or less since 2023, and 8 kgCO<sub>2</sub>-eq/m<sup>2</sup>/year was set for voluntary regulations. The evaluation period for LCAs is 50 years, and the life-cycle stages accounted for in the calculation are A1 (material production), A2 (transportation to the factory), A3 (manufacturing of products), B4 (replacement), B6 (energy use during operation), C3 (waste processing), C4 (disposal), and D (reuse, recovery, and recycling potential). A key point is that embodied and operational carbon are combined and evaluated as

whole life carbon, making it necessary to reduce carbon emissions comprehensively rather than simply selecting low-carbon materials or increasing energy efficiency. Previous studies have reported that actions aimed at reducing operational energy and carbon emissions often result in increased embodied carbon [22]. Therefore, a balance between operational and embodied carbon should be carefully considered in the design of buildings. In addition, Zimmermann et al. [23] conducted an LCA analysis of 60 buildings in Denmark with the life-cycle stages suggested in BR18 [21]. The results showed that the values of embodied carbon were remarkably higher than those of operational carbon in both residential and office buildings. The median value of operational carbon emissions for office buildings and those of embodied carbon were 2.0 kgCO<sub>2</sub>-eq/m<sup>2</sup>/year and 6.9 kgCO<sub>2</sub>-eq/m<sup>2</sup>/year, respectively. The balance between operational and embodied carbon can vary in different countries, depending on local energy and electricity mixes. Robati et al. [24] suggested that in Australia embodied carbon could vary from 27% to 58% of whole life carbon emissions, depending on future electricity mixes.

In France, environmental regulations (RE2020) [25] were introduced, and the major differences from the previous thermal regulation, RT2012 [26], were the requirements regarding the reduction of carbon emissions during construction stages, thermal comfort during heatwaves, and energy efficiency of buildings. The benchmark values for upfront carbon emissions were set to 640 kgCO<sub>2</sub>-eq/m<sup>2</sup> for single houses and 740 kgCO<sub>2</sub>-eq/m<sup>2</sup> for apartment buildings in 2022 (Table 1-2). In the Netherlands, calculation of the Environmental Performance of Buildings (Milieu Prestatie Berekening, MPG) [27] is mandatory for new offices and residential buildings exceeding 100 m<sup>2</sup>. The MPG involves the LCA of buildings, and the calculation results are expressed in €/m<sup>2</sup>/year.

Table 1-2. Benchmark of upfront carbon in RE2020 (France) [25]

Year		2022	2025	2028	2031
Upfront carbon for residential buildings [kgCO <sub>2</sub> -eq/m <sup>2</sup> ]	Single house	640	530	475	415
	Apartment	740	650	580	490

London Plan 2021 [28] outlines London’s urban development strategy for the next 20–25 years, and one of the policies recommended in the plan is the reduction of GHGs. For development proposals related to London, it is necessary to calculate and reduce carbon emissions during the entire building life cycle. Furthermore, guidelines for whole life carbon calculations [29] were issued in March 2022; the benchmark values are listed in Table 1-3. As shown in Table 1-3, the benchmark values and aspirational targets for carbon emissions over a building’s life cycle are provided for four types of building applications: office, residential, school, and retail. Looking at the breakdown of each building material, foundations and structures accounted for a large percentage of the building construction category (A1 to A5), whereas equipment and envelope parts accounted for a large percentage of the building operation and demolition categories (B to

C). The basic LCA calculation method in the London Plan was based on EN15978:2011 [12]; however, practical and detailed calculation procedures can be found in the reports of the Royal Institute of Chartered Surveyors [30] and the London Energy Transformation Initiative, an expert group in the built environment sector [31]. Furthermore, it was recommended to refer to the guidelines of IstructE, the UK’s Institute of Building and Structural Engineers [32], when EPDs for concrete and other structures are not available and to the Chartered Institution of Building Services Engineers (CIBSE) [33] guidelines when EPDs for MEP are not available.

Table 1-3. Benchmark of whole life carbon in the London Plan [29]

Building use	Life cycle stage	Benchmark [kgCO <sub>2</sub> -eq/m <sup>2</sup> GIA]	Aspirational benchmark	Breakdown of a typical development [%]						
			[kgCO <sub>2</sub> -eq/m <sup>2</sup> GIA]	Sub-structure	Super-structure	Facade	Internal finishes	FFE**	Service MEP	External work
Office	A1–A5	<950	<600	19	36	17	10	2	14	2
	B–C: excluding	<450	<370	1	4	21	27	9	35	3
	B6, B7									
Residential	A1–A5	<850	<500	21	33	18	10	1	16	1
	B–C: excluding	<350	<300	6	6	34	19	3	30	2
	B6, B7									
School	A1–A5	<750	<500	33	30	13	6	-	11	7
	B–C: excluding	<250	<175	2	4	37	14	-	29	14
	B6, B7									
Retail	A1–A5	<850	<550	35	38	9	5	1	6	6
	B–C: excluding	<200	<140	0	5	18	22	8	40	7
	B6, B7									

\*GIA: Gross Internal Area \*\*FFE: Furniture, Fixtures, and Equipment

Heating, Ventilation, and Air Conditioning (HVAC) systems that could contribute to reducing whole life carbon emissions. The HVAC of a building is usually made from high-impact carbon emission materials, such as steel, iron, and aluminum, which affect embodied carbon emissions. Therefore, it has become more important to evaluate HVAC systems in terms of carbon emissions in addition to operational energy use. CIBSE TM65 [33] reported embodied carbon emissions at the MEP scale and developed a consistent methodology for embodied carbon assessment in the absence of EPDs.



As shown in the Table 1-4, progress of building regulations and climate declarations related to whole life carbon differ from country to country. For example, the scopes covered by BR18 in Denmark and the DGNB certification system in Germany are very limited to A1-A3: product stage, B4: replacement, B6: operational energy use, C3: waste processing, and C4: disposal. In contrast, France RE2020 covered basically all scopes from cradle to gate (A-C). Some European countries such as Norway and Sweden were limited to climate declarations. Differences in the scope should not be overlooked as they have a significant impact on the value of whole life carbon.

Table 1-4. Overview of the whole life carbon scope covered in selected countries in Europe with regulation already in place or expected come into force [34]

Country	Building regulation/ Certification system	A1-A5: Upfront carbon			B1-B5: Use stage embodied carbon					B6-B7: Operational carbon		C1-C4: End of life stage embodied carbon				D: Beyond the building system		
		A1-A3			A4	A5	B1	B2	B3	B4	B5	B6	B7	C1	C2	C3	C4	D
		A1-A3	A4	A5	B1	B2	B3	B4	B5	B6	B7	C1	C2	C3	C4	D		
Denmark	BR18 [21]	Blue	White	White	White	White	White	White	Blue	White	Blue	White	White	White	Blue	White	Pink	
France	RE2020 [25]	Blue	Blue	Blue	Blue	Blue	Blue	Blue	Blue	Blue	Blue	Blue	Blue	Blue	Blue	Blue	Blue	Blue
Netherlands	MPG [27]	Blue	Blue	Blue	White	White	White	White	White	Blue	White	Pink	White	White	Blue	White	White	Pink
Finland	Proposed method for climate declaration [35]	Blue	Blue	Blue	White	White	White	White	Blue	White	Blue	White	White	White	Blue	White	White	Pink
Norway	TEK17 [36]	Pink	Pink	Pink	White	Pink	White	White	Pink	White	White	White	White	White	White	White	White	White
Sweden	Climate declaration 2022 [37]	Pink	Pink	Pink	White	Pink	White	White	White	White	White	White	White	White	White	White	White	White
Sweden	Proposal for limit values 2025	Blue	Blue	Blue	White	Pink	White	White	Pink	White	Pink	White	White	White	Pink	White	White	White
Germany	DGNB certification system [38]	Blue	White	White	White	White	White	White	Blue	White	Blue	White	White	White	Blue	White	White	Pink

\*Note: blue denotes the scope in limit value and pink in climate declaration.

### 1.2.3 Electrical grid and district heat

The ratio of embodied carbon to operational carbon changed significantly as demand-side electrification progressed. With the higher efficiency of power generation obtained using fossil fuels and the increased use of renewable resources, the amount of carbon emitted required to generate 1 kWh of electricity is expected to decrease. As a result, the standards and building regulation values of carbon emissions are expected to be country dependent. Therefore, the actual and estimated future carbon emission intensities of electricity in European countries and Japan were compared.

Figure 1-3 shows current and future carbon intensities based on electricity. Filled markers are measured values and empty markers are estimated values. The Japanese carbon intensity was based on the actual and estimated values provided by the Ministry of the Environment in “Draft Approach to Contracts for Electricity Supply” [39] released in October 2022. Actual carbon intensities were used until 2020, and future-scenario-based values were used after 2021. The future average carbon intensity for all power sources in 2030 is 0.250 kgCO<sub>2</sub>-eq/kWh, assuming an increase in the ratio of renewable energy sources in the future. The Danish carbon intensities were obtained from the building regulation BR18 [40], which summarizes carbon intensities after 2023, with a future value of 0.047 kgCO<sub>2</sub>-eq/kWh for 2030. In Denmark, the current high share of wind and biomass power sources results in a value of 0.187 kgCO<sub>2</sub>-eq/kWh for 2023. The carbon intensities for the UK were based on the future carbon intensity proposed in the Future Energy Scenarios (FES) [41] described in the WBCSD [14] on building decarbonization. Various future scenarios were proposed, and the estimates were based on future projections on the demand side, including the spread of renewable energy and technological innovation, consumer behavior, enhanced home insulation, and increased use of electric vehicles. For this comparison, a steady progress forecast was used for the FES. Dutch guidelines for buildings, NTA8800:2022 [42], have set the carbon intensity for the grid to 0.340 kgCO<sub>2</sub>-eq/kWh. The estimated carbon intensity for 2030, published by the Dutch research institute “Netherlands Organization for Applied Scientific Research” (TNO) [43], is 0.190 kgCO<sub>2</sub>-eq/kWh, assuming further penetration of renewable energy in the future. Although this comparison focused on only four countries, all of them assumed a significant reduction in the carbon intensity of grid electricity by 2030. This suggests the need to evaluate the LCA of buildings as represented by whole life carbon, based on the assumption of a reduction in the carbon intensity of electricity in the near future.

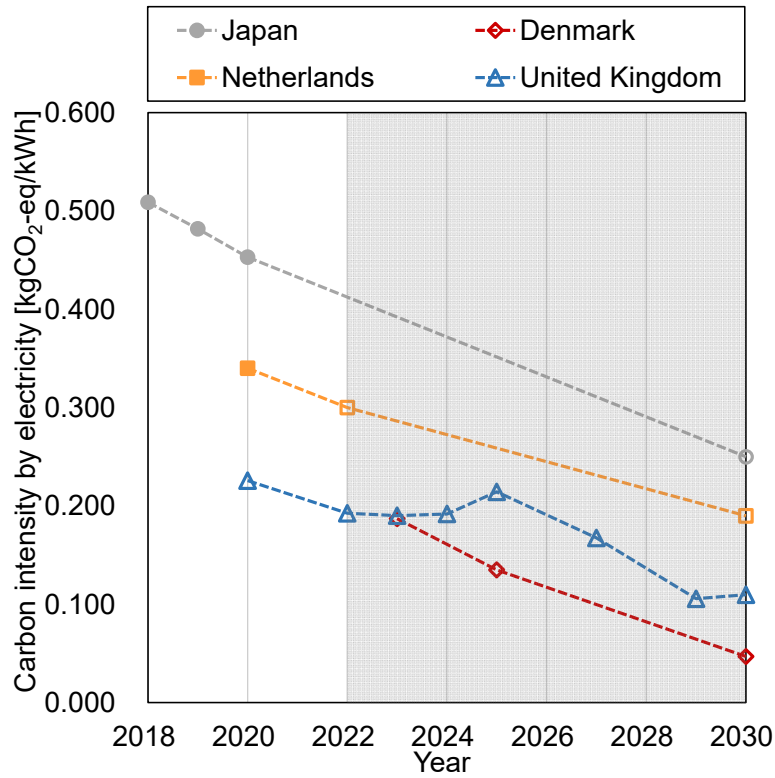


Figure 1-3. Current and future carbon intensity by electricity

\* Filled markers are measured values and empty markers are estimated values

Figure 1-4 shows the installed capacity of solar power generation by the city in Tokyo. As the renewable energy market itself expands and becomes more base-loaded, the possibility that renewable resources such as solar and wind, whose power generation fluctuates greatly depending on the time, may threaten the stability of power transmission and distribution networks will increase. To cope with this, it will become more critical to produce renewable energy for local consumption locally. However, in many cases, the amount of on-site renewable energy installed is minimal in urban areas. As shown in the case study in Fig. 1-3, the latest PV installed capacity in Shinjuku City is only 771 kW. Therefore, new solutions are needed to expand the amount of renewable energy installation [44].

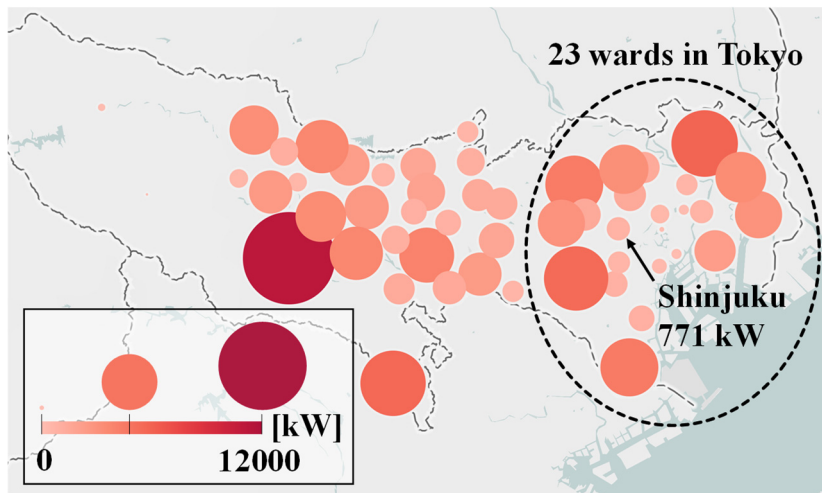


Figure 1-4. Installed capacity of solar power generation by city in Tokyo

In the field of photovoltaics, the development of perovskite solar cells [45], the next generation of lightweight, flexible, and inexpensive solar cells, has been underway in recent years. If commercialized in the future, it will increase the feasibility of PV installation on building facades, resulting in a significant increase in the total PV power generation capacity on-site. Thus, in addition to the energy efficiency and off-site renewable energy of buildings, it is also important to confirm the potential and limitations of on-site renewable energy by comparing it with the current carbon emissions to promote the decarbonization of buildings in the future.

#### 1.2.4 Recent studies related to the zero carbon buildings

##### **Operational and embodied carbon**

Studies on the LCA of buildings have mainly focused on the building construction such as the building envelope. Echenagucia et al. [46] conducted a simplified case study to examine the trade-offs between embodied and operational carbon in building envelopes for a medium-sized office building in the United States. Parametric optimization simulations were conducted with window-to-wall ratios (WWRs), glazing, exterior walls, and shading as the parameters. The results indicated that maintaining a low WWR was beneficial for the low whole life carbon content of buildings. In addition to new construction, some studies have focused on building retrofitting and refurbishment [47,48]. Results showed that optimal refurbishment archetypes generally performed better than replacements in terms of their life-cycle carbon footprint and life-cycle cost. Several studies have focused on the effects of structural timber on embodied carbon [49,50].

Only a few studies focused on the embodied carbon impact of MEP systems. A case study by Rodriguez et al. [51] investigated the impact of MEP and tenant improvements on embodied carbon over the whole lifetime of the building. The results showed that the initial embodied carbon of MEP and tenant improvements components were smaller compared to the building core and shell. However, due to the recurring installments of MEP and tenant improvements components over the building lifetime, their impact on the whole life carbon of the building becomes significant. A post-construction

study by Ylmén et al. [52] conducted an LCA of a building using data provided by contractors involved in the construction of the building. Their analysis revealed that the technical installations (HVAC) contributed significantly (14-32% of the total impact) on multiple environmental impact categories including the GWP. Both studies have shown that MEP has a major impact on the whole life carbon emissions of a building.

**Resilient cooling of buildings**

Figure 1-5 shows the resilient cooling of buildings. IEA EBC Annex 80 – Resilient Cooling of Buildings [53,54] focused on defining resiliency and its key concepts in terms of building cooling, developing qualitative and quantitative key performance indicators (KPIs), and evaluating different cooling systems based on these indicators. Dynamic simulation guidelines for the performance testing of resilient cooling strategies [55] were proposed to compare several cooling strategies in a similar way. Annex 80 developed two types of weather files: typical meteorological years (TMY) and years containing extreme heatwave weather years (HWY). Two types of building geometry, single-family detached house and medium office, developed by U.S Department of Energy (DOE) were shown in the guideline. For the output, four types of KPIs were proposed: overheating and climate resistance assessment, thermal comfort metrics, energy metrics, and emission metrics.

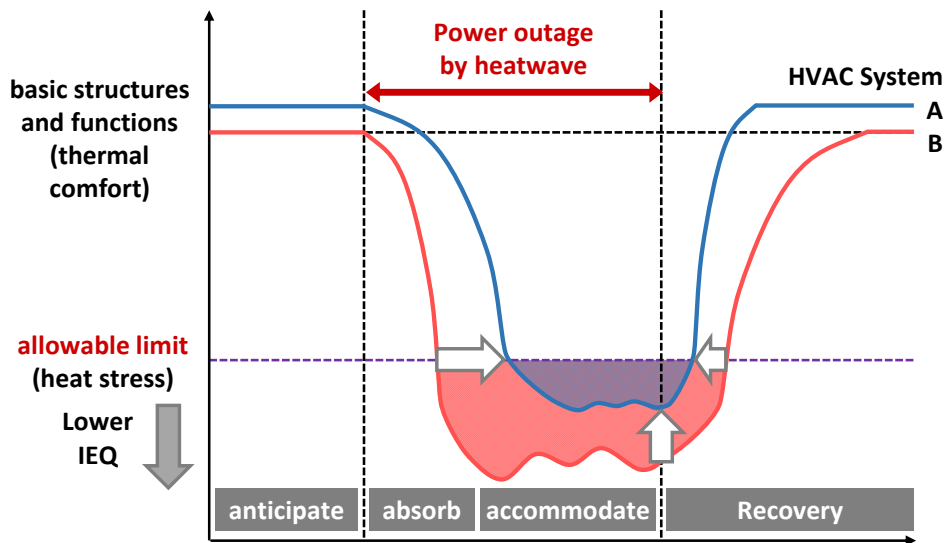


Figure 1-5. Resilient cooling of buildings [53]

In addition to mitigation strategies, it has become necessary to consider adaptation to climate disasters. In this context, the importance of flexible responses to the frequent heatwaves caused by climate change through architectural design and behaviour change, rather than simply increasing cooling capacity, has been pointed out.

### 1.3 Outline of This Study

Figure 1-6 shows the outline of the thesis. There is an urgent need to reduce embodied carbon emissions in addition to the operational carbon emissions as typified by net zero emission buildings. In this study, net zero carbon buildings (ZCB) were defined as consisting of three parts: (i) overheating risk of indoor environment, (ii) operational carbon, and (iii) embodied carbon of the building. The objective of this study is to verify the possibilities and limitations of using radiant heating and cooling systems for achieving zero carbon building. The outline of this thesis is as follows:

Chapter 1 gave the background and objective of this study and a summary of related studies, Chapter 2 explains the definition, characteristics, and limitation of radiant heating and cooling systems with previous research. Installation surveys of radiant systems and expert interviews in Japan were conducted and the key topics that would be important in the designing radiant systems were clearly presented. Chapter 3 gives field measurement results of Thermally Active Building System (TABS) ceiling slits with both daylight harvesting and prevent overheating in the office environment. Chapter 4 presents dynamic simulation results of radiant systems and all-air system in terms of overheating risk assessment and operational carbon emissions of buildings. Typical meteorological year (TMY) and Heatwave weather year (HWY) data were used to assess the resilience performance of buildings against heatwaves. Chapter 5 examines the comparative study of the whole life carbon of a radiant system and an all-air system in a non-residential building with boundary conditions in Danish building regulation. Indoor thermal comfort was integrated into the life cycle assessment framework. A methodology to compare the whole life carbon of HVAC systems was developed. Chapter 6 indicates the comparative study of the upfront and operational carbon of a radiant system and an all-air system in a university building in Japan. Chapter 7 discusses the conclusions of the thesis and the implications for future research.

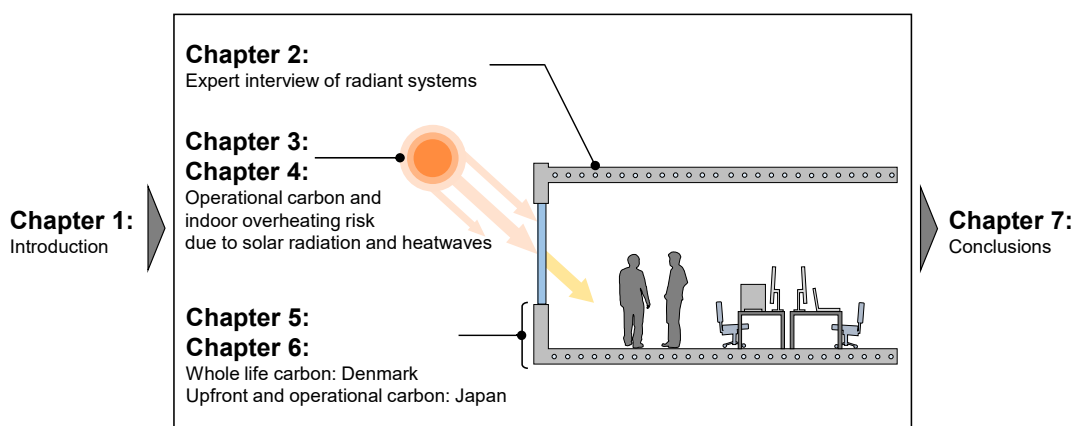


Figure 1-6. Outline of the thesis

## References

- [1] IEA EBC Annex 80, Resilient Cooling of Buildings. IEA. <https://annex80.iea-ebc.org/> (accessed January 16, 2024)
- [2] ISO/TS 23764:2021, Methodology for achieving non-residential zero-energy buildings (ZEBs), International Organization for Standardization, 2021.
- [3] ZEB Roadmap Follow-up Committee, ZEB desing guideline - medium office version, Sustainable open innovation initiative, 2018.
- [4] International Energy Agency, Tracking Buildings, 2022. <https://www.iea.org/energy-system/buildings#overview> (accessed January 16, 2024)
- [5] Embodied Carbon Primer, London Energy Transformation Initiative (LETI), 2020. <https://www.leti.uk/ecp> (accessed January 16, 2024)
- [6] O. B. Kazanci, Low Temperature Heating and High Temperature Cooling in Buildings, PhD Thesis, Kgs. Lyngby: Technical University of Denmark, 2016.
- [7] IPCC DDC Glossary, Intergovernmental Panel on Climate Change, 2020. [https://www.ipcc-data.org/guidelines/pages/glossary/glossary\\_c.html](https://www.ipcc-data.org/guidelines/pages/glossary/glossary_c.html) (accessed July 20, 2023)
- [8] IPCC, Synthesis report of the IPCC sixth assessment report (AR6), 2023. <https://www.ipcc.ch/report/sixth-assessment-report-cycle/> (accessed July 20, 2023)
- [9] International Energy Agency, CO2 emissions by fuel type, 2022. <https://ourworldindata.org/emissions-by-fuel> (accessed July 20, 2023)
- [10] WBCSD. Greenhouse Gas Protocol, Corporate Value Chain (Scope3) Accounting and Reporting Standard. [https://ghgprotocol.org/sites/default/files/standards/Corporate-Value-Chain-Accounting-Reporting-Standard\\_041613\\_2.pdf](https://ghgprotocol.org/sites/default/files/standards/Corporate-Value-Chain-Accounting-Reporting-Standard_041613_2.pdf) (accessed July 20, 2023)
- [11] International Energy Agency, Global energy and process emissions from buildings, including embodied emissions from new construction, 2021. <https://www.iea.org/data-and-statistics/charts> (accessed July 20, 2023)
- [12] EN 15978:2011, Sustainability of construction works – Assessment of environmental performance of buildings – Calculation method, CEN, 2011.
- [13] ISO 21930:2017, Sustainability in buildings and civil engineering works — Core rules for environmental product declarations of construction products and services, International Organization for Standardization, 2017.
- [14] WBCSD, Net-zero buildings Where do we stand?, 2021.
- [15] ASHRAE, ASHRAE task force for building decarbonization (TFBD). <https://www.ashrae.org/about/ashrae-task-force-for-building-decarbonization> (accessed July 20, 2023)
- [16] WLCN, Improving consistency in whole life carbon assessment and reporting, carbon definitions for the built environment, buildings and infrastructure, Royal Institute of British Architects (RIBA), 2021.
- [17] PAS 2080, guideline document for PAS 2080, construction leadership council and green construction board, 2016.
- [18] H. Birgisdottir, A. Moncaster, A.H. Wiberg, C. Chae, K. Yokoyama, M. Balouktsi, S. Seo, T. Oka, T. Lützkendorf, T. Malmqvist, IEA EBC annex 57 ‘evaluation of embodied energy and CO<sub>2</sub>e<sub>q</sub> for building construction’, Energy

- and Buildings, 154, 72–80, 2017. <https://doi.org/10.1016/j.enbuild.2017.08.030>.
- [19] EN 15804:2012+A2:2019, Sustainability of construction works. Environmental product declarations. Core rules for the product category of construction products, CEN, 2019.
- [20] ISO 14025:2006, Environmental labels and declarations — Type III environmental declarations — Principles and procedures, International Organization for Standardization, 2021.
- [21] Building regulation 2018 (BR18), 2018. <https://byggningsreglementet.dk/> (accessed July 20, 2023)
- [22] I. Sartori, A.G. Hestnes, Energy use in the life cycle of conventional and low-energy buildings: A review article, *Energy and Buildings*, 39, 249–257, 2007. <https://doi.org/10.1016/j.enbuild.2006.07.001>.
- [23] R.K. Zimmermann, C.M. Ernst Andersen, K. Kanafani, H. Birgisdottir, Whole life carbon assessment of 60 buildings – possibilities to develop benchmark values for LCA of buildings, BUILD, Aalborg university, 2021.
- [24] M. Robati, P. Oldfield, A. A. Nezhad, D. G. Carmichael, A. Kuru, Carbon value engineering: A framework for integrating embodied carbon and cost reduction strategies in building design, *Building and Environment*, 192, 107620, 2021. <https://doi.org/10.1016/j.buildenv.2021.107620>
- [25] Guide RE2020: Environmental regulations. <https://www.ecologie.gouv.fr/reglementation-environnementale-re2020> (accessed July 20, 2023)
- [26] Thermal regulation RT2012. <https://www.ecologie.gouv.fr/reglementation-thermique-rt2012> (accessed July 20, 2023)
- [27] Environmental Performance Buildings - MPG (Milieu Prestatie Berekening), Netherlands Enterprise Agency. <https://www.rvo.nl/onderwerpen/wetten-en-regels-gebouwen/milieuprestatie-gebouwen-mpg> (accessed July 20, 2023)
- [28] Mayor of London, The London Plan: The Spatial Development Strategy for Greater London, pp. 342–347, 2021.
- [29] Mayor of London, London plan guideline – Whole Life-Cycle Carbon Assessments, 2022. <https://www.london.gov.uk/programmes-strategies/planning/implementing-london-plan/london-plan-guidance/whole-life-cycle-carbon-assessments-guidance> (accessed July 20, 2023)
- [30] Royal Institution of Chartered Surveyors (RICS), Whole Life Carbon Assessment for the Built Environment, 1st edition, 2017.
- [31] London Energy Transformation Initiative (LETI), LETI Embodied Carbon Primer, 2020.
- [32] IstructE, How to calculate embodied carbon (Second edition), 2022.
- [33] CIBSE, TM65 Embodied carbon in building services: A calculation methodology, 2021.
- [34] B. Maria, B. Harpa, Analysis of new modules in connection with calculation of the climate impact of buildings, BUILD: Aalborg university, Denmark, 2023
- [35] M. Kuittinen, Method for the whole life carbon assessment of buildings. Helsinki: Ministry of the Environment, 2019. <http://urn.fi/URN:ISBN:978-952-361-030-9>. (accessed January 17, 2024)
- [36] Ministry of Local Government and Regional Development, Regulations amending the Regulations relating to technical requirements for buildings (Building Regulations), Norway, 2022. <https://lovdata.no/dokument/LTI/forskrift/2022-05-29-945> (accessed January 17, 2024)



- [37] Boverket, Limit values for climate impact from buildings, Boverket, 2023.
- [38] GERMAN SUSTAINABLE BUILDING COUNCIL (DGNB), DGNB Certification system, <https://www.dgnb.de/en/certification/important-facts-about-dgnb-certification/about-the-dgnb-system> (accessed January 17, 2024)
- [39] Ministry of the Environment in its "Draft Approach to Contracts for Electricity Supply. <https://www.env.go.jp/content/000081247.pdf> (accessed July 20, 2023)
- [40] BR18 Executive order amending the executive order on building regulations 2018.
- [41] National Grid ESO, Future Energy Scenarios, 2021. <https://www.nationalgrideso.com/future-energy/future-energy-scenarios> (accessed July 20, 2023)
- [42] Dutch technical agreement (NTA) 8800, Energy Performance of buildings – Determination method, Dutch Standard (NEN standard), 2022.
- [43] Niessink, R.J.M, Gerdes, J., Primary fossil energy factor electricity at upper value (HHV) for application in the energy performance standard NTA 8800, TNO. <https://repository.tno.nl/islandora/object/uuid%3Ad2efd0b0-5b6b-4c47-ad7d-ebb421440c94> (accessed July 20, 2023)
- [44] K. Shindo, R. Nitta, R. Matsumura, K. Ikai, M. Tazaki, Y. Ogawa, Y. Saito, S. Tanabe, Using CityGML to Study Embodied Carbon and Renewable Energy in Tokyo, Indoor Air 2022, 2022.
- [45] M. Lee, J. Teuscher, T. Miyasaka, T. Murakami, H. J. Snath, Efficient hybrid solar cells based on meso-structured organometal halide perovskites, Science, Vol 338, 643-647, 2012. DOI: 10.1126/science.1228604
- [46] T.M. Echenagucia, T. Moroseos, C. Meek, On the tradeoffs between embodied and operational carbon in building envelope design: The impact of local climates and energy grids, Energy and Buildings, 278, 112589, 2023. <https://doi.org/10.1016/j.enbuild.2022.112589>
- [47] K. Simonen, M. Huang, C. Aicher, P. Morris, Embodied carbon as a proxy for the environmental impact of earthquake damage repair, Energy and Buildings, 164, 131–139, 2018. <https://doi.org/10.1016/j.enbuild.2017.12.065>
- [48] Y. Schwartz, R. Raslan, D. Mumovic, Refurbish or replace? The Life Cycle Carbon Footprint and Life Cycle Cost of Refurbished and New Residential Archetype Buildings in London, Energy, 248, 123585, 2022. <https://doi.org/10.1016/j.energy.2022.123585>
- [49] F. Morris, S. Allen, W. Hawkins, On the embodied carbon of structural timber versus steel, and the influence of LCA methodology, Building and Environment, 206, 108285, 2021. <https://doi.org/10.1016/j.buildenv.2021.108285>
- [50] J.M. Greene., H.R. Hosanna., B. Willson., J.C. Quinn, Whole life embodied emissions and net-zero emissions potential for a mid-rise office building constructed with mass timber, Sustainable Materials and Technologies, 35, e00528, 2023. <https://doi.org/10.1016/j.susmat.2022.e00528>
- [51] B.X. Rodriguez, M. Huang, H.W. Lee, K. Simonen, J. Ditto, Mechanical, electrical, plumbing and tenant improvements over the building lifetime: Estimating material quantities and embodied carbon for climate change mitigation, Energy and Buildings, 226, 110324, 2020. <https://doi.org/10.1016/j.enbuild.2020.110324>
- [52] P. Ylmén, D. Peñaloza, K. Mjörnell, Life cycle assessment of an office building based on site-specific data, Energies,

12, 1–11, 2019. <https://doi.org/10.3390/en12132588>.

- [53] S. Attia, R. Levinson, E. Ndong, P. Holzer, O. B. Kazanci, S. Homaei, C. Zhang, B.W. Olesen, D. Qi, M. Hamdy, P. Heiselberg, Resilient cooling of buildings to protect against heat waves and power outages: Key concepts and definition, *Energy and Buildings*, 239, 110869, 2021.
- [54] C. Zhang, O. B. Kazanci, R. Levinson, P. Heiselberg, B. W. Olesen, G.Chiesa et al. Resilient cooling strategies – A critical review and qualitative assessment. *Energy and Buildings*, 251, 111312, 2021.
- [55] C. Zhang, O. B. Kazanci, S. Attia, R. Levinson, S. H. Lee, P. Holzer, R. Rahif, A. Salvati, A. Machard, M. Pourabdollahtookaboni, A. Gauri, B. W. Olesen, P. K. Heiselberg, IEA EBC Annex 80 - Dynamic simulation guideline for the performance testing of resilient cooling strategies Version 2, 2023.

## **Chapter 2:**

# **Design and control of radiant heating and cooling systems in Japan: Results from expert interviews**

### **Abstract**

This research conducted surveys of buildings equipped with radiant systems and expert interviews in 2021-2022 with manufacturers and mechanical, electrical, and plumbing (MEP) engineers in Japan who had experience in designing radiant heating and cooling systems. In total, interviews were conducted with 56 respondents from 15 companies. Results from the building survey showed that the 69% of the identified buildings had radiant ceilings, and 30% had radiant floors. In terms of working fluid, 56% were water-based, and 43% were air-based. For the expert interview, 79% of all respondents answered that the use of radiant systems will continue to increase in the future. 54% of all respondents answered that it has become easier to design radiant systems at present compared to the 2010s.

### **KEYWORDS:**

Radiant heating and cooling system, Survey, Expert interview, Practical design, Building decarbonization

## 2.1 Introduction

### 2.1.1 Background

There is an urgent need to reduce global greenhouse gas (GHG) emissions from the building sector to prevent the further acceleration of global warming. Climate change is a severe problem, with natural disasters causing extensive damage to buildings and cities [1]. Energy and process emissions from buildings in 2021 indicated that the building sector accounts for 33% of the global energy and process emissions [2]. In the last decades, net zero energy buildings [3] and other initiatives have been implemented worldwide to reduce building energy consumption during the operational stage [4]. In addition to reducing operational energy/carbon from the building, there is an urgent need to reduce carbon emissions throughout the life cycle stages, including the manufacturing, construction, use, disposal, and recycling phases of building parts [5].

### 2.1.2 Definition, characteristics, and limitation of radiant systems

One solution to reduce carbon emissions by designing an HVAC system might be installing radiant heating and cooling systems (radiant systems). Radiant systems provide cooling/heating by radiation and convection from a cooled/heated surface. Radiant systems are now commonly used as a comfortable, energy-efficient, and resource-effective heating and cooling alternative in buildings [6]. Radiant systems are mainly classified into Radiant Ceiling Panels (RCP) [7], Embedded Surface Systems (ESS) [8], and Thermally Active Building Systems (TABS) [9], with different characteristics depending on the heat transfer fluid, the radiant surface structure, and the location of the cooled/heated surface.

There are many previous research cases and installations of radiant systems in many countries. Rhee et al. [10] reviewed studies related to radiant systems, which were conducted over a 50-year period until 2015. The results showed that radiant systems have been continuously developed, modified, and improved to achieve better indoor thermal comfort and energy efficiency. Radiant systems can provide the same quality of indoor thermal comfort with a lower air temperature for heating and a higher air temperature for cooling [11,12]. These characteristics are also beneficial for energy efficiency. Hydronic radiant systems with ventilation system can also operate with less airflow than all-air systems, contributing to less draught [13,14] and reducing operational energy due to high efficiency heat sources and less fan power.

Compared to all-air systems, radiant cooling systems remove heat differently, especially for solar radiation [15]. Previous studies have reported enhanced cooling capacity of radiant cooling systems due to the absorption of solar radiation at cooled surfaces [16-19]; this characteristic has the potential to increase the design flexibility of windows and facades in daylight harvesting spaces. Other research has been conducted from different perspectives, such as control of radiant systems, condensation problems by the moisture air, Computational Fluid Dynamics (CFD), and heat balance simulations [20]. Radiant systems have been adopted in a variety of spaces, such as in office buildings [21-24], entrance spaces (large spaces) [25,26], patient rooms [27].

### 2.1.3 Previous research with expert interviews

Previous studies have also conducted surveys and interviews with professionals with substantial experience designing, constructing, and operating radiant systems. In 2016, a committee of the Society of Heating, Air-Conditioning and Sanitary Engineers of Japan (SHASE) released a report from surveys and interviews with mechanical, electrical, and plumbing (MEP) engineers in Japan who had experience designing radiant systems [28]. The survey was developed based on interviews with four experts and 24 engineers in eight companies (design firms or general construction companies) from 2013 to 2014. Results showed that high initial cost was listed as the primary concern, and humidity control was the second most serious concern in the difficulties and concerns regarding the design of radiant systems. In addition, half or more than half of the engineers involved in recent building projects pointed out the difficulties related to the heat transfer of the radiant system, such as the lack of cooling capacity, slow response time, and control. In 2017, a team from UC Berkeley Center for the Built Environment (CBE) interviewed eleven professionals with substantial experience with the design, construction, and operation of embedded radiant systems, especially TABS, in North America, having collectively designed more than 330 radiant cooled buildings [29]. Interviewees had a common understanding that the maximum cooling capacity of TABS is lower than that of air systems but has a self-regulating effect in response to temporal and spatial variations in the room air or radiant surface temperatures. For the ventilation system, a dedicated outdoor air system (DOAS) was used in most cases, and condensation was rarely encountered. The feedback from these MEP designers is beneficial when exploring and determining the next research topics for radiant systems in the future.

### 2.1.4 Objective

An installation survey and expert interviews for radiant systems in Japan were conducted from 2013 to 2014 [28]. In the 2010s, net zero energy buildings rapidly became popular in Japan, and the number of radiant systems installations is expected to increase yearly. In addition, buildings are being evaluated with new Key Performance Indicators (KPIs) such as whole life carbon (building decarbonization) [30-32] and building resilience [33]. In order to respond to these changes, it is worthwhile to conduct expert interviews and installation surveys to find out what designers require in the research of radiant systems, and what new issues are being raised. The objective of the study was to investigate design and control strategies currently used for radiant systems in Japan, highlight themes of common practice and variations in practical approaches, and identify research areas that serve practitioner needs.

## 2.2 Methods

Figure 2-1 shows the methodology for installation survey and expert interview in this study. This research consists of two parts.

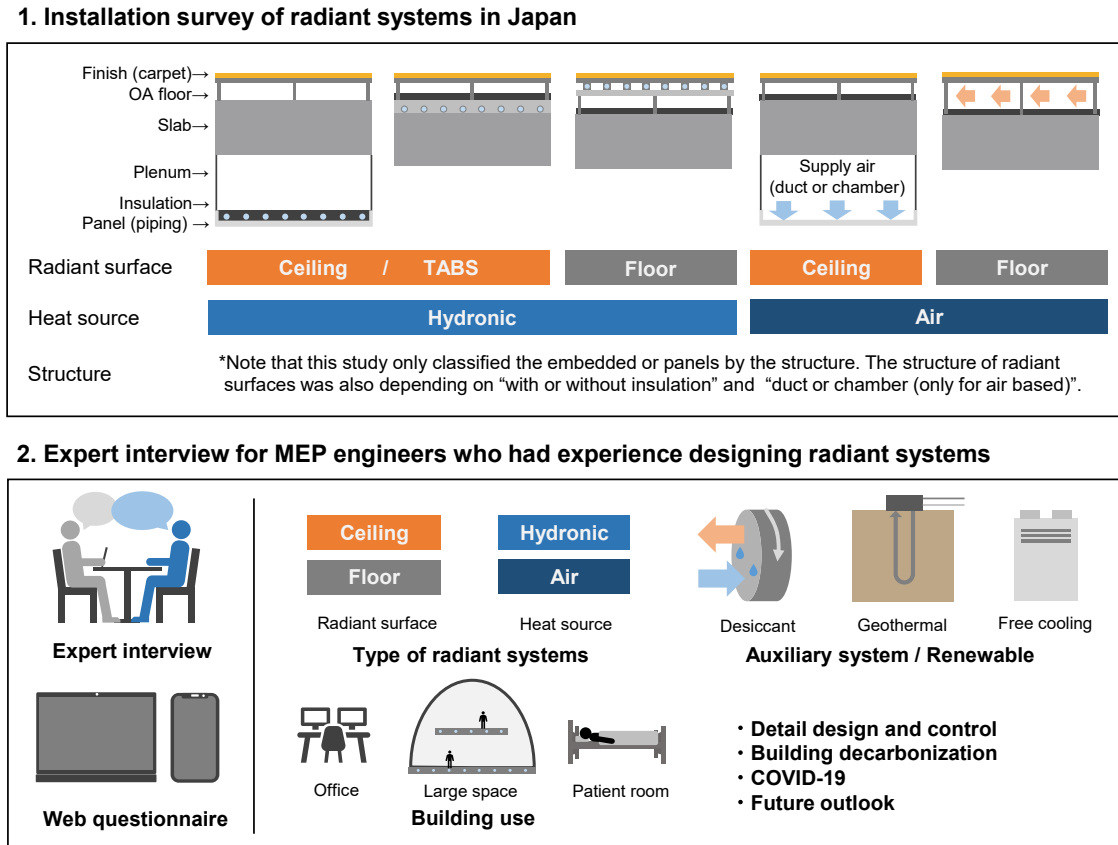


Figure 2-1. Methodology for installation survey and expert interview in this study

### • Installation survey of radiant systems in Japan

The installation survey was based mainly on data provided from two radiant system manufacturers in Japan and papers published in the Architectural Institute of Japan (AIJ) [34] and SHASE [35]. These manufacturers are part of the standard of radiant ceiling panels in Japan (ARCH) [36] and cover a large share of radiant systems in a non-residential buildings in Japan. Radiant systems were classified by radiant surface position, heat transfer fluid, and structure. In this study, radiant surfaces were classified into the ceiling (including TABS) and the floor. The heat transfer fluid was classified into hydronic and air. Note that this study only classified embedded surfaces or panels by the structure. The structure of radiant surfaces, i.e., “with or without insulation” and “duct or chamber” (only for air-based), was asked but not used in this study. The following types of radiant systems were excluded in this study: electric panel heaters, radiant cooling walls. Floor heating systems in residential buildings were also excluded from the study. There is a new type of

radiant systems, which is radiant ceiling panels combined with phase change materials [37], but this system doesn't exist in Japan.

**•Interview for radiant systems experts (mainly for MEP engineers)**

The survey was developed based on interviews with 56 engineers working in 15 different companies (design firms, construction companies, and manufacturers) from July 2021 to June 2022. Interviews were conducted with 32 engineers either in person or in online meetings, and the detailed survey were asked with 31 engineers to respond in the form of a web questionnaire. Some of the questions were the same in the interview (n=32) and the detailed survey (n=31). In these cases, the questions were answered by a total of 56 respondents, merging 7 duplicates who cooperated in both the interviews and the web-based detailed survey. In the general questions, engineers were asked about the characteristics of radiant systems which they have designed and installed in the building (radiant surface, heat transfer fluid, building use, auxiliary system, and combination with renewable resource). The survey also looked at the impact of the global movement towards building decarbonization and the respondents' future outlook for radiant systems. In the detailed survey, some questions were asked in same ways as the SHASE report [28], and results of the questionnaire could be compared with that of 2010s.

### **2.3 Results from the installation survey of radiant systems in Japan**

Figure 2-2 and Table2-1 shows the number of building projects with radiant heating and cooling systems in Japan in the past twenty years. The survey yielded a total of 661 buildings with radiant heating and cooling systems. This database consists of the data from company A, company B, other companies, and AIJ conference papers. If a building had a radiant system installed, it was counted as one project. A detailed survey of the area where the radiant system was installed or the other air-conditioning systems were not conducted this survey. Radiant ceilings were installed in 69% of the buildings, and radiant floors were installed in 30%. In terms of heat transfer fluids, 56% were water-based (hydronic), and 43% were air-based. Before 2010, the number of installations each year was less than 20, but after 2010, the number of installations increased up to 79 projects in 2017. In particular, the ratios of "air-based radiant ceiling " and "water-based radiant floor" have increased since 2010. Air-based systems tend to be chosen because of avoiding hydronic systems in the room, where avoids water leakage. Hydronic floor systems tend to be used in spaces such as entrance hall where there are a lot of glazing, in relation to direct solar load [38]. In addition, there was a constant demand for “water-based radiant ceiling” every year.

Since 2017, the number of installations of the radiation system had remained between 70 and 80 projects. Although the number of radiant systems installed has not changed much recently in Japan, if regulations regarding refrigerant leakage become stricter in the future, radiant systems that use less high-GWP refrigerants compared to packaged systems may be installed in even more buildings. With about 10,000 new office buildings being constructed in Japan each year [39], there may be a possibility that even more buildings will be implemented radiant systems in the future.

Table2-1. Total installed radiant heating and cooling system in Japan

Data source	Water, Ceiling	Air, Ceiling	Water, Floor	Air, Floor	TABS
Company A	106	245	157	36	
Company B	99				
Other companies	6		4	2	
AIJ conference paper					6
Subtotal	211	245	161	38	6
Total					661

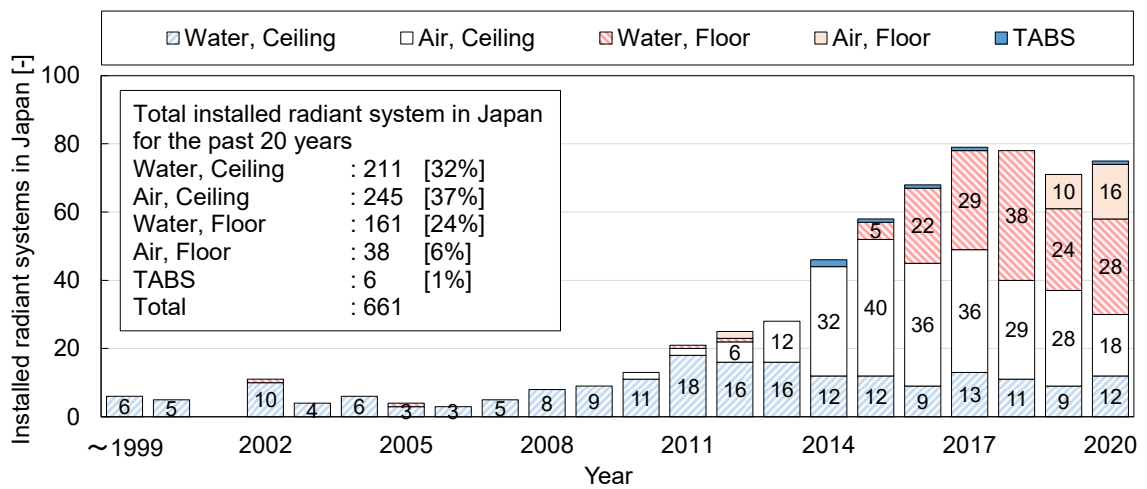


Figure 2-2. Total installed radiant heating and cooling system in Japan for the past twenty years



## 2.4 Results from expert interviews

### 2.4.1 General survey (n=56)

Table 2-2 shows the outlook for future installation of radiant systems for installing radiant systems in buildings. Excerpts of comments corresponding to each response group were listed as reference. When the “increase” and “partial increase” responses were combined, 79% of all respondents indicated that the use of radiant heating and cooling systems would continue to increase in Japan. One of the reasons for the “increase” was that radiant systems can provide both energy saving and thermal comfort. Many respondents answered that the future installation of radiant systems would be limited to specific building uses/rooms, such as patient rooms and office buildings. Many designers pointed out the high initial cost of radiant systems, regardless of their answer. Some MEP engineers mentioned that designing radiant systems requires advanced design with understanding of its characteristics.

Table 2-2. Outlook for future installation of radiant systems

What do you think about outlook for installing radiant systems in the building?		Number of respondents 2022 N=56
<b>Increase</b>		
Comments	<ul style="list-style-type: none"> <li>• Radiant systems can provide both energy savings and thermal comfort.</li> <li>• Internal gain has decreased due to reduced equipment gain (conversion to laptop), and building envelope performance has improved.</li> <li>• More real estate developers are willing to install radiant systems as long as the high initial cost is lowered.</li> </ul>	16 (29%)
<b>Partial increase</b>		
Comments	<ul style="list-style-type: none"> <li>• Because of the high initial cost, the installation of radiant systems is expected to increase slightly only for specific applications (entrance rooms, large spaces) and for rooms where thermal comfort is important.</li> <li>• For draft-sensitive spaces (e.g. patient rooms), the installation of radiant systems are expected to increase.</li> </ul>	28 (50%)
<b>No change</b>		
Comments	<ul style="list-style-type: none"> <li>• High initial cost</li> <li>• Requires advanced design with an understanding of the characteristics of radiant systems (e.g. handling the heat load of perimeter zones, the use of separate sensible and latent cooling technology [40], etc.)</li> </ul>	8 (14%)
<b>Decrease</b>		3 (5%)
<b>No answer</b>		1 (2%)

Table 2-3 shows the responses on whether designing radiant systems has become easier or more difficult compared to the 2010s. More than half (54%) of the respondents answered that it is easier to design radiant systems at present compared to the 2010s. Some engineers indicated that the increased number of building projects with radiant systems made it easier for them to reference and design. At present, radiant systems are listed in the Building Equipment Design Standard of the Ministry of Land, Infrastructure, Transport and Tourism in Japan [41] in 2015. The national standard of radiant ceiling panels (ARCH [36], developed in 2017) being listed in the national guidelines for design standards was one of the reasons many respondents answered that it has become easier to design.

Table 2-3. Whether designing radiant systems has been easier or more difficult compared to the 2010s

What do you think about whether designing radiant systems has been easier or more difficult compared to the 2010s?	Number of respondents 2022 N=56
<b>More difficult</b>	
<b>Comments</b> <ul style="list-style-type: none"> <li>· Clients are becoming more cost-conscious than before, and it is becoming more difficult to install radiant systems due to high initial costs.</li> </ul>	1 (2%)
<b>No change</b>	12 (21%)
<b>Easier</b>	
<b>Comments</b> <ul style="list-style-type: none"> <li>· The number of buildings with radiant systems is increasing, and they are becoming more common as one of the HVAC systems.</li> <li>· Manufacturers have established their technologies, and there are no longer any special concerns, regardless of whether water-based or air-based radiant systems are used.</li> <li>· Compared to the past, it is now easier to design radiant systems. A radiant ceiling panel system is now listed in the Building Equipment Design Standard of the Ministry of Land, Infrastructure, Transport and Tourism in Japan.</li> </ul>	30 (54%)
<b>No answer</b>	13 (23%)

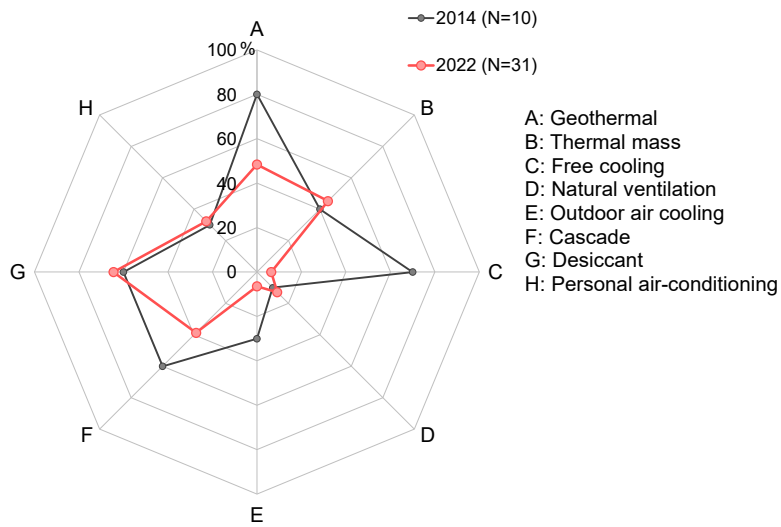
Table 2-4 shows the respondents’ view of whether building decarbonization will have an impact on the installation of radiant systems for the building. When “high impact” and “low impact” responses were merged, 53% of all respondents answered that building decarbonization would have an impact on the installation of radiant systems. Respondents who answered “high impact” indicated that radiant systems are becoming a powerful item for building decarbonization to reduce operational energy and carbon emissions. Other respondents expressed doubts whether radiant systems would be beneficial in terms of whole life carbon [31,32]. This doubt comes from the fact that radiant systems use materials with high carbon footprint (e.g., aluminum for radiant panels). One of the respondents who answered “no change” indicated that an appropriate design of the entire system is a prerequisite for achieving carbon neutrality, such as improving the coefficient of performance (COP) of the chiller and designing an auxiliary system.

Table 2-4. Whether building decarbonization will impact the installation of radiant systems for the building

What do you think about whether building decarbonization will impact the installation of radiant systems for the building?	Number of respondents 2022 (N=56)
<b>High impact</b>	
<ul style="list-style-type: none"> <li>• Radiant systems are becoming a powerful item for achieving a carbon neutral building.</li> <li>• Because of the limited energy savings by all-air systems, radiant systems are definitely one of the keys to building decarbonization.</li> <li>• Radiant system can use low exergy heat sources, making it easier to use renewable resources and more compatible with decarbonization.</li> </ul>	8 (14%)
<b>Low impact</b>	
<ul style="list-style-type: none"> <li>• I doubt that the radiant system is beneficial in terms of life cycle carbon emissions (LCCO<sub>2</sub>).</li> <li>• The reduction of distribution energy (fans, pumps) in radiant systems are effective for reducing running costs (operational carbon), so there will be a certain impact.</li> </ul>	22 (39%)
<b>No change</b>	
<ul style="list-style-type: none"> <li>• I do not consider radiant systems to have any notable advantages in energy saving.</li> <li>• The installation of radiant heating and cooling does not directly lead to energy efficiency of the building. Appropriate design of the entire system is a prerequisite, such as improving the coefficient of performance (COP) of the chiller and designing an auxiliary system.</li> </ul>	13 (23%)
<b>No answer</b>	13 (23%)

2.4.2 Detailed survey (n=31, web-based questionnaires)

Figure 2-3 indicates auxiliary systems and renewable resources that were preferred in combination with radiant systems. Answers were obtained from 10 respondents in 2014 and 31 respondents in 2022, respectively. One of the reasons for the particularly high percentage of desiccant technology in both 2014 (60%) and 2022 (65%) was that dehumidification is essential to avoid condensation at radiant surfaces during the summer season in Japan, which becomes hot and humid. Natural ventilation had a few responses for both 2014 and 2022, and the reason was expected to be the difficulty in controlling window opening and radiant surface temperatures to avoid condensation.



\* Percentage of respondents for each auxiliary systems and renewable resources

Figure 2-3. Auxiliary systems and renewable resources which were preferred in combination with radiant systems. (Multiple answers allowed)

Figure 2-4 shows that the percentage of respondents for concerns and difficulties of designing radiant systems (multiple answers allowed). Answers were obtained from 24 respondents in 2014 and 31 respondents in 2022, respectively. The category with the highest response rate was “L: high initial cost”, both in 2014 (n=20, 83%) and 2022 (n=23, 74%). For both 2014 and 2022, categories “B: slow response time” and “C: response to fluctuation and uneven distribution of cooling load” were selected by 40-50% of the respondents. In categories “G: latent cooling, humidity control” and “H: preventing condensation”, 40% of the respondents in 2022 indicated that there were concerns and difficulties of a condensation problem. The number of respondents who answered “I: control” decreased from 25% in 2014 to 6% in 2022. Probably due to the learning effect, MEP engineers have a better understanding of how to control radiant systems.

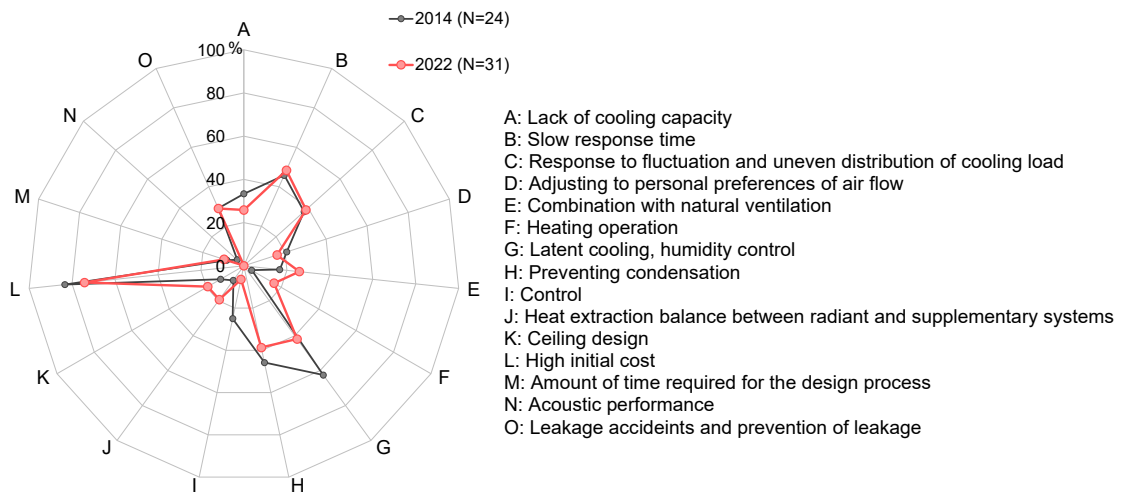


Figure 2-4. Percentage of respondents for concerns and difficulties of designing radiant systems (multiple answers allowed)

Table 2-5 shows the knowledge gaps in designing radiant systems. Answers were obtained from 24 respondents in 2014 and 31 respondents in 2022, respectively. For the lack of design guidelines, recommended design values, and design methods for radiant systems, 4 respondents in 2014 and 9 in 2022 answered. One of the respondents was unsure about whether to control by room temperature or surface temperature, and how to cover low circulating air volume. The REHVA guideline [12] and ISO 11855 [42] for radiant heating and cooling systems describes how to control radiant systems based on room temperature. These standards and guidelines recommended that it is preferable to control based on the operative temperature in the occupied area. Previous studies have investigated the optimal position, shape, size, and color of the room temperature sensor to express heat transfer between sensor and space similarly as for a person [12] [43-45]. For the knowledge gaps related to the effects of radiant systems on the human body, and occupant thermal comfort, many designers indicated that there was a lack of general knowledge about radiant systems with thermal mass, such as TABS. One of the reasons could be that there are currently no TABS guidelines for Japanese design practices (e.g., preparing for an earthquake, combination with raised floor). However, it must be noted that the ISO 11855 standard provides a method for evaluating the indoor comfort of TABS [46], as well as design and sizing methods [47]. There was also a request for

guidelines on how to determine the indoor setpoint for radiant systems, in contrast to the conventional all-air systems. One of the Japanese office buildings used the equivalent temperature (ET) to control radiant ceiling panels [48,49].

Table 2-5. Knowledge gaps in designing radiant systems

What do you think about the lack of knowledge in designing radiant systems?		Number of respondents *	
		2014 (N=24)	2022 (N=31)
<b>Design guidelines, recommended design values (indoor environmental conditions/panel surface temperature), and design method for radiant systems</b>			
Comments (2022)	· There are many examples of heating, such as floor heating, but it would be good to have more design guidelines for cooling.	4 (17%)	9 (29%)
	· Until a few years ago, a certain manufacturer had a well compiled design guideline, but the current status is unknown.		
	· Whether to control by room temperature or surface temperature, how to cover low circulating air volume, etc.		
<b>Effects of radiant systems on the human body, occupant thermal comfort, etc.</b>			
Comments (2022)	· It is difficult to evaluate thermal comfort for radiant wall systems		
	· Fluctuation of heat flux in case of TABS.		
	· There are no design guidelines of radiant systems for indoor thermal comfort, so there is still a needed to verify indoor thermal comfort in the operation phase by the field measurement.	5 (20%)	12 (39%)
	· Radiant systems should have a different setpoint temperature compared to all-air systems, but because there are no standards, there is a tendency for operators to overcool or overwarm the indoor environment.		
	· Dynamic thermal performance of TABS, including its heat transfer, are very difficult to predict.		
	· The large thermal capacity of concrete may make it difficult to find a control method.		
<b>Heat flux and the indoor environment when radiant systems are in operation</b>		5 (20%)	3 (10%)

\* ( %) indicates the percentage of responses for each question to all respondents.

## 2.5 Discussion

Installation surveys of radiant systems and expert interviews were conducted to identify what designers require to design radiant systems and to investigate any new issues or perspectives in practice. Hence, topics that were commonly discussed in the surveys and interviews were discussed below.

### Country-specific Factors

Results of installed survey indicated that there were less than 10 building projects with radiant systems each year before the 2010s, but since 2016, radiant systems were continuously installed in 60 to 80 building projects per year. It should be noted that this survey was a collection of building projects from two major Japanese radiant systems manufacturers and from research papers. Since the 2010s, the number of net zero energy buildings in Japan has increased, and this is expected to contribute to a further increase in the installation of radiant systems. Many MEP designers pointed out the high initial cost of radiant systems regardless of the interview period (2014 or 2022).

This study showed that air-based radiant systems were installed in 43% of the total in the past 20 years. In Japan, where earthquakes often occur, water-based radiant systems are sometimes avoided because of the risk of water leakage. Embedding TABS piping directly into the structure of the building are also not common in Japan in terms of maintenance, replacement, and the risk of water leakage by earthquakes.

### Difficulty of designing radiant systems

From the interview survey, more than half of the MEP designers answered that it was easier to design radiant systems compared to the 2010s. The publication of the standard of radiant ceiling panels and the increase in case studies have helped to design and control radiant systems more easily. The decrease in internal heat gain of the building due to the widespread use of Light-Emitting Diode (LED) lighting [50] and personal computers [51] has also contributed to the increase in the installation of radiant systems. Studies documenting the benefits and limitations of the desiccant dehumidification system and coupling of the radiant system with renewable sources have helped in the broader use of radiant systems as well. Compared to the all-air system, which typically uses a chilled water temperature of 7°C, radiant systems have the potential to use chilled water of 16 to 20°C for cooling, which is compatible with renewable sources, such as well water and geothermal heat. One research conducted a comparative case study of radiant ceiling panels that use well water and the potential for their installation in Japanese office buildings in different regions [52]. The results showed that more floor area could be cooled with well water as the heat source, in areas with cooler outdoor climates. the lower well water temperature, and the high pumping allowance.

As shown in the Table 2-5, many MEP designers commented on the knowledge gap in the research area of thermal mass of the building represented by TABS. Radiant ceiling panels and radiant floor systems are relatively easy to design and size because the heating and cooling capacities under standard conditions are described in the manufacturers' catalogues. On the other hand, it is difficult to determine how much heating and cooling capacity to expect from TABS. The heating

and cooling capacity also depends on the facade, structure of the radiant surface, and the occupancy behaviors. It would be beneficial to develop guidelines and calculation tools of TABS to bridge the gap between research and practice.

### **Building Decarbonization and radiant systems**

There were also many comments on the topic of building decarbonization, which was not present in the survey conducted in 2014. There were divided opinions within the respondents on whether or not radiant performs well in terms of whole life carbon. One research conducted a comparative case study of the whole life carbon of a radiant system and an all-air system in a non-residential Danish building [53]. Results showed that implementing TABS reduced operational carbon (-0.75) and increased embodied carbon (+0.21) compared to a packaged variable air volume system. Although implementing TABS could lower the floor height, reducing ducting, and downsize the HVAC equipment, installing the pipework for TABS increased the embodied carbon in the Danish case study. Similar comparisons should be considered in Japan, as calculation boundaries are different for each country, e.g., carbon emission factors for electricity and gas, selection of life cycle modules, accounting refrigerant leakage [54], and climatic conditions.

## **2.6 Conclusions**

The objective of the study was to examine the current trend in the design and control of radiant systems in practice in Japan. A survey of existing building projects and expert interviews and questionnaires of radiant systems in Japan were conducted from 2021 to 2022. The conclusions are as follows:

- In Japan, 661 buildings with radiant systems have been constructed, as of 2020. Radiant ceilings were installed in 69% of the buildings, and radiant floors were installed in 30%. In terms of the heat transfer fluid, 56% of the buildings had water-based (hydronic) radiant systems, and 43% were air-based. Since 2017, the number of installations of the radiation system had remained between 70 and 80 projects. If regulations regarding refrigerant leakage become stricter in the future, radiant systems that use less high-GWP refrigerants compared to packaged systems may be installed in even more buildings.
- 79% of all respondents answered that the use of radiant systems will continue to increase in the future.
- 54% of all respondents answered that it has become easier to design radiant systems compared to the 2010s, due to the development of national standards and guidelines and the increased number of implementations in new building projects. Many MEP engineers emphasized that radiant systems could provide energy savings and thermal comfort for buildings.
- Regarding the impact of building decarbonization on the installation of radiant systems, 53% of the respondents answered that it would impact the installation of radiant systems. Those who answered “high impact” asserted that radiant systems were becoming a powerful tool for building decarbonization, specifically in reducing operational energy and carbon emissions. Additionally, other respondents pointed out that radiant system would be beneficial or not in terms of whole-life carbon emissions.
- Based on the above, from next chapters, several studies were conducted focusing on indoor thermal comfort and



carbon emission of radiant systems.

## References

- [1] IPCC DDC Glossary, Intergovernmental Panel on Climate Change, 2020. [https://www.ipcc-data.org/guidelines/pages/glossary/glossary\\_c.html](https://www.ipcc-data.org/guidelines/pages/glossary/glossary_c.html) (accessed August 30, 2023)
- [2] International Energy Agency, Global energy and process emissions from buildings, including embodied emissions from new construction, 2021. <https://www.iea.org/data-and-statistics/charts> (accessed August 30, 2023)
- [3] ISO/TS 23764:2021, Methodology for achieving non-residential zero-energy buildings (ZEBs), International Organization for Standardization, 2021.
- [4] ANSI/ASHRAE/IES Standard 90.1-2019, Energy Standard for Buildings Except Low-Rise Residential Buildings, ASHRAE, 2019.
- [5] 5EN 1597:2011, Sustainability of construction works – Assessment of environmental performance of buildings – Calculation method, European Committee for Standardization, 2011.
- [6] O.B. Kazanci, Low Temperature Heating and High Temperature Cooling in Buildings, PhD Thesis, Kgs. Lyngby: Technical University of Denmark, 2016.
- [7] EN14240, Ventilation for buildings - Chilled ceilings - Testing and rating, European Committee for Standardization, 2004.
- [8] EN 1264-5:2021, Water based surface embedded heating and cooling systems - Part 5: Determination of the thermal output for wall and ceiling heating and for floor, wall and ceiling cooling, European Committee for Standardization, 2021.
- [9] ISO 11855-1:2021, Building environment design — Embedded radiant heating and cooling systems — Part 1: Definitions, symbols, and comfort criteria. International Organization for Standardization, 2021.
- [10] K. Rhee, K. W. Kim, A 50 year review of basic and applied research in radiant heating and cooling systems for the built environment. *Building and Environment*. 2015; 91: 166-190. <https://doi.org/10.1016/j.buildenv.2015.03.040>
- [11] H. E. Feustel, C. Stetiu, Hydronic radiant cooling — preliminary assessment. 1995; 22: 193-205. [https://doi.org/10.1016/0378-7788\(95\)00922-K](https://doi.org/10.1016/0378-7788(95)00922-K)
- [12] J. Babiak, B.W. Olesen, D. Petras, Low temperature heating and high temperature cooling. REHVA guidebook. 2007.
- [13] S. Corgnati, M. Perino, G. Fracastoro, P. Nielsen, Experimental and numerical analysis of air and radiant cooling systems in offices. *Building and Environment*. 2009; 44: 801-806. <https://doi.org/10.1016/j.buildenv.2008.05.022>
- [14] B. Lin, Z. Wang, H. Sun, Y. Zhu, Q. Ouyang, Evaluation and comparison of thermal comfort of convective and radiant heating terminals in office buildings, *Building and Environment*, 2016; 106: 91-102. <https://doi.org/10.1016/j.buildenv.2016.06.015>
- [15] J. Feng, S. Schiavon, F. Bauman, Cooling load differences between radiant and air systems. *Energy and Buildings*. 2013; 65: 310-321. <https://doi.org/10.1016/j.enbuild.2013.06.009>
- [16] B. W. Olesen, Possibilities and limitations of radiant floor cooling. *ASHRAE Transaction*, 1997; 103: 42–48.

- [17] K. Zhao, X. Liu, Y. Jiang, On-site measured performance of a radiant floor cooling/heating system in Xi'an Xianyang International Airport. *Solar Energy*. 2014; 108: 274–286. <https://doi.org/10.1016/j.solener.2014.07.012>
- [18] J. Pantelic, S. Schiavon, B. Ning, E. Bourdakos, P. Raftery, F. Bauman, Full scale laboratory experiment on the cooling capacity of a radiant floor system. *Energy and Buildings*. 2018; 170: 134–144. <https://doi.org/10.1016/j.enbuild.2018.03.002>
- [19] K. Shindo, J. Shinoda, K. Ikai, T. Takenaka, S. Tamura, T. Kobori, S. Tanabe, Application of a slit ceiling based on thermally activated building systems in a daylight-harvesting office space with direct solar radiation. *Japan Architectural review*. 2021; 5: 548-559. <https://doi.org/10.1002/2475-8876.12292>
- [20] K. Rhee, B.W. Olesen, K. W. Kim, Ten questions about radiant heating and cooling systems. *Building and Environment*. 2017; 112: 367-381. <https://doi.org/10.1016/j.buildenv.2016.11.030>
- [21] J. Shinoda, O. B. Kazanci, S. Tanabe, K. Hidari, H. Watanabe, Y. Takahashi, Room-side and Plenum-side Cooling Prediction of Suspended Radiant Ceiling Panels. *Proceedings of CLIMA 2022 Conference*. 2022. <https://doi.org/10.34641/clima.2022.137>
- [22] K. Sato, E. Kataoka, S. Horikawa, Thermo Active Building System creates comfort, energy efficiency. *ASHRAE Journal*. 2020; 62.
- [23] N. Hirasuga, S. Kato, T. Akimoto, Y. Sakamoto, Comparing convection vs. radiant air-conditioning systems in office. *ASHRAE Journal*. 2023; 65.
- [24] B.W. Olesen, F. C. Dossi, Operation and control of activated slab heating and cooling systems. *CIB World Buildings Congress*. 2004.
- [25] P. Simmonds, S. Holst, S. Reuss, W. Gaw, Using radiant cooled floors to condition large spaces and maintain comfort conditions. *ASHRAE Transact*. 2000; 106: 695–701.
- [26] K. Zhao, X. Liu, Y. Jiang, Application of radiant floor cooling in a large open space building with high-intensity solar radiation. *Energy and Buildings*. 2013; 66: 246–257. <https://doi.org/10.1016/j.enbuild.2013.07.014>
- [27] S. Mori, M. B. Barova, D. Zhecho, A. K. Melikov, S. Tanabe, Radiant Ceiling Panels Combined with Localized Methods for Improved Thermal Comfort of Both Patient and Medical Staff in Patient Room. *Proceedings of 9th International Meeting for manikins and Modeling*. 2012.
- [28] Report of HVAC Systems adapting to New Design Conditions [in Japanese], The Society of Heating, Air-Conditioning and Sanitary Engineers of Japan. 2016.
- [29] G. Paliaga, F. Farahmand, P. Raftery, J. Woolley, TABS Radiant Cooling Design & Control in North America: Results from Expert Interviews. 2017.
- [30] IEA EBC Annex 89, Ways to Implement Net-zero Whole Life Carbon Buildings. IEA. <https://annex89.iea-ebc.org/> (accessed August 30, 2023)
- [31] WBCSD, Net-zero buildings Where do we stand?. 2021.
- [32] ASHRAE, ASHRAE task force for building decarbonization (TFBD). <https://www.ashrae.org/about/ashrae-task-force-for-building-decarbonization> (accessed August 30, 2023)
- [33] IEA EBC Annex 80, Resilient Cooling of Buildings. IEA. <https://annex80.iea-ebc.org/> (accessed August 30, 2023)

- [34] Technical papers of annual meeting; Architectural Institute of Japan
- [35] Technical Papers of Annual Meeting; The Society of Heating, Air-Conditioning and Sanitary Engineers of Japan. <https://www.jstage.jst.go.jp/browse/shasetaikai/-char/en> (accessed August 30, 2023)
- [36] ARCH Cooling and Heating - Testing and Rating Standard (CHTRS), The Association of Radiant Cooling and Heating systems of Japan (ARCH), 2022. <http://www.archsj.jp/img/file35.pdf> (accessed August 30, 2023)
- [37] D. Bogatu, O. B. Kazanci, B. W. Olesen, An experimental study of the active cooling performance of a novel radiant ceiling panel containing phase change material (PCM). *Energy and Buildings*. 2021; 110981. <https://doi.org/10.1016/j.enbuild.2021.110981>
- [38] F. Causone, S. Corgnati, M. Filippi, B. W. Olesen, Solar radiation and cooling load calculation for radiant systems: Definition and evaluation of the direct solar load. *Energy and Build.* 2010; 42(3):305–314.
- [39] Construction Economics and Statistics Research, Building Construction Statistics Survey in Japan, Policy Bureau of Ministry of Land, Infrastructure and Transport in Japan. <https://www.mlit.go.jp/report/press/content/kencha405.pdf> (accessed August 30, 2023)
- [40] O. Zaki, R. Mohammed, O. Abdelaziz, Separate sensible and latent cooling technologies: A comprehensive review, *Energy Conversion and Management*, 2022; 256(15): 115380.
- [41] Building design standard of mechanical, electrical, and plumbing systems in Japan, Government Buildings Department of Ministry of Land, Infrastructure and Transport in Japan. <https://www.mlit.go.jp/gobuild/content/001390961.pdf> (accessed August 30, 2023)
- [42] ISO 11855-6:2018, Building environment design — Embedded radiant heating and cooling systems — Part 6: Control, International Organization for Standardization, 2018.
- [43] A. Simone, J. Babiak, M. Bullo, G. Landkilde, B.W. Olesen, Operative temperature control of radiant surface heating and cooling systems, *Proceedings of Clima 2007 Wellbeing Indoors*, 2007.
- [44] J. Shinoda, A. Mylonas, O. B. Kazanci, S. Tanabe, B. W. Olesen, Differences in temperature measurement by commercial room temperature sensors: Effects of room cooling system, loads, sensor type and position, *Energy and Buildings*. 2021; 231: 15. <https://doi.org/10.1016/j.enbuild.2020.110630>
- [45] E. Teitelbaum, K. W. Chen, F. Meggers, H. Guo, N. Houchois, J. Pantelic, A. Rysanek, Globe thermometer free convection error potentials, *Scientific Reports*, 2020; 2652: 10. <https://doi.org/10.1038/s41598-020-59441-1>
- [46] ISO 11855-2:2021, Building environment design — Embedded radiant heating and cooling systems — Part 2: Determination of the design heating and cooling capacity, International Organization for Standardization, 2021.
- [47] ISO 11855-2:2021, Building environment design — Embedded radiant heating and cooling systems — Part 4: Dimensioning and calculation of the dynamic heating and cooling capacity of Thermo Active Building Systems (TABS), International Organization for Standardization, 2021.
- [48] K. Hidari, Y. Takahashi, T. Nobe, Study on the City Hall in SDGs Future City for Zero Energy Building Part 8. Preparation and verification of MRT estimation equation used to calculate Equivalent Temperature when controlling radiant heating and cooling system with Equivalent Temperature, *Technical Papers of Annual Meeting The Society of Heating, Air-Conditioning and Sanitary Engineers of Japan* 2021.
- [49] T. M. Madsen, Measurement of thermal comfort and discomfort, Indoor Climate Danish Building Research Institute,

1979: 591-613.

- [50] Y. Narishima, J. Munakata, T. Iwata, T. Taniguchi, E. Mochizuki, A study on the changes of light environment and evaluations by workers in Japanese office, *The Architectural Institute of Japan's Journal of Environmental Engineering*, 2016; 81: 49-56. <https://doi.org/10.3130/aije.81.49>
- [51] A. Danowitz, K. Kelley, J. Mao, J. P. Stevenson, M. Horowitz, CPU DB: Recording Microprocessor History: With this open database, you can mine microprocessor trends over the past 40 years, 2012; 10. <https://queue.acm.org/detail.cfm?id=2181798>
- [52] H. Ito, I. Hasegawa, Evaluation of Effectiveness for Radiative Cooling and Heating System Utilizing Underground Water No.1: Study on Potential of Introduction for Office Buildings, *Technical Papers of Annual Meeting The Society of Heating, Air-Conditioning and Sanitary Engineers of Japan* 2018. [https://doi.org/10.18948/shasetaikai.2018.3.0\\_321](https://doi.org/10.18948/shasetaikai.2018.3.0_321)
- [53] K. Shindo, J. Shinoda, O. B. Kazanci, D. O. Bogatu, S. Tanabe, B.W. Olesen, A comparative study on the embodied carbon and operational carbon of a radiant cooling system and an all-air system, 18th Healthy Buildings Europe Conference, 2023.
- [54] ANSI/ASHRAE/IES Standard 228-2023, Standard Method Of Evaluating Zero Net Energy And Zero Net Carbon Building Performance, ASHRAE, 2023.

## **Chapter 3:**

# **Application of a slit ceiling on thermally activated building system in a daylight-harvesting office space**

### **Abstract**

In recent years, an increasing number of offices have actively harvested daylight for the well-being of occupants. However, if large windows are provided for daylight harvesting, the amount of solar heat gain increases, leading to poor energy efficiency and deteriorated indoor environment. Therefore, the objective of this study was to verify the radiant cooling effect of ceiling slits in an office building based on thermally activated building systems to achieve both daylight harvesting and solar heat removal through field measurements. In this study, the radiant cooling capacity of a slit ceiling and the indoor radiant environment were measured in a research facility in Fukui City, Japan, during spring (16–30 March) and summer (17–31 August) in 2020.

### **KEYWORDS:**

Daylight use, Solar radiation, Radiant cooling capacity, Surface heat flux, Radiant Asymmetry, TABS

### 3.1 Introduction

The effects of solar radiation on indoor environmental quality and occupants' well-being have received increasing interest in recent years [1], revealing that a balance should be established between daylight harvesting and reducing solar load. The larger the window size for daylight harvesting, the higher the increase in solar heat gain. In this context, the following problems should be solved: reduced energy efficiency due to increased solar radiation and non-uniform radiation in the indoor environment due to high temperature of the inner glass of windows when daylight is introduced through a skylight.

To deal with these problems, radiant cooling systems are used to introduce daylight while ensuring energy efficiency and indoor thermal comfort [2]. Radiant heating and cooling systems are systems that directly cool and heat floors and ceilings and use longwave radiation and natural convection for heating and cooling. Generally, radiant ceiling panels are installed in office spaces, and the internal heat from the occupants, equipment, and lighting are extracted by the cooled surface. Previous studies have reported enhanced cooling capacity of radiant cooling systems owing to the absorption of solar radiation at cooled surfaces [3]; this characteristic can increase the design flexibility of windows and facades in daylight harvesting spaces.

The objective of this study was to verify the radiant cooling effect of a slit ceiling that can introduce daylight into and remove solar heat from a research building. In this study, the radiant cooling effect was defined as the absorption and removal of solar heat by the cooled surface and thermal comfort in the office space. Midterm and summer measurements were conducted in the office building to verify the performance of the cooling surface in removing solar heat and determine the thermal environment of the office space. The radiant cooling effect of the slit ceiling was quantitatively evaluated to ensure an energy-saving and comfortable office space and verify the usefulness of the radiant cooling system under direct solar radiation conditions.

### 3.2 Literature review of radiant cooling capacity enhancement under direct solar radiation

#### 3.2.1 Radiant cooling capacity enhancement under direct solar radiation

Table 3-1 lists the cooling capacity enhancement under high-intensity solar radiation as reported in literature. Previous studies have reported a significant increase in radiant cooling capacity owing to absorption of solar radiation on the cooling surfaces. Several case studies have investigated radiant floor cooling in large glass-fronted spaces, such as atriums and airports, which are sensitive to solar radiation. These studies have primarily explored the difference in the radiant cooling capacity with and without absorption of solar radiation. Olesen [3] showed that radiant floor cooling capacity reaches 100–150 W/m<sup>2</sup> when the floor is exposed to direct solar radiation.

Simmonds et al. [4] reported that the average radiant floor cooling capacity reached 70–80 W/m<sup>2</sup> for mixed loads at Bangkok International Airport. The efficient removal of solar radiation by radiant cooling significantly affects ventilation and air-conditioning systems (Simmonds et al. 2006) [2]. Causone et al. [5,6] stated that the increase in the cooling capacity of solar-exposed radiant systems occurs due to the direct removal of a fraction of the solar heat gain from the cooled surface before contributing to the room load, which is defined as the direct solar load (DSL). The ratio of the DSL to total transmitted solar heat gain is known as the F ratio. Compared to the conventional calculation method, when the DSL is considered in load calculations and system sizing, the room load of the auxiliary air and/or ventilation system can be reduced.

Because radiant cooling and heating systems are usually driven by convection and longwave radiative heat transfer, the upper limit of the cooling capacity in a radiant system is determined by the difference in temperature between the radiant surface and room. In hot and humid climates, the lower temperature limit of the radiation surface is also limited due to condensation. DSL is the amount of solar radiation absorbed by the cooling surface and is independent of the cooling surface temperature. Therefore, the absorption of solar radiation at the cooling surface increases the radiant cooling capacity within the capacity of the heat-source equipment, supply temperature, and flow rate.

Table 3-1. Cooling capacity enhancement under high-intensity solar radiation reported in literature

Author(s)	Year	Method	Floor Area (m <sup>2</sup> )	Radiant Surface Type	Supply Water Temperature (°C)	Time (h)	Radiant Cooling Capacity (W/m <sup>2</sup> )		
							Without Solar Radiation	Under Solar Radiation	Description
Olesen [3]	1997	Literature review	–	Floor	15, 20, and 25	–	30–50	148, 129, and 107	Peak value
Simmonds et al. [4]	2000	Simulation	1,082	Floor	13	–	–	83	Peak value
Causone et al. [5][6]	2010	Simulation	56	Ceiling	–	13:00	98	108	Peak value
De Carli et al. [7]	2011	Simulation	23	Floor	20	13:00–14:00	–	130	Peak value
						17:00	27	–	Mean value
						–	35–40 Office	60–120 Large space	Peak value
Zhao et al. [8]	2013	Simulation	9,600	Floor	18	–	35–40 Office	60–120 Large space	Peak value
Zhao et al. [9]	2014	Field measurement	15,000	Floor	18	13:50–16:00	35–40	130–140	Peak value
Feng et al. [10]	2016	Simulation	48	Floor	12, 15, and 18	–	35.6–44.0 $\Delta T_h = 10^\circ\text{C}^*$	130–140 $\Delta T_h = 10^\circ\text{C}^*$	Peak value
Pantelic et al. [11]	2018	Chamber	62	Floor	12, 15, and 18	9:00–21:00	30–40	95–115	Peak value

\*  $\Delta T_h$  the temperature difference between the cooling medium and the room temperature. [12]

### 3.2.2 Issues arising during cooling of radiant surfaces under solar radiation

Radiant heating and cooling systems are classified according to their radiant surface, heat transfer medium, and radiant surface structure. Perimeter zones in atriums, large spaces, and office spaces are also listed as spaces that are susceptible to solar radiation. Several studies have been conducted on radiant cooling systems that are introduced into spaces susceptible to solar radiation, wherein the radiant surface is the floor, and its structure is a thermally activated building system (TABS) [13]. Therefore, to clarify the novelty of this study, we present a list of issues associated with solar radiation removal using TABS in spaces that are significantly affected by solar radiation.

#### (1) Solar heat gain

Design methods for radiant cooling in solar radiation environments have not been established because previous studies are primarily based on numerical calculations and lack detailed measured data. Moreover, the peak values of the cooling capacity, which affect equipment selection, vary across different literature. The variation in cooling capacity is mostly due to changes in solar heat gain, but factors that may lead to such changes include building facades (primarily aperture and radiant surface layout), season, time of day, and weather conditions.

#### (2) Radiant surface heat flux and heat extraction rate

Previous studies have confirmed that the surface heat flux and heat extraction rate are different for cooled surfaces with large heat capacities [7]. As shown in Table 3-1, enhanced radiant cooling capacity under direct solar radiation has been reported based on measured and numerical results; however, most of these studies considered the surface heat flux as the radiant cooling capacity. When designing an HVAC system, the radiant cooling capacity should be evaluated as the heat extraction rate. However, most existing studies did not distinguish between surface heat flux and heat extraction rate, and only surface heat flux measured by heat flow sensors was used to evaluate the cooling capacity, even if the cooled surface was a TABS or ESS.

An advantage of the TABS is peak load shifting by heat capacity. However, previous studies have not quantitatively verified whether a TABS is effective for high-intensity thermal loads, such as solar radiation, or determined the appropriate heat capacity of the cooled surface.

#### (3) Solar radiation absorption rate of cooled surface

The radiant cooling capacity varies significantly depending on the solar radiation absorption rate of the cooled surface. De Carli et al. [7] showed that the radiant cooling capacity reaches 130 W/m<sup>2</sup> when solar radiation is absorbed and 260 W/m<sup>2</sup> when the cooled surface is a low-reflectance material. However, their study did not clarify whether the surface temperature also varies with the solar radiation absorption rate of the cooling surface and its effect on heat removal by convection and radiative heat transfer.

#### (4) Supply water temperature and water flow rate



Radiant panels and TABS can use chilled water at 16–20°C, resulting in high energy savings. The flow rate of TABS is usually determined to achieve an inlet/outlet water temperature difference of 3.0–5.0°C to ensure efficient heat treatment. Additionally, the difference between indoor temperature and supply water temperature should be small to prevent condensation. However, these determinations of supply water temperature and flow rate do not account for solar absorption at the cooled surface.

Radiant heating and cooling systems control the temperature of ceilings, walls, floors, and other surfaces by longwave radiative and convective heat transfer. Therefore, the radiant cooling capacity depends on the surface temperature. However, the absorption of solar radiation at the cooling surface occurs independently of the surface temperature, resulting in a heat removal process that differs from that of a normal radiant cooling system. Thus, the appropriate water supply temperature, water supply flow rate, and water supply schedule must be considered in such systems.

### 3.2.3 Relationship to this study

Based on the reviewed literature, this study verified the cooling characteristics of radiant surfaces through a field measurement by taking the surface heat flux and heat extraction rates. During the actual measurement period, the water flow rate of the radiant cooling system was set as constant, and the effect of the solar heat gain on the radiant cooling capacity was examined.

## **3.3 Methods**

### 3.3.1 Outline of the research building

Table 3-2 presents the dimensions and other details of the building used in this research. The office building is a research facility located in Fukui City, Japan [14,15]. The building was constructed to serve as a space for global chemical product development and manufacturing companies to develop innovative ideas by encouraging the active exchange of information, discussions, and presentations by researchers, and by providing hospitality and interaction for visitors from Japan and abroad. The building has a floor area of 2,839 m<sup>2</sup>, total floor area of 7,496 m<sup>2</sup>, and a four-story steel reinforced concrete structure (partially steel structure).

Table 3-2. Building outline

---

Location	Fukui, Japan
Building use	Office, research facility
Structure type	Steel reinforced concrete construction (SRC)
Floor area/Total floor area	2,839 m <sup>2</sup> /7,496 m <sup>2</sup>
Floors	Four

---

Figure 3-1 shows the sectional view of the office building [16], Figure 3-2 shows the interior of the building, and Figure 3-3 shows a sectional view of the TABS ceiling slits. The atrium space has a height difference of approximately 15 m from the first to the top of the fourth floor, and the various office spaces created by the randomly sprung slabs are known as “common spaces”. The architectural design of the room layout, where the central atrium office space was surrounded by a perimeter laboratory space, resulted in the top light being installed on the third office space for daylight harvesting. The daylight is reflected and diffused by slits in the ceiling at the bottom of the atrium and poured into the office space. Because Fukui experiences few hours of sunlight annually, the office space has a large skylight to maximize daylight. TABS were also installed on some of the ceiling slits (solar heat removal system) and daylight harvesting walls of the building. The solar heat removal system directly removes the solar heat and uses well water for cooling, resulting in high energy efficiency. In addition to TABS ceiling slits and harvest walls, radiant floor systems with underfloor air distribution systems were installed in the atrium office spaces on the third floor. A natural ventilation system using both horizontal and gravity ventilation was designed by taking advantage of the prevailing winds in the north-south direction and the height of the atrium office space. In this study, field measurements were conducted on the TABS ceiling slits and harvesting walls, the atrium office space on the third floor, and the corridor space on the fourth floor of the building in Figure 3-1.

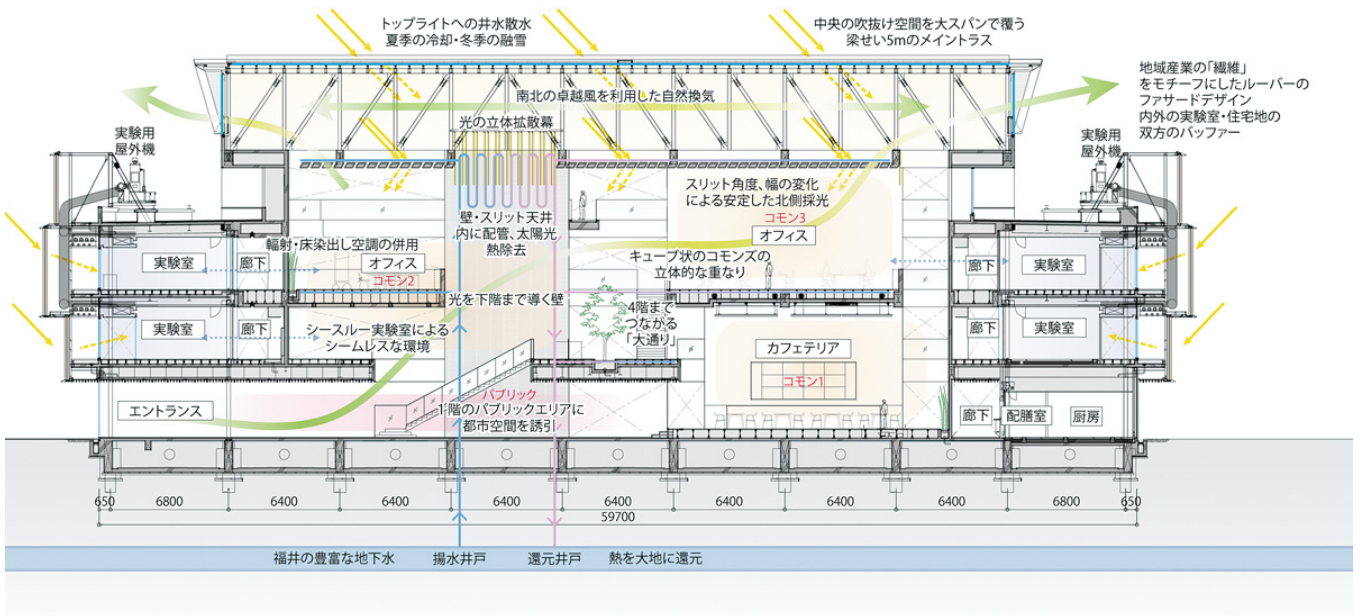


Figure 3-1. Sectional view of the office building selected in this study [16]



Figure 3-2. Interior view of the office building selected in this study

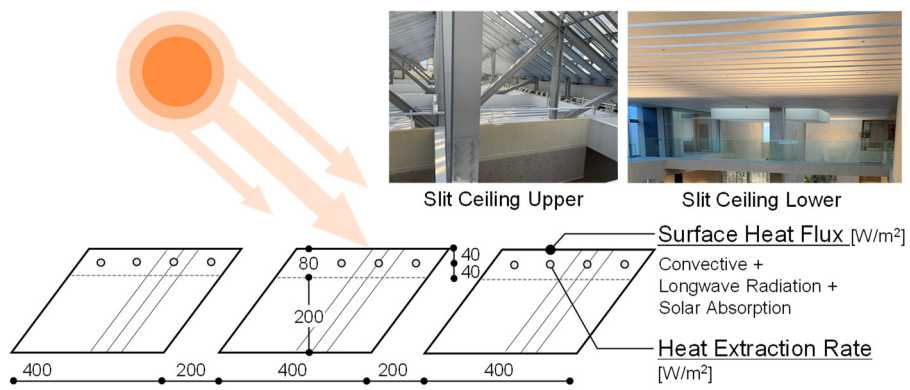


Figure 3-3. Sectional view of the slit ceiling in the building



3.3.2 Method

Table 3-3 presents the measurement period and Table 3-4 lists the operational pattern of the radiant cooling system installed in the office space. The midterm measurement was conducted from 16–30 March 2020, and the summer measurement was conducted from 17–31 August 2020. Field measurements were conducted on the rooftop floor (RF), where TABS [13] ceiling slits were installed, and on the second through fourth floors, where the TABS floor and walls were installed.

Table 3-3. Measurement period

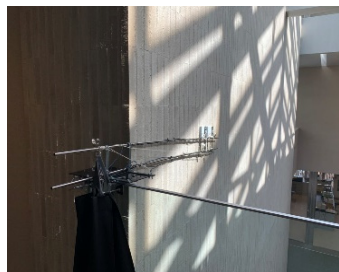
Measurement period (day and date)
Monday, 16 March 2020 – Monday, 30 March 2020
Monday 17 August 2020 – Monday, 31 August 2020

Table 3-4. Operational pattern of radiant cooling system

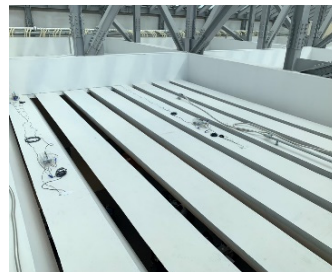
	0	2	4	6	8	10	12	14	16	18	20	22	0	Total Operative Time (h)
Radiant cooling system • Slit ceiling • Daylight harvesting wall														12 (6:00–18:00)
Radiant cooling system • 2F–3F														12 (7:00–19:00)
Under floor air distribution system • 2F–3F														12 (7:00–19:00)

Figures 3-5 presents the thermal environment measurement. In the midterm measurement, the solar heat removal performance of a daylight harvesting wall on 4F was measured. Because normally air conditioning was not used during this period, chilled water was not pumped to the TABS ceiling slits on the rooftop floor, but only to the daylight harvesting wall on 4F. During this period, the water was pumped to the daylight harvesting wall from 6 a.m. to 6 p.m. on weekdays at a supply water temperature of 18°C and a water flow rate of 75 L/min.

In the measurement conducted during summer, the solar heat removal performance of TABS ceiling slits on the rooftop floor and the thermal environment of the office space were measured. During this measurement period, the chilled water was pumped to the daylight harvesting wall at the same time and temperature on weekdays but at a water flow rate of 65 L/min. Operation hours of radiant heating and cooling on the third to fourth floors (3F and 4F) and underfloor air distribution (UFAD) on the third floor were from 7 a.m. to 7 p.m.



(A) Harvest wall



(B) Ceiling slits



(C) Thermal environment measurement devices








(D) Thermal image measurement devices

Figure 3-5. View of the thermal environment measurement

Table 3-5 lists the measured parameters and Figure 3-6 shows the sectional view and measurement points in the study area. Previous studies have reported that the behaviors of (1) the radiant surface heat flux and (2) heat extraction rate are different for cooled surfaces with large cooling capacities when receiving solar radiation; therefore, both parameters were measured separately. A heat flow sensor was used to measure the radiant surface heat flux, and a thin type of solar radiometer was used to measure the amount of heat received from solar radiation on the cooling surface. The heat extraction rate was evaluated from the inlet and outlet water temperatures and the water flow rate at the secondary side of the heat exchanger in the solar heat removal system was obtained from the Building Energy Management System (BEMS) data.

Table 3-5. Measured parameters

Symbol	Floor level	Parameter	Type	Resolution/accuracy	Time interval (min)
	RF	Surface heat flux [W/m <sup>2</sup> ]	M55A, THERMIC 2300A (ETODENKI)	0.1 W/m <sup>2</sup> ±0.02%	10
	4F and RF	Global solar irradiance [W/m <sup>2</sup> ]	Low-profile pyranometers ML-02 (400nm-1100nm, EKO) THERMIC 2300A (ETODENKI)	0.1 W/m <sup>2</sup> ±0.02%	10
	2F-4F RF	Air temperature [°C] Globe temperature [°C] Relative humidity [%] Illuminance [lux]	TR-74Ui (T&D)	±0.5°C ±0.5°C ±5%RH (25°C, 50%RH) ±5%	10
	3F	Air temperature [°C] Globe temperature [°C] Relative humidity [%] Air velocity [m/s]	PMV meter AM101 (KYOTO ELECTRONICS)	±0.5°C (15-35°C) ±0.5°C (15-35°C) ±3%RH (20-80%RH) ±0.1 m/s (0-1 m/s) ±0.5 m/s (1-5 m/s)	30
	3F	Thermal image	InfRec ThermoGEAR (Thermography corporation)	0.04°C/±2%	30

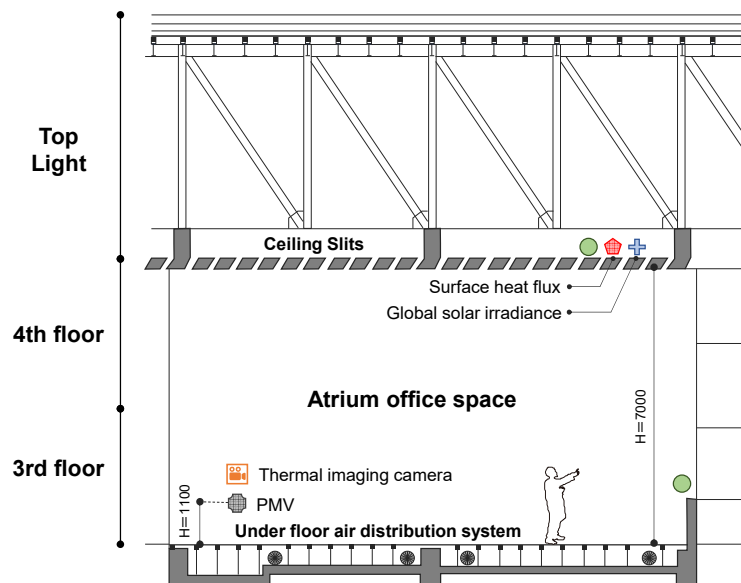


Figure 3-6. Sectional view and measurement points



To verify the thermal environment of the office space, temperature and humidity measurements were conducted on each floor. Moreover, a Predicted Mean Vote (PMV) meter was installed in the third-floor office space, which is highly affected by longwave radiation from the slit ceiling, and the air temperature, radiation temperature, relative humidity, and air velocity were measured. In addition, the temperature of the cooling surface was determined through thermal images of the TABS-based slit ceiling. The illuminance of the office space from second floor to fourth floor was measured using an illuminance meter.

### 3.4 Results

#### 3.4.1 Midterm field measurement

The following subsections present the results of the measurements conducted at 4F harvesting wall on Friday, 26 March 2020, when the daytime weather was clear during the two-week measurement period.

##### (1) Solar radiation and surface heat flux

Figure 3-7 shows the global solar irradiance and radiant surface heat flux at 4F. Due to the location of the heat flow sensor and pyranometer, solar radiation was observed in the space between 9 a.m. and noon. Based on the measured results, the maximum solar radiation received by the cooling surface and its maximum surface heat flux were  $214 \text{ W/m}^2$  and  $69 \text{ W/m}^2$ , respectively. During the period when the cooled surface did not receive solar radiation, the heat absorption and dissipation rates of the cooled surface were less than  $20 \text{ W/m}^2$ , confirming that the surface heat flux of the cooled surface was significantly enhanced by solar radiation.

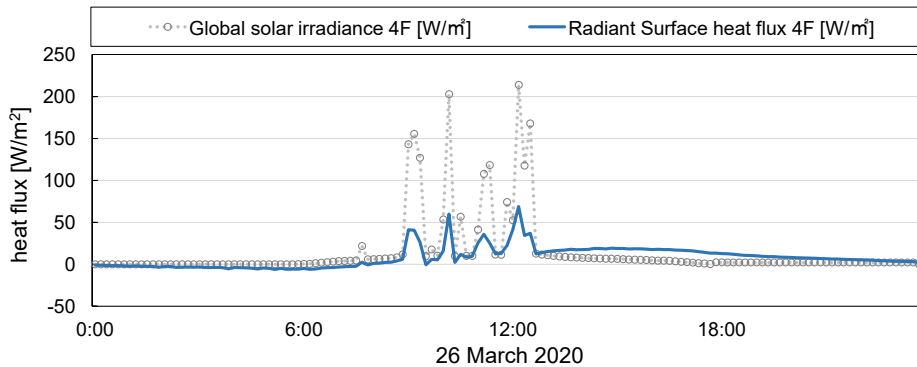


Figure 3-7. Plot showing the measured 4F global solar irradiance and radiant surface heat flux

##### (2) Surface temperature of the daylight harvesting wall and fourth floor air temperature

Figure 3-8 shows the air temperature and the surface temperature of the radiant cooled surface at 4F. Direct solar radiation increased the surface temperature of the cooled surfaces to  $24^\circ\text{C}$ . Room air temperature on 4F ranged from  $18$  to  $22^\circ\text{C}$ . This suggests that an increase in the surface temperature of the cooled surface under direct solar radiation may also change the convective and (longwave) radiative heat transfer at the cooled surface.

During the measurements, we attempted to calculate the heat extraction rate from both the daylight harvesting wall and



slit ceiling. However, only the water flow rate of the entire system and supply water temperature at both the inlet and outlet could be measured. Therefore, the water flow rate was adjusted to prevent water supply to the slit ceiling and only allow supply to the daylight harvesting wall. However, the ratio of water supplied was originally highly biased (93% to the slit ceiling and 7% to the daylight harvesting wall); thus, the range of flow rate adjustment was limited. Therefore, the results of the heat extraction rate from the daylight harvesting wall were omitted from this study.

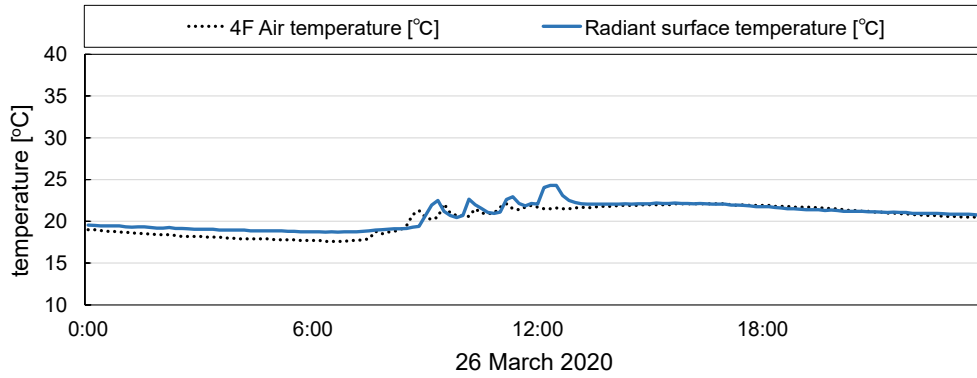


Figure 3-8. Plot showing the measured 4F air temperature and radiant surface temperature

3.4.2 Summer field measurement

The main results of the measurements conducted during summer from 27 August (Thursday) to 29 August (Saturday) are discussed in the following sections. All the three days were sunny.

(1) Horizontal illuminance in an office space with daylight harvesting

Figure 3-9 shows the horizontal illuminance in the third-floor office space. The illuminance meter was installed at a height of 1.1 m above the floor. Since it was sunny throughout the three days, the horizontal illuminance in the third-floor office space reached a maximum of approximately 3,000 lux around noon. During working hours, the measured illuminance was generally within the range of 300–3,000 lux and an appropriate illuminance environment was maintained.

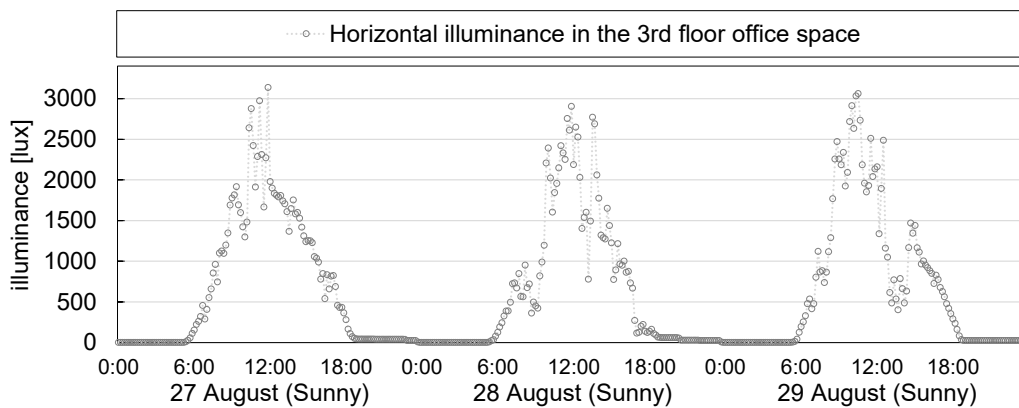


Figure 3-9. Horizontal illuminance in the third floor (3F) office space during summer

(2) Global solar irradiance of the outdoor environment and slit ceiling

Figure 3-10 shows the global solar irradiance of the outdoors and the slit ceiling. The outdoor solar irradiance was obtained from BEMS data, and the solar radiation on the cooled surface of the slit ceiling was measured using a solar radiation meter. The measured data revealed that the maximum outdoor solar radiation was 972 W/m<sup>2</sup> (at 11:40 on 27 August 2020), and the maximum solar radiation at the slit ceiling was 352 W/m<sup>2</sup> during the day (at 14:10 on 27 August 2020).

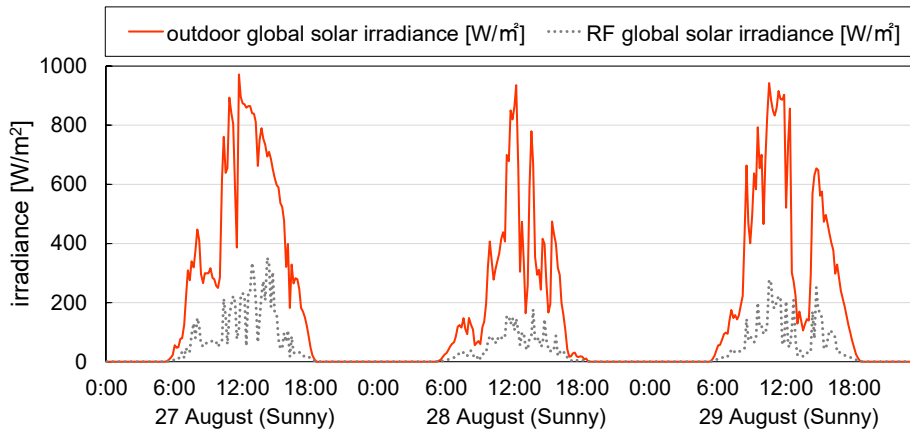


Figure 3-10. Plot showing the measured outdoor and RF global solar radiance values during summer

(3) Air temperature and inner temperature of the slit ceiling

Figure 3-11 shows the air temperature and inner temperature of the slit ceiling. Throughout the three days, the outdoor temperature ranged from 25.1°C to 37.5°C, and the air temperature on RF ranged from 30.4°C to 59.4°C. When the chilled water was pumped to the slit ceiling and daylight harvesting wall, the temperature in the concrete of the slit ceiling was generally within 30°C. The air temperature on the RF and the surface temperature of the slit ceiling were higher than the outdoor temperature during the day.

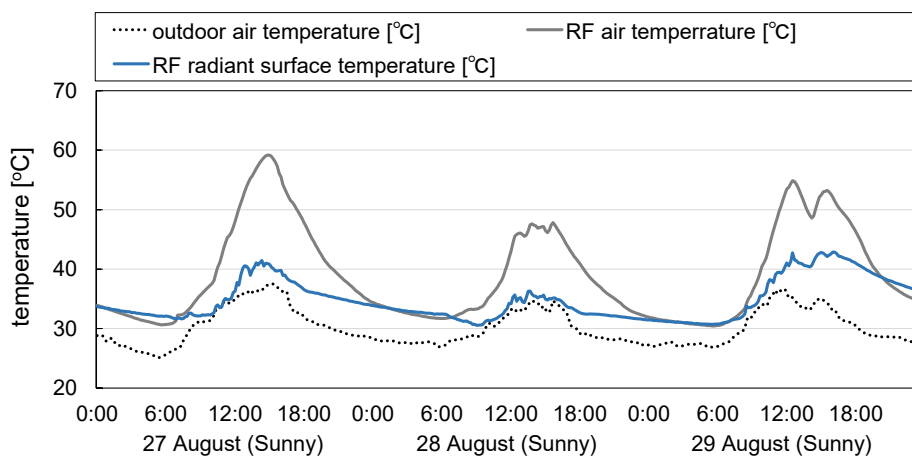


Figure 3-11. Plot showing the measured outdoor and RF air temperatures, and the inner temperature of the slit ceiling

(4) Surface heat flux and heat extraction rate of the slit ceiling

Figure 3-12 presents the radiant surface heat flux and heat extraction of the slit ceiling. The maximum surface heat flux reached 190 W/m<sup>2</sup> during the day. In contrast, the maximum heat extraction rate through the water side was approximately 126 W/m<sup>2</sup> during the day, except for the measurement during the start-up of radiant cooling system. These results confirmed that the peak values of surface heat flux and heat extraction rate are different and that the solar absorption rate at the cooled surface was leveled off by the time it was removed by the cooling water.

The obtained results also showed that the maximum surface heat flux (heat-absorbing side) reached 138 W/m<sup>2</sup> during the day, even on 29 August 2020, when no cooling water was pumped into the slit ceiling. When the air temperature of the RF was lower than the surface temperature of the slit ceiling from midnight to early morning, the surface heat flux was negative (heat dissipation side). Therefore, the measurement results reveal that when estimating the radiant cooling capacity under solar radiation, the heat extraction rate through the water side should be used instead of the surface heat flux of the radiant cooled surface.

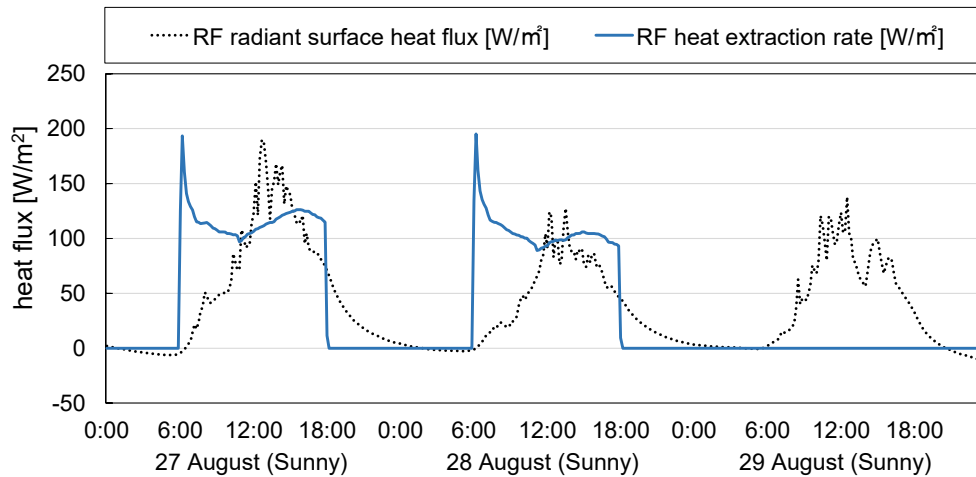


Figure 3-12. Radiant surface heat flux and heat extraction rate of the slit ceiling during summer

(5) Relationship between radiant cooling capacity and outdoor conditions

Figure 3-13 shows the relationship between the surface heat flux of the cooled surface and outdoor conditions. During the summer measurement, the analysis period was from 6 a.m. to 6 p.m. on weekdays when the chilled water was pumped to the slit ceiling. Furthermore, the results were classified into analysis periods of 6 a.m. to 11 a.m. and 11 a.m. to 6 p.m., considering the effect of heat accumulation at the start-up of the radiant cooling system. The radiant surface heat flux increased in response to the increase in solar radiation; similarly, the radiant surface heat flux increased as the outdoor temperature increased.

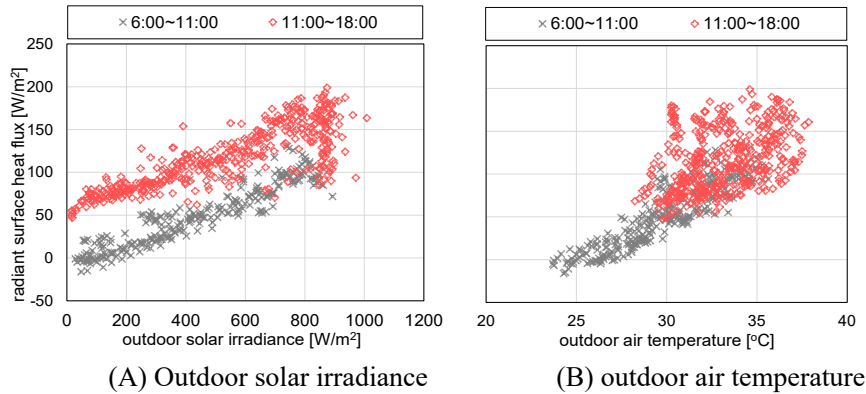


Figure 3-13. Radiant surface heat flux and outdoor conditions

Figures 3-14 shows the heat extraction rate and outdoor conditions determined through the measurements. Regardless of changes in solar radiation and outdoor temperature, the heat extraction rate of the water side remained between 100 W/m<sup>2</sup> and 150 W/m<sup>2</sup> for most of the day. However, the heat extraction rate exceeded 200 W/m<sup>2</sup> during 6 a.m. to 11 a.m., when the solar radiation was less than 200 W/m<sup>2</sup> or the outdoor temperature was less than 30°C. This could be due to the effect of heat accumulation at the start-up of radiant cooling systems.

A reason for the small fluctuation range of the heat extraction rate compared with that of the radiant surface heat flux may be the peak shifting effect of the thermal load that occurs by utilizing the heat capacity of TABS. Thus, a time difference occurs between the heat flowing into the slit ceiling and that reaching the chilled water piping, resulting in a leveled load.

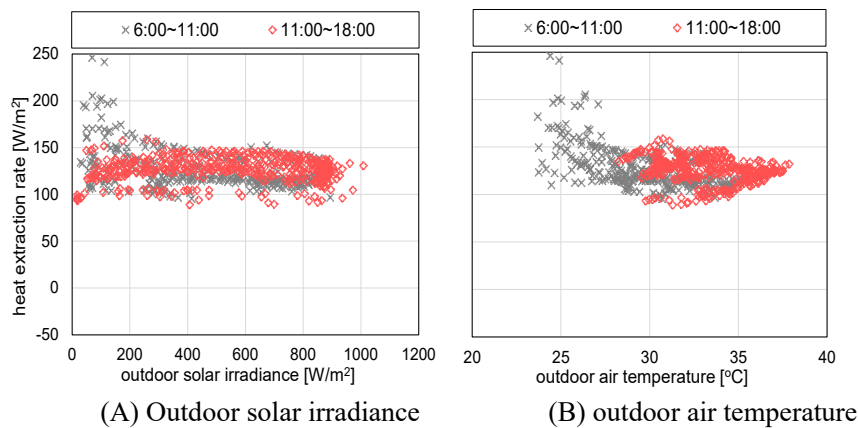


Figure 3-14. Heat extraction rate and outdoor conditions

(6) Daily integrated radiant cooling capacity of the slit ceiling

Figure 3-15 shows the cumulative radiant surface heat flow and heat removal by radiant systems per day of the slit ceiling. The daily cumulative values were calculated from the measurements taken 24h at from 27–29 August 2020. The daily cumulative values of surface heat flow and heat removal were 1.2 kWh/m<sup>2</sup> and 1.4 kWh/m<sup>2</sup>, respectively, on August 27. The larger daily cumulative value of the heat removal than that of the radiant surface heat flow might be due to the following four reasons.

- (i) In this measurement, the heat flux sensors were installed on the upper surface of the slit ceiling; therefore, the surface heat flow rate on the side and bottom surfaces of the slit ceiling was not included.
- (ii) The daily cumulative value was calculated by including the negative value of the surface heat flow (heat radiation side).
- (iii) The solar absorption of the daylight harvesting wall was also included in the total heat extraction rate.
- (iv) The total heat absorption/desorption of the entire slit ceiling was estimated using the values from the four locally installed heat flux sensors.

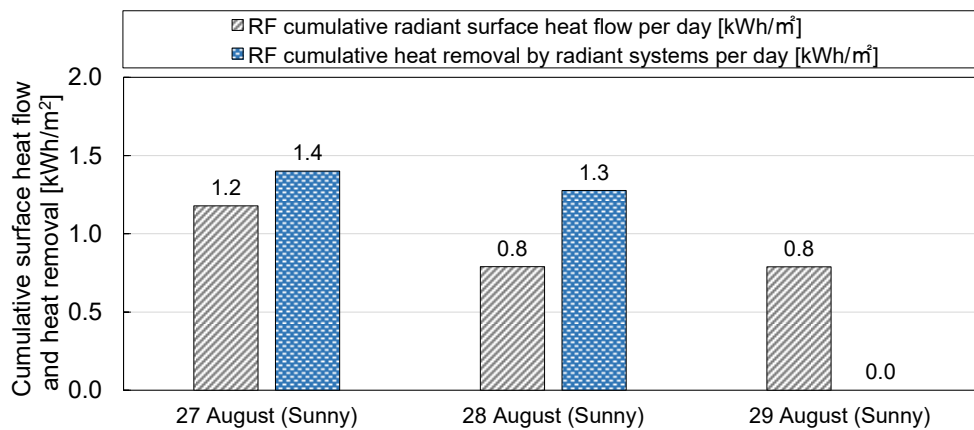
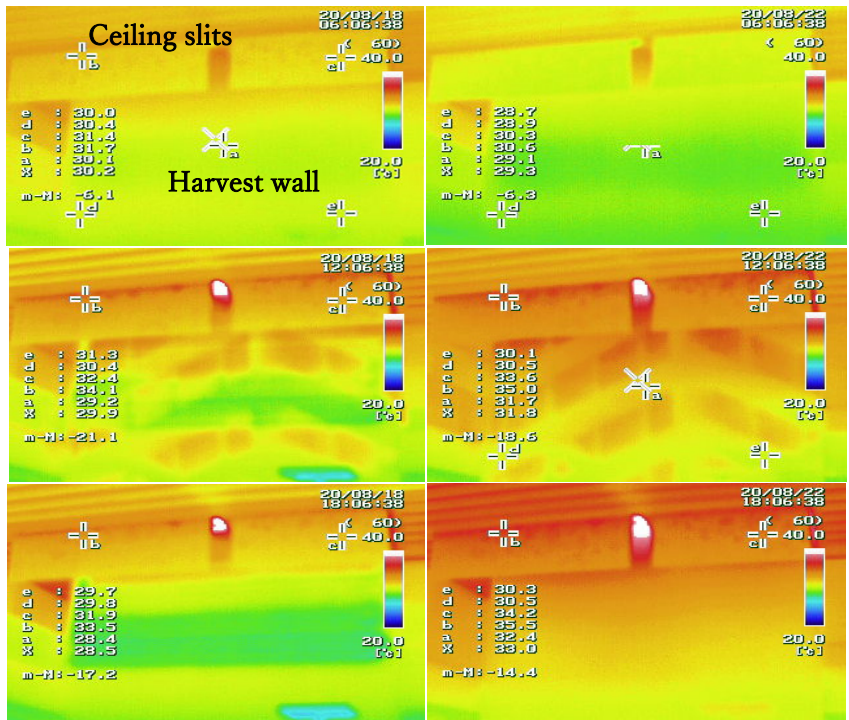


Figure 3-15. Cumulative radiant surface heat flow and heat removal by radiant systems per day of the slit ceiling

(7) Surface temperature measurement of the cooled surface

Figure 3-16 shows the thermal images of the radiant surfaces (6:00, 12:00, and 18:00) that were obtained to demonstrate the changes in the surface temperature over time throughout the day. These thermal images of the daylight harvesting wall and slit ceiling were taken at fixed points when viewed from the 3F office space during the actual summer measurement period. To compare surface temperatures with and without water supply to the slit ceiling, 18 August (Tuesday) and 22 August (Saturday) 2020 were considered as representative days.

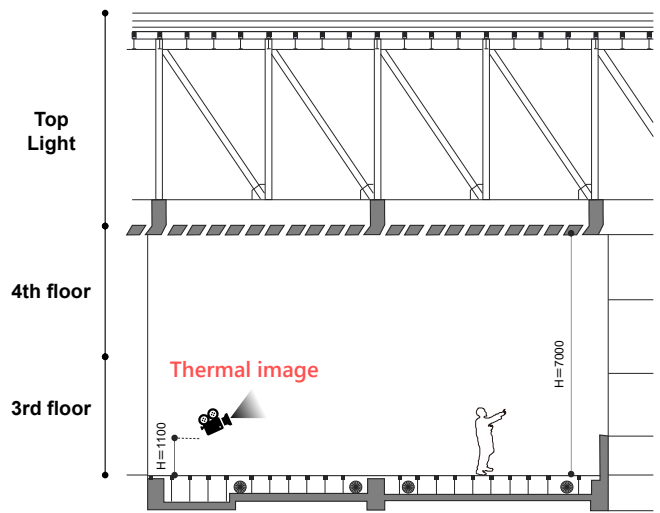


(A) 18 August 2020 (Tuesday)

(B) 22 August 2020 (Saturday)



(C) Thermal image position



(D) View direction of the thermal image

Figure 3-16. Thermal images of the radiant surface at different times and dates (6:00, 12:00, and 18:00)

The surface temperatures of the daylight harvesting wall were 30.1°C (6:00), 29.2°C (12:00), and 28.4°C (18:00) on Tuesday, 18 August 2020, and 29.1°C (6:00), 31.7°C (12:00), and 32.4°C (18:00) on Saturday 22 August 2020. These results confirm that the surface temperature of the cooling surface was reduced by pumping chilled water into the pipes from 6:00 to 18:00. In contrast, the surface temperature of the cooling surface continued to increase from 6:00 to 18:00 h on the day the air conditioning was stopped. The thermal image at 18:00 on 22 August revealed that the surface temperature near the slit ceiling reached 35.5°C. Moreover, the thermal image at 12:00 on 18 August confirmed that under direct solar radiation, the increase in radiant surface temperature on the wall with embedded piping was suppressed compared to that on the wall without buried piping.

(8) Thermal comfort of the office space with daylight harvesting

Figure 3-17 shows the operative temperature (OT) of the office space. The OT was calculated from the additive mean value of air temperature and globe temperature of the 3F office space measured by a PMV meter under low air wind speed. The comfort range of the OT during the cooling period was calculated by referring to the three categories (Categories A to C) indicated in ISO 7730 [17]. The comfort zone was also calculated based on a metabolic rate of 0.90 met [18], considering that the occupants were Japanese. During working hours on 27 and 28 August 2020, the OT of the 3F office space was generally within category A ( $OT = 25.8 \pm 1.0^\circ C$ ), and thus, a comfortable thermal environment was ensured.

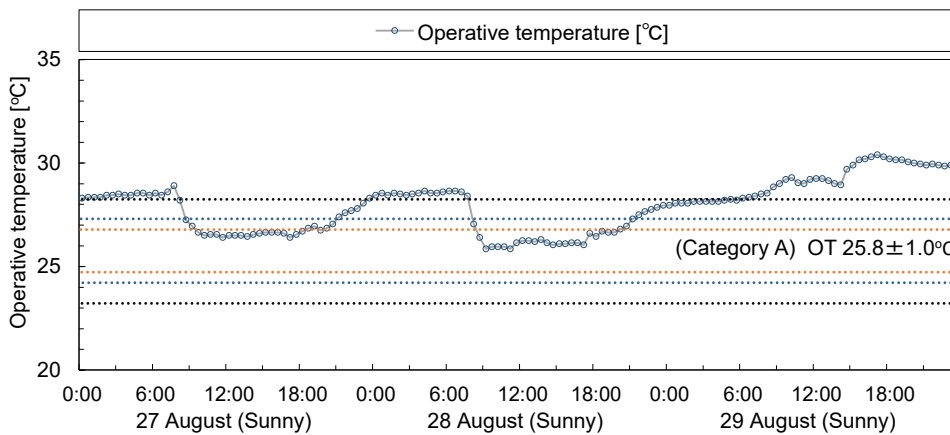


Figure 3-17. Operative temperature (OT) of the office space during summer



Figure 3-18 shows the thermal comfort ranges based on the psychrometric chart. In the ASHRAE 55-2017 standard [19], the thermal comfort zone is defined as the range where the Predicted Percent of Dissatisfied (PPD) is less than 20% under metabolic rates of 1.0–1.3 met and clothing levels of 0.5–1.0 clo. The thermal environment data obtained using the PMV meter over a two-week period were categorized as air-conditioning operation (Monday through Friday, 6 a.m. to 6 p.m.) and shutdown (Saturday and Sunday, 6 a.m. to 6 p.m.) periods and then plotted on the psychrometric chart. When the air-conditioning system was in operation, the air temperature was generally within the comfort zone (cooling period: 0.5 clo zone); however, when the air-conditioning system was stopped, the air temperature was significantly beyond the comfort zone.

These results suggest that a comfortable office space was ensured by air-conditioning the office space while directly absorbing and treating solar radiation as well as heat accumulation from the skylights through the daylight harvesting wall and slit ceiling in an office space.

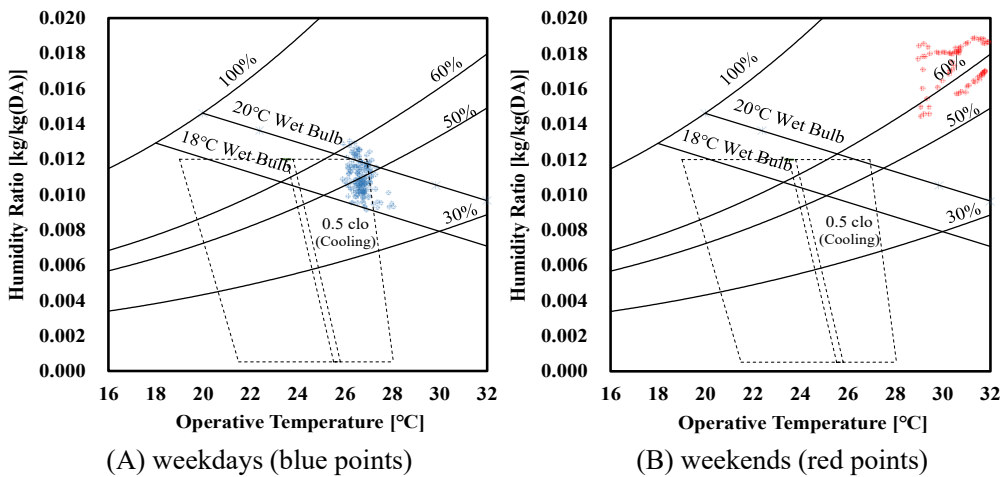


Figure 3-18. Thermal comfort range in the studied office space based on the psychrometric chart



### 3.5 Discussion and conclusions

The aim of this study is to verify the radiant cooling effect of a slit ceiling for both daylight harvesting and solar heat removal in a research building. First, previous studies on radiant cooling capacity enhancement under solar radiation were reviewed. During the midterm and summer periods, field measurements were conducted to measure the solar heat removal performance of the cooled surface and thermal environment of the office space. Consequently, the obtained results verified that an energy-saving and comfortable office space was ensured. The following are the main findings of this study.

- The use of radiant cooling as a method to introduce daylight while ensuring energy efficiency and indoor thermal comfort has attracted significant attention in recent years. A review of previous studies was conducted on the significant increase in radiant cooling capacity owing to solar absorption at the cooled surface. The literature review showed that the peak cooling capacity values, which affect equipment selection, vary widely across literature, which is one of the main reasons for the lack of established design methodologies.
- The surface heat flux and heat extraction rate were calculated to verify the solar heat removal performance of the slit ceiling. Under the effect of solar radiation, the maximum surface heat flux was  $190 \text{ W/m}^2$  and the maximum heat extraction rate was  $126 \text{ W/m}^2$ . The field measurement results confirmed that the radiant cooling capacity was considerably enhanced when the building was absorbing solar radiation.
- The maximum surface heat flux (heat-absorbing side) reached  $138 \text{ W/m}^2$  during the day, even when no cooling water was pumped into the slit ceiling. Therefore, the measured results reveal that when estimating the radiant cooling capacity under solar radiation, the heat extraction rate from the water side should be used instead of the surface heat flux of the radiant cooled surface.
- The surface heat flux and heat extraction rate varied from approximately  $-20$  to  $200 \text{ W/m}^2$  and from approximately  $100$  to  $150 \text{ W/m}^2$ , respectively, in response to changes in solar radiation and outdoor temperature. The variation range of the heat extraction rate was smaller than that of the surface heat flux. Thus, the heat extraction rate from the slit ceiling generally remained constant regardless of the solar radiation intensity, owing to the peak shift of the thermal load by utilizing the TABS heat capacity.
- During working hours on 27 and 28 August 2020, the OT of the 3F office space was generally within category A ( $\text{OT} = 25.8 \pm 1.0^\circ\text{C}$ ), which confirmed that a comfortable thermal environment was ensured.

## References

- [1] International Well Building Institute, “WELL v2™ pilot”, [online]. <https://v2.wellcertified.com/v2.2/en/overview>. Accessed July 01, 2021.
- [2] P. Simmonds, B. Mehlomakulu, T. Eibert, Radiant cooled floors - Operation and control dependent upon solar radiation. *ASHRAE Transact.* 2006;112:358–367.
- [3] B. W. Olesen, Possibilities and limitations of radiant floor cooling. *ASHRAE Transact.* 1997;103(1):42–48.
- [4] P. Simmonds, S. Holst, S. Reuss, W. Gaw, Using radiant cooled floors to condition large spaces and maintain comfort conditions. *ASHRAE Transact.* 2000;106:695–701.
- [5] F. Causone, S. Corgnati, M. Filippi, Calculation method for summer cooling with radiant panels. *CLIMA.* 2007.
- [6] F. Causone, S. Corgnati, M. Filippi, B. W. Olesen., Solar radiation and cooling load calculation for radiant systems: Definition and evaluation of the direct solar load. *Energy and Build.* 2010;42(3):305–314.
- [7] M. De Carli, M. Tonon, Effect of modelling solar radiation on the cooling performance of radiant floors. *Solar Energy.* 2011;85(5):689–712.
- [8] K. Zhao, X. Liu, Y. Jiang, Application of radiant floor cooling in a large open space building with high-intensity solar radiation. *Energy and Build.* 2013; 66:246–257.
- [9] K. Zhao, X. Liu, Y. Jiang, On-site measured performance of a radiant floor cooling/heating system in Xi'an Xianyang International Airport. *Solar Energy.* 2014; 108:274–286.
- [10] J. Feng, S. Schiavon, F. Bauman, New method for the design of radiant floor cooling systems with solar radiation. *Energy and Build.* 2016;125:9–18.
- [11] J. Pantelic, S. Schiavon, B. Ning, E. Bourdakos, P. Raftery, F. Bauman, Full scale laboratory experiment on the cooling capacity of a radiant floor system. *Energy and Build.* 2018;170:134–144.
- [12] ISO 11855-2. Building environment design – Design, dimensioning, installation and control of embedded radiant heating and cooling systems – Part 2: Determination of the design heating and cooling capacity. ISO; 2012.
- [13] B. W. Olesen, Thermo active building systems: Using building mass to heat and cool. *ASHRAE J.* 2012;54(2):44–52.
- [14] T. Takenaka, S. Tamura, K. Shindo, J. Shinoda, T. Kabori, S. Tanabe, Evaluation of the environmental and equipment system performance of a building aimed for intellectual creativity and energy conservation (Part 1). Outline of the building and verification of daylight environment by the ceiling louvers. *Technical Papers of Annual Meeting the Society of Heating, Air-conditioning and Sanitary Engineers of Japan.* 2020.
- [15] K. Shindo, J. Shinoda, T. Takenaka, S. Tamura, T. Kabori, S. Tanabe, Evaluation of the environmental and equipment system performance of a building aimed for intellectual creativity and energy conservation (Part 2). Verification of solar radiation removal by concrete ceiling louvers. *Technical Papers of Annual Meeting the Society of Heating, Air-conditioning and Sanitary Engineers of Japan.* 2020.
- [16] Tetsuo Kabori Architects. <https://tk-a.jp/> (accessed January 21, 2024)
- [17] ISO 7730. Moderate thermal environments. Determination of the PMV and PPD indices and specification of the

conditions for thermal comfort. ISO; 2005.

[18] A. Nomoto, R. Hisayama, S. Yoda, M. Akimoto, M. Ogata, H. Tsutsumi, S. Tanabe, Indirect calorimetry of metabolic rate in college-age Japanese subjects during various office activities, *Build Environ.* 2021;199.

[19] ANSI/ASHRAE Standard 55-2017. Thermal environmental conditions for human occupancy. ASHRAE; 2017.



## **Chapter 4:**

# **Resilient cooling comparison of an all-air system and a radiant system**

### **Abstract**

Radiant systems have been proven to be an energy-efficient and resource-effective heating and cooling solution for buildings. A key feature of a thermally active building system (TABS), one type of a radiant cooling system, is its ability to activate and control the thermal mass of the building structure. The advantage of this feature is the peak load shifting effect by the thermal mass, which leads to energy saving compared to a conventional system, e.g., an all-air system. This feature of the radiant cooling system could be particularly beneficial under a heatwave and power outage event. Dynamic building simulations were carried out to quantify the resilience of TABS to heatwaves and power outages. An all-air system (i.e., air-conditioning) was used as the reference cooling system. The simulations were carried out using EnergyPlus. Future weather files (typical meteorological years and heatwave weather year) developed in IEA EBC Annex 80 were used for the simulations. In both HVAC systems. Simulation results for future weather data resulted in a decrease in heating demand and an increase in cooling demand.

### **KEYWORDS:**

Heatwave, Resilient cooling, All-air system, Thermally Active Building System (TABS), Operational carbon

## 4.1 Introduction

Climate change has become a severe problem globally, with natural disasters causing extensive damages [1]. In response to climate change, resilience of the built environment has been increasingly significant. There are a variety of shocks to buildings, such as floods, heat and cold waves, associated power outages, and earthquakes. This study focuses on heatwaves and power outages. Previous studies have shown that frequent heatwaves and power outages caused by climate change are significant disruptors that make it challenging to maintain Heating, ventilation, and air-conditioning (HVAC) systems [2,3]. If HVAC systems cannot maintain comfort conditions during events such as power outages, it could result in declining occupant productivity and health and having serious and long-term adverse economic consequences. Therefore, there is a need to identify effective resilient cooling solutions to deal with climate change.

International Energy Agency (IEA), Energy in Buildings and Communities Programme (EBC) Annex 80 – Resilient Cooling of Buildings [4] is working on defining resiliency and its key concepts in terms of building cooling [5-7], developing qualitative and quantitative key performance indicators [8] and evaluating different cooling systems based on these indicators.

Radiant cooling systems have been proven to be an energy-efficient and resource-effective heating and cooling solution for buildings [9]. A key feature of a Thermally Active Building System (TABS), one type of a radiant cooling system, is its ability to activate and control the thermal mass of the building structure [10]. The advantage of this feature is the peak load shifting effect by the thermal mass, which leads to energy saving compared to a conventional system, e.g., an all-air system. This feature of TABS could be particularly beneficial under a heatwave and power outage event by natural disasters [11,12].

Figure 4-1 shows the framework for evaluating the building resilience of different weather locations and cooling technologies. The present study compared the resiliency performance of TABS with that of a packaged Variable Air Volume system with reheating (VAV system). Indoor temperature and primary energy consumption of the HVAC systems under typical weather conditions and future heatwaves and power outages were compared.

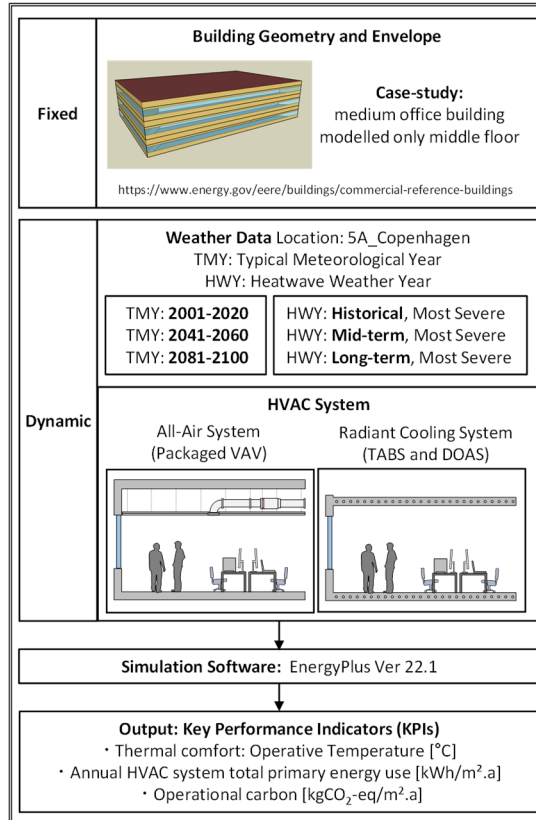


Figure 4-1. Framework for evaluating the building resilience of different weather locations and cooling technologies

## 4.2 Methods

### 4.2.1 Building model

Figure 4-2 shows the schedule of internal heat gain and Figure 4-3 shows the zone layout of for the building model. A medium office building to represent commercial buildings, one of the prototypes building models provided by the U.S. department of Energy, was used for the simulations. The prototype building models are based on ANSI/ASHRAE/IES Standard 90.1 [13]. In this study, only the middle floor was modelled with the simulation software EnergyPlus version 22.1 [14]. The middle floor was separated in 5 zones, comprising 4 perimeter zones and a core zone. The construction and material of the building is presented in Table 4-1. [15].

For the boundary conditions of the building, only the exterior walls exchanged heat with the external environment. The interior walls were set to adjacent, and the floor and ceiling were set to adiabatic. Air change rate of infiltration was 0.6 h<sup>-1</sup>. 30 m<sup>3</sup>/h of outdoor air was supplied per person by the ventilation system. Outdoor supply air for each zone was calculated based on ASHRAE Standard 62.1-2019 [16]. The maximum values of density of occupants, lighting gain, and equipment gain were 0.05 person/m<sup>2</sup>, 6.9 W/m<sup>2</sup>, and 8.0 W/m<sup>2</sup>, respectively. As shown in Figure 4-2, the internal heat gain was varied according to the schedule. During power outage periods, all internal heat gain were set to zero.

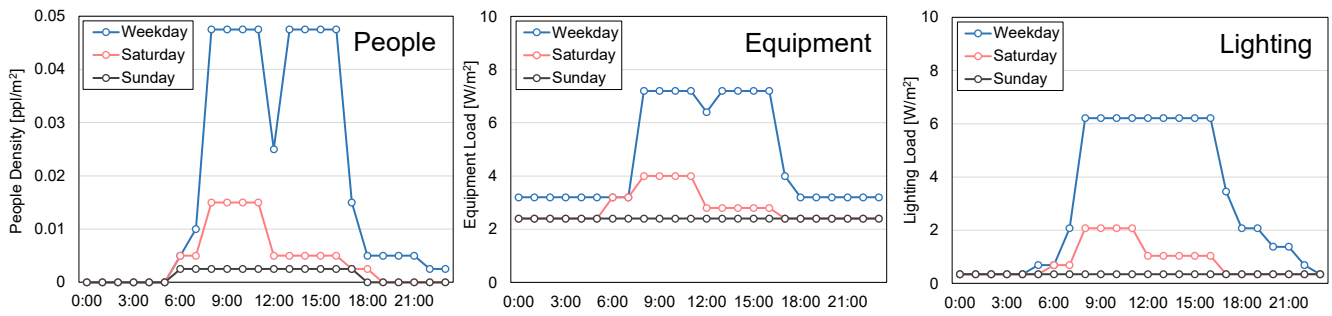


Figure 4-2. Schedule of internal heat gain

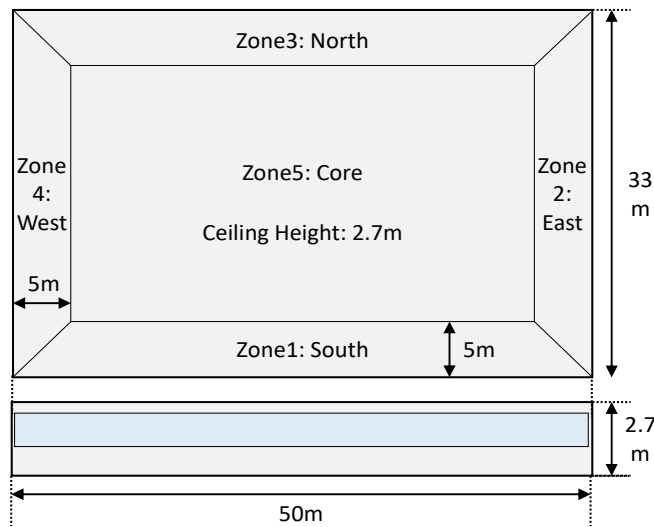


Figure 4-3. Zone layout for medium office building

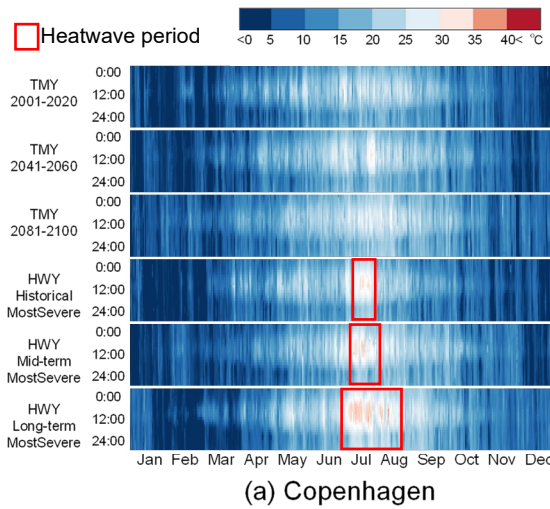
Table 4-1. Construction and material of the building envelope

Construction	Material	R value [(m <sup>2</sup> ·K)/W]	Thickness [mm]	Conductivity [W/(m·K)]	Density [kg/m <sup>3</sup> ]	Thermal capacity [J/(kg·K)]
Floor/ceiling	Carpet pad	0.22	—	—	—	—
	Concrete	—	101.6	2.31	2,322	832
Outside wall	Stucco	—	25.4	0.72	1,856	840
	Gypsum board	—	15.9	0.16	800	1,090
	Insulation	2.37	—	—	—	—
	Gypsum board	—	15.9	0.16	800	1,090
Interior wall	Gypsum board	—	25.4	0.16	800	1,090



4.2.2 Weather data

The future typical meteorological year (TMY) weather files and future heatwave weather year (HWY) developed in Annex 80 [4] were used for the simulations. Singapore and Copenhagen were selected as representative very hot–humid and cold–humid weather locations. Heat balance simulations were run using three TMY files (2001-2020, 2041-2060, and 2081-2100) and three HWY files for most severe conditions (Historical, Mid-term, and Long-term), respectively. Historical, mid-term future, and long-term future refer to the 2000-2020, 2041-2060, and 2081-2100 periods, respectively. As shown in Fig. 4, heatwaves will be more frequent in both Copenhagen and Singapore in the future, and the duration of the heatwave period will be longer.



(a) Copenhagen  
Figure 4-4. Outdoor dry bulb temperature

4.2.3 HVAC strategies

Figure 4-5. Shows the heat source system diagram both VAV system and TABS. Two types of HVAC systems were modelled for comparison: TABS (coupled with a dedicated outside air system, DOAS) and VAV system. Input values and settings presented in this section were taken from [15-18]. Cooling setpoint was 24°C and heating setpoint was 21°C. Setpoints were used air temperature. Annual simulations were conducted, i.e., the analysis period was from 1st January to 31st December. Simulation interval was 1 hour. The VAV system operated from 7:00 to 23:00 on weekdays. The supply air temperature was maintained at 12.8°C and 35°C with a variable air volume fan during the cooling and heating season. The HVAC system cools or heats the required outdoor air and return air. This supplies by coil cooling DX and reheat coil and supplies it to each 5 rooms. The TABS was operated from 18:00 to 6:00 on weekdays. Cold or hot water was supplied to each room for a fixed period with variable water flow rates, depending on the heat load. The ceiling was set as the radiant surface, and the supply water temperature for the cooling and heating season was set to 18°C and 30°C. Pipe inner diameter was 0.020 m, and one circuit length of TABS is 106.7 m. Operative temperature was adopted for temperature control for TABS. DOAS was used to remove the latent heat load and the sensible heat load that could not be removed by TABS.

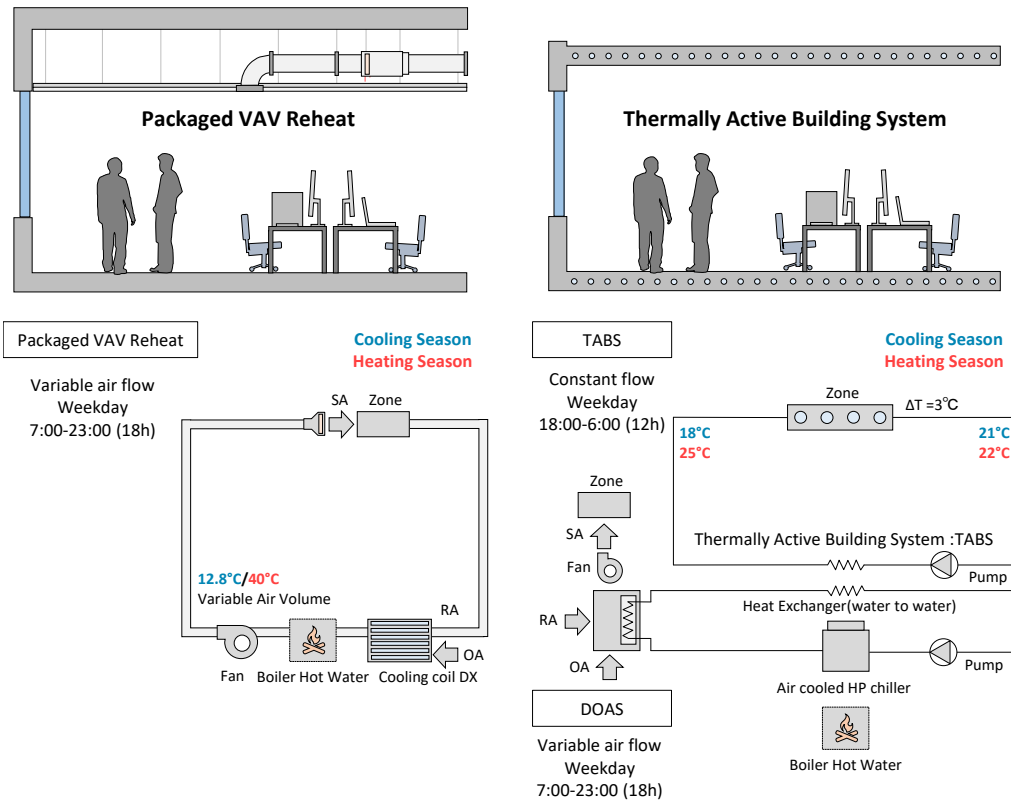


Figure 4-5. Heat source system diagram both VAV system and TABS

Table 4-2. Boundary conditions of TABS [17-18]

Radiant surface	Ceiling
Supply water temperature	18°C (Cooling) 30°C (Heating)
Pipe inside diameter	0.020 m
Circuit length	106.7 m
Temperature control	Operative temperature

### 4.3 Results and Discussion

#### 4.3.1 Indoor thermal comfort

Table 4-3 shows the Percentage of time in comfort range (EN16798-1: 2019) under future typical meteorological year weather conditions in Copenhagen. The period from May to September was set as the cooling season and the rest of the year as the heating season and operative temperature during occupied hours (8:00 to 17:00 on weekdays) were used. In office spaces, the default indoor operative temperature range corresponding to Category II of EN16798-1: 2019 [19] is 20-24 °C for the heating season and 23-26 °C for the cooling season. Indoor operative temperature was kept within the comfort range for all cases for both TABS and all-air system. However, energy use related to the HVAC systems were greatly dependent on weather data and the selected system.

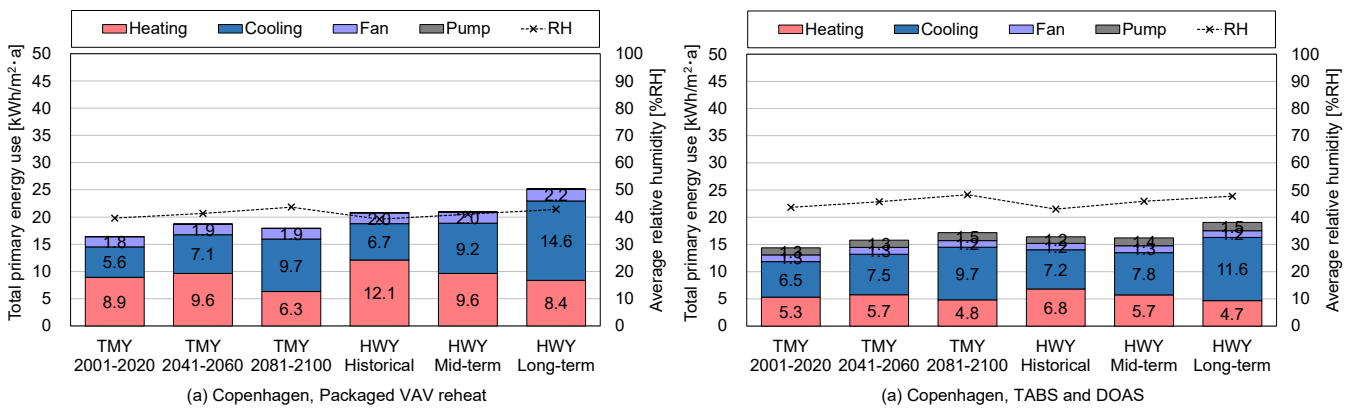
Table 4-3. Percentage of time in comfort range in Copenhagen (EN16798-1: 2019)

HVAC System	Packaged VAV reheat				Thermally Active Building System: TABS			
Period	Average Operative Temp 1 May – 30 September	EN16978 Category II 23-26°C 1 May – 30 September	Average Operative Temp 1 January – 30 April, 1 October – 31 December	EN16978 Category II 20-24°C, 1 January – 30 April, 1 October – 31 December	Average Operative Temp 1 May – 30 September	EN16978 Category II 23-26°C 1 May – 30 September	Average Operative Temp 1 January – 30 April, 1 October – 31 December	EN16978 Category II 20-24°C, 1 January – 30 April, 1 October – 31 December
Unit	°C	%	°C	%	°C	%	°C	%
TMY 2001-2020	24.4	99	22.2	90	24.1	98	22.5	94
TMY 2041-2060	24.3	99	22.1	88	24.1	97	22.6	91
TMY 2081-2100	24.4	99	22.6	83	24.0	98	22.7	90
Heatwave Historical	24.2	97	21.8	93	24.1	97	22.3	95
Heatwave Mid-term	24.3	97	22.1	89	24.3	92	22.6	93
Heatwave Long-term	24.5	98	22.2	92	24.2	98	22.7	95

4.3.2 Energy use and operational carbon

Annual cooling and heating primary energy use per conditioned floor area are one of the Key Performance Indicators (KPI) for the IEA EBC Annex 80 – Dynamic simulation guideline for the performance testing or resilient cooling strategies [4]. The primary energy factor (PEF) was used to 1.9 for electricity and 1.0 for gaseous fossil fuel for Danish building regulation BR18 [20]. The carbon emission factor of BR18 [20] was also used to 0.187 kgCO<sub>2</sub>-eq/kWh for electricity and 0.225 kgCO<sub>2</sub>-eq/kWh for gaseous fossil fuel.

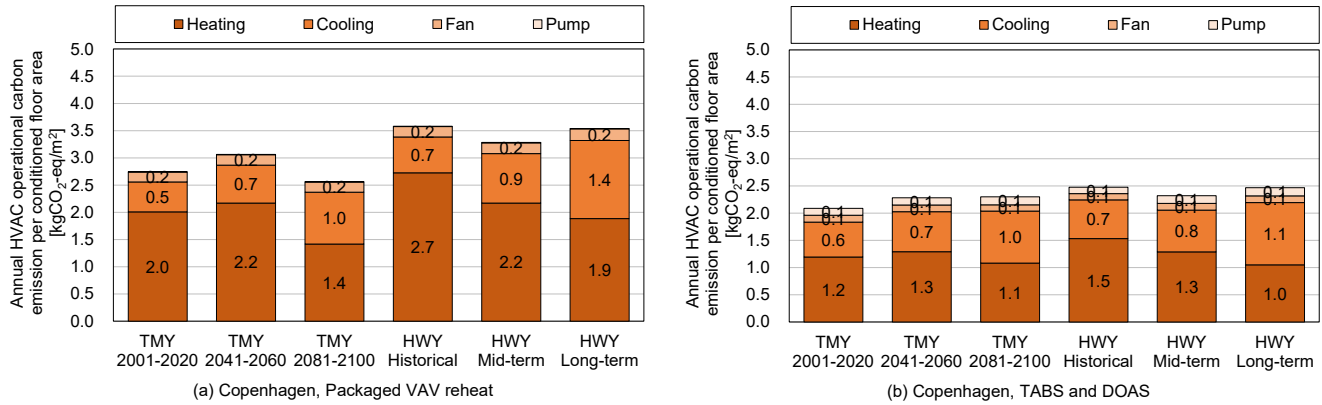
Figure 4-6 shows annual HVAC system total primary energy uses per conditioned floor area. Results shows that the primary energy use for cooling and heating of TABS was lower than that of VAV system. One reason for this result was that the peak heating and cooling load shifting due to the thermal mass of the TABS resulted in a smaller heat source capacity and consequently less energy use for HVAC systems. In both HVAC systems, Simulation results for future weather data mostly resulted in a decrease in heating demand and an increase in cooling demand. Total primary energy use was expected to increase with future rising outdoor temperatures. Another advantage of installing TABS was that the energy increase in heatwave weather year data from mid-term to long-term was smaller for TABS than for the all-air system.



\* Primary energy factors (PEF) of BR18 were applied.

Figure 4-6. Annual HVAC system total primary energy uses per conditioned floor area in Copenhagen

Figure 4-7 shows annual HVAC system operational carbon per conditioned floor area in Copenhagen. The operational carbon for cooling and heating in TABS were also less than in VAV system. Under HWY conditions, both the VAV system and TABS showed little change or a decrease in operational carbon values from the present value (historical) in the event of more frequent heatwaves in the future.



\* Carbon emission factors of BR18 were applied.

Figure 4-7. Annual HVAC system operational carbon per conditioned floor area in Copenhagen

Under HWY conditions, the total primary energy use increased with respect to the future decrease in heating demand and increase in cooling demand, but the total operational carbon was equal to or partially reduced, a contrary result. As shown in Table 4-4, the primary energy factor of electricity in BR18 is 1.90 times that of gas. In contrast, the carbon emission factor of electricity in BR18 is 0.83 times that of gas. Since gas was assumed for heating and electricity was assumed for cooling in this simulation case study, the ratio of heating and cooling to primary energy and operational carbon might differ depending on these conversion factors. The result of the operational carbon implies that the impact of the decrease in gas-based heating demand was equal to or larger than the impact of the increase in electricity-based cooling demand due to the higher outdoor temperatures caused by the event of more frequent heatwaves in the future.

Table 4-4. Primary energy factor and carbon emission factors for natural gas, district heating, and electricity

Weighting factor	Primary energy conversion factor		Carbon emission factor	
	ISO52000 [21]	BR18: Danish building regulation [20]	ISO52000 [21]	BR18: Danish building regulation [20]
Units	kWh/kWh	kWh/kWh	kgCO <sub>2</sub> -eq/kWh	kgCO <sub>2</sub> -eq/kWh
Natural gas	1.1	1.0	0.220	0.225
District heating	1.3	0.85	0.260	0.105
Electricity	2.5	1.9	0.420	0.187

This study focused on the energy and operational carbon impact of the more frequent heatwaves in the future. Further possibilities and limitations of this study were discussed below.

#### **Operation and combination of heat sources for HVAC systems**

It should be noted that the typical operation of TABS is night operation only and the simulated buildings was low thermal mass. In this study, gas-fired boilers were assumed as the heat source for heating, but electrification, such as the use of an air source heat pump for heating and cooling, is an option. When boilers are replaced by heat pumps, electrification might be expected to reduce operational carbon. On the other hand, if outdoor temperature increases due to frequent heatwaves in the future, the efficiency of air source heat pumps might be expected to decrease due to higher outdoor temperatures during cooling. Another option is the use of district heating. According to the energy and carbon conversion factors in BR18, heating system from district heating instead of using gas is expected to reduce primary energy use and operational carbon of the HVAC systems.

#### **Dynamic simulation settings**

In this study, the comparison of VAV system and TABS should be done in terms of indoor thermal comfort, energy use, or maybe those simulations should consider the sizing of the systems as well. It should be noted that under the boundary conditions of this study, the sizing of air conditioning equipment and heat sources were calculated automatically according to the heat load, resulting in a stable indoor environment and significant changes in energy consumption related to HVAC systems.

#### **Embodied carbon impact**

In this study, operational carbon impact of the HVAC system was conducted by dynamic simulation. In addition to operational carbon, embodied carbon throughout the building life cycle, including the material production, construction, use, demolition, and reuse stages should also be verified. Comparative studies of operational and embodied carbon for HVAC systems were discussed in the next chapters.

## **4.4 Conclusions**

Dynamic building simulations were carried out to quantify the resilience of a thermally active building system and an all-air system (i.e., air-conditioning) to heatwaves and power outages using EnergyPlus. Future weather files of typical meteorological years and heatwave weather years were used.

For any future typical meteorological years and future heatwave weather years, both TABS and VAV system were able to provide an indoor temperature within a comfortable range. In Copenhagen, the primary energy use for cooling and heating of TABS was lower than that of VAV system. In both HVAC systems. Simulation results for future weather data resulted in a decrease in heating demand and an increase in cooling demand. Total primary energy use was expected to increase

with future rising outdoor temperatures. In contrast, under HWY conditions, both the VAV system and TABS showed little change or a decrease in operational carbon values from the present value (historical) in the event of more frequent heatwaves in the future.

## References

- [1] The Intergovernmental Panel on Climate Change, “IPCC DDC Glossary,” 2020. [https://www.ipcc-data.org/guidelines/pages/glossary/glossary\\_c.html](https://www.ipcc-data.org/guidelines/pages/glossary/glossary_c.html) (accessed Dec. 11, 2022).
- [2] A. Baniassadi, J. Heusinger, D. J. Sailor, Energy efficiency vs resiliency to extreme heat and power outages: The role of evolving building energy codes, *Building and Environment*, 139, 86-94 (2018)
- [3] A. De Bono, Peduzzi, S. Kluser, G. Giuliani, Impacts of summer 2003 heat wave in Europe, <https://wedocs.unep.org/handle/20.500.11822/40942> (accessed Dec. 14, 2022)
- [4] IEA Annex 80- Resilient Cooling for Buildings, Dynamic simulation guideline for the performance testing of resilient cooling strategies (2021)
- [5] S. Attia, R. Levinson, E. Ndongo, P. Holzer, O. B. Kazanci, S. Homaei, C. Zhang, B.W. Olesen, D. Qi, M. Hamdy, P. Heiselberg, Resilient cooling of buildings to protect against heat waves and power outages: Key concepts and definition, *Energy and Buildings*, 239, 110869 (2021)
- [6] W. Miller, A. Machard, E. Bozonnet, N. Yoon, D. Qi, C. Zhang, A. Liu, A. Sengupta, J. Akander, A. Hayati, M. Cehlin, O. B. Kazanci, R. Levinson, Conceptualising a resilient cooling system: A socio-technical approach. *City and Environment Interactions*, 11, 100065 (2021)
- [7] E. Elnagar, V. Lemort, Cooling Concepts for Residential Buildings: A Comparison Under Climate Change Scenarios, *International High Performance Buildings Conference*, 406 (2022)
- [8] C. Zhang, O. B. Kazanci, R. Levinson, P. Heiselberg, B. W. Olesen, G.Chiesa et al. Resilient cooling strategies – A critical review and qualitative assessment. *Energy and Buildings*, 251, 111312 (2021)
- [9] O. B. Kazanci, Low Temperature Heating and High Temperature Cooling in Buildings, PhDThesis, Kgs. Lyngby: Technical University of Denmark. (2016)
- [10] ISO 11855-2, Building environment design – Embedded radiant heating and cooling systems – Part 2: Determination of the design heating and cooling capacity, ISO. (2012)
- [11] O. B. Kazanci, J. Shinoda, B. W. Olesen, Revisiting radiant cooling systems from a resiliency perspective: A preliminary study, CLIMA (2022)
- [12] J. Shinoda, D. Bogatu, B. W. Olesen, O. B. Kazanci, A qualitative evaluation of the resiliency of Personalized Environmental Control Systems (PECS), 42nd AIVC (2022)
- [13] ANSI/ASHRAE/IES Standard 90.1-2019, Energy Standard for Buildings Except Low-Rise Residential Buildings, ASHRAE. (2019)
- [14] National Renewable Energy Laboratory (NREL), EnergyPlus, <https://energyplus.net/> (accessed Dec. 11, 2022).
- [15] National Renewable Energy Laboratory (NREL), Commercial Reference Buildings, <https://www.energy.gov/eere/buildings/commercial-reference-buildings> (accessed Dec. 14, 2022).

- [16] ANSI/ASHRAE Standard 62.1-2022, Ventilation and Acceptable Indoor Air Quality, ASHRAE. (2022)
- [17] M. Achermann, G. Zweifel, RADTEST – Radiant Heating and Cooling Test Cases, International Energy Agency (2003)
- [18] B. W. Olesen, F. C. Dossi, Operation and control of activated slab heating and cooling systems, in Proceedings of CIB World Buildings Congress, Toronto, Canada (2004)
- [19] EN 16798-1, Energy Performance of buildings–Ventilation for buildings – Part 1: Indoor environmental input parameters for design and assessment of energy performance of buildings addressing indoor air quality, thermal environment, lighting and acoustics, European Committee for Standardization (2019)
- [20] Building regulation 2018 (BR18) (2018). <https://byggningsreglementet.dk>
- [21] ISO 52000-1, Energy performance of buildings – Overarching EPB assessment – Part 1: General framework and procedures, ISO (2017)



## **Chapter 5:**

# **A comparative study of the whole life carbon of an all-air system and a radiant system in Denmark**

### **Abstract**

There is an urgent need to reduce carbon emissions from the building sector. This study focused on the whole life carbon of a building's heating, ventilation, and air conditioning system. A methodology to compare the whole life carbon of different HVAC systems was proposed and used in a case study with boundary conditions in Denmark. All-air system and radiant systems were compared, as they have different working principles and the potential for differences in both their embodied and operational carbon. The radiant system was a Thermally Active Building System (TABS), and the all-air system was a packaged variable-air-volume system with reheat. The building model was based on the medium-sized office of prototype buildings developed by the U.S. Department of Energy. Life cycle stages of the building were classified based on EN15978:2011. Two models, one for dynamic building simulation and the other for measuring the mass of materials (e.g., concrete), were adopted in a novel approach. The operational carbon of the HVAC systems was calculated under very similar indoor thermal comfort conditions. The whole life carbon was 10.1 kgCO<sub>2</sub>-eq/m<sup>2</sup>/year and 9.0 kgCO<sub>2</sub>-eq/m<sup>2</sup>/year for the all-air system and TABS, respectively. Compared to the all-air system, TABS reduced annual total primary energy use by 34% and whole life carbon by 11%. If dynamic carbon intensity of the grid were to be implemented, further reduction of carbon emission is expected with TABS, owing to its flexibility in operation with the activated thermal mass.

### **KEYWORDS:**

Building energy, Embodied carbon, Whole life carbon, Thermally active building system (TABS), All-air system, Circular economy

## 5.1 Introduction

Previous studies have highlighted that the MEP can be a major contributor to the whole life carbon emission of a building. Therefore, in the present study, the selection of the HVAC system was investigated, as different HVAC systems have different working principles and the potential for differences in both embodied and operational carbon. As a simplified case study of different HVAC systems, all-air and radiant systems were compared. Radiant systems are energy-efficient and resource-effective heating and cooling solutions for buildings [1]. A Thermally Active Building System (TABS) is a radiant system that embeds water pipes in a concrete structure for heating and cooling [2]. A key feature of a TABS is that it reduces the required peak cooling and heating power by utilizing the thermal mass of the building. This reduces the size of the heating and cooling system components, including the heat source [3]. If the supply water temperature is close to room temperature, the efficiencies of the chiller and heat pump will increase. Another feature of a TABS is that it does not require a suspended ceiling, which reduces the floor height and building materials required during construction. Given these features, it was hypothesized that radiant systems would perform better than all-air systems in terms of whole life carbon emissions.

The aim of this study was to quantify the effect of HVAC systems on whole life carbon emissions. An all-air system, that is, a packaged variable air volume (VAV) system with reheat, was used as the reference (all-air) system for comparison with a TABS. Two models were used: one for dynamic building simulation and the other for calculating the mass of materials (e.g., concrete). Dynamic building simulations were conducted to evaluate the indoor operative temperature and operational carbon emissions related to the HVAC systems. The embodied carbon emissions of the building were calculated based on the values given in the Building Regulation 2018 of Denmark [4]. The entire life-cycle stages of a building were classified according to EN 15978:2011 [5].

## 5.2 Methods

Whole life carbon is the sum of operational and embodied carbon. As shown in Figure 5-1, two types of models—a building surface model and a building geometry model—were used to calculate whole life carbon. A building surface model was used for the dynamic energy performance simulations, in which the operative temperature in the reference zone and the energy use of the HVAC system were calculated. The obtained energy use was converted to operational carbon emissions (B6) by multiplying it with the carbon intensity. Dynamic simulations were conducted using EnergyPlus version 22.1 [6]. The simulation interval was set to one hour. The simulation results were also utilized to size the equipment, and the sizing information was used to calculate the embodied carbon emissions of HVAC. To calculate the embodied carbon emissions of building components, information regarding their volumes and surface areas is required. A building geometry model was developed to obtain these values, which were then multiplied by the respective carbon-emission factors per unit in the LCA database. Appendix B lists the emission factors used in this study.

Danish regulations were selected for this case study, and the calculation procedure complied with their requirements. The lifespan, life-cycle stage, calculation methodology, LCA inventory database, and emission factors of the utilities were used based on the Danish building code BR18 [4]. In this study, the lifespan of the building was assumed to be 50 years. However, this lifespan does not necessarily correspond to the expected lifespan of the building. Fixing the lifespan allows for a comparison of the climate impact calculations for individual buildings. The requirements for building regulation includes A1–A3: Products, B4: Replacement, B6: Operational use, C3: Waste, C4: Disposal, and D: Recycling; all the required stages were calculated in this study. As shown in Table 5-1, the carbon emission factor for electricity and district heating has already been considerably reduced in Denmark compared to the values given in ISO 52000 (2017) [7] because of progress in the energy mix (i.e., a larger share of renewable energy in the grid). For BR18, emission factors of 0.187 kgCO<sub>2</sub>-eq/kWh, 0.105 kgCO<sub>2</sub>-eq/kWh, and 0.225 kgCO<sub>2</sub>-eq/kWh for electricity, district heating, and gas, respectively, were used.

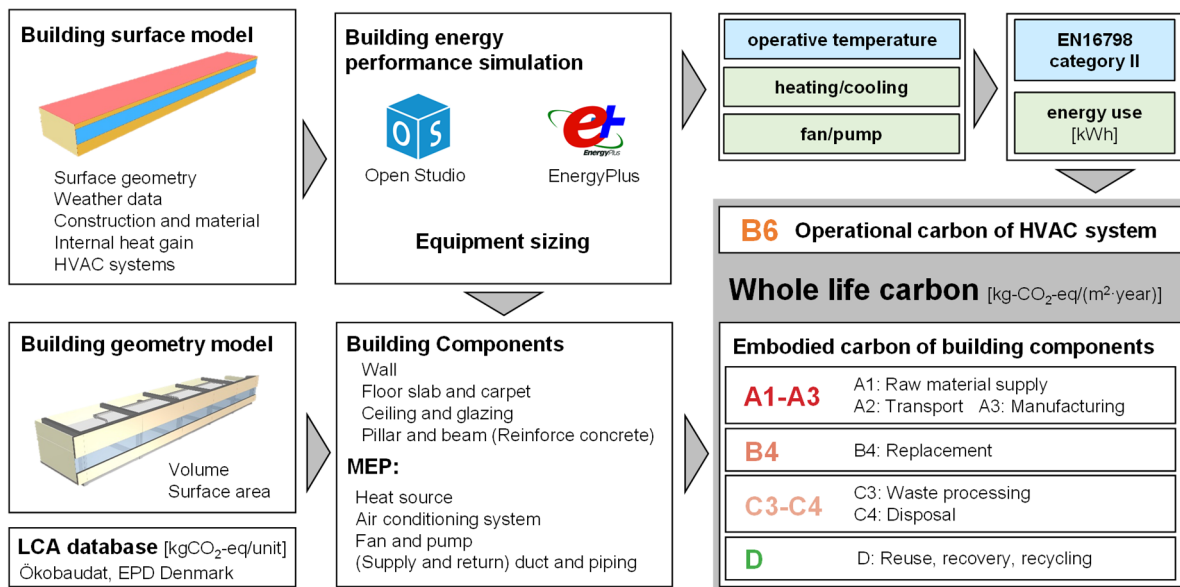


Figure 5-1. Methodology for calculating operational and embodied carbon emissions in this study

Table 5-1. Primary conversion and carbon emission factors for natural gas, district heating, and electricity

Weighting factor	Primary energy conversion factor		Carbon emission factor	
	ISO52000	BR18: Danish building regulation	ISO52000	BR18: Danish building regulation
Guideline, regulation				
Units	kWh/kWh	kWh/kWh	kgCO <sub>2</sub> -eq/kWh	kgCO <sub>2</sub> -eq/kWh
Natural gas	1.1	1.0	0.220	0.225
District heating	1.3	0.85	0.260	0.105
Electricity	2.5	1.9	0.420	0.187

5.2.1 Building model

Figure 5-2 shows the layout of the building model. The building model is based on a medium-sized office of prototype building models provided by the U.S. Department of Energy [8]. The original floor plan of the medium-sized office comprises four perimeter zones and a core zone. Moreover, an updated detailed medium office prototype model proposed by Im et al. [9] was used. The prototype model must contain information regarding the building structure. Therefore, the locations and sizes of the columns and beams were estimated from a detailed floor plan, and a reinforced concrete structure was assumed. It must be noted that the building structures and foundations differ in each region’s building regulations; however, this is beyond the scope of the present study. Only the office room on the south side of the middle floor was included in the calculation to quantify the impact of the HVAC systems on operational and embodied carbon. The plenum zone was removed when using the TABS. When the plenum was removed, materials in facade for TABS were also less because of the lower floor height.

Table 5-2 lists the system boundaries of the life-cycle stages referenced from the guidelines from IEA EBC Annex 57 [10]. For the superstructure, the pillars, beams, external walls, windows, internal walls, floors, ceilings, and roofs were considered for estimating the embodied carbon in the office building. For the building service, only heating, cooling, and ventilation systems were considered for both operational and embodied carbon. The main objective of this study is to compare two different HVAC systems in terms of the whole life carbon emissions. Therefore, water, sewage, electrical, and conveying systems were excluded from the building services.

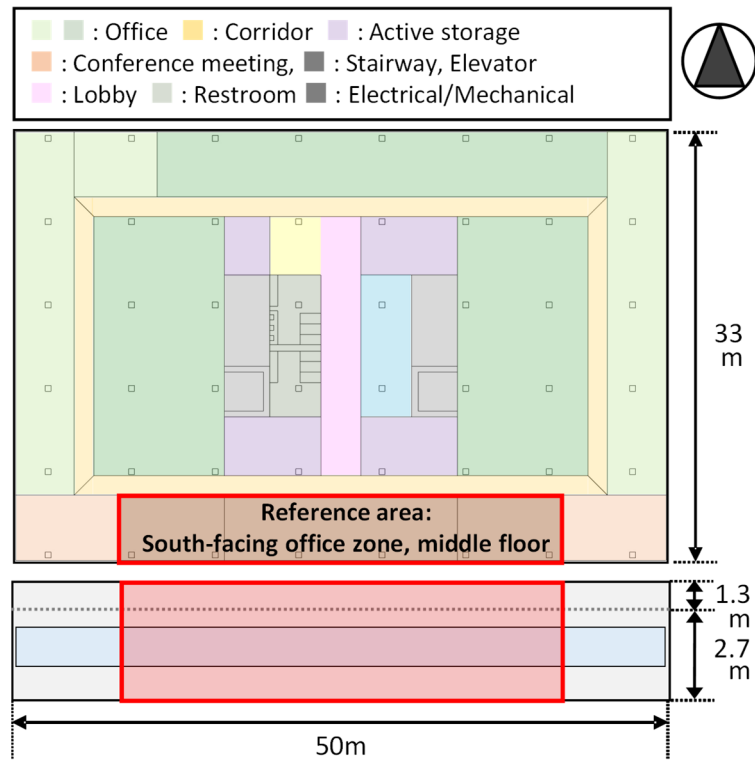


Figure 5-2. Zone layout of the building model [8,9]

Table 5-2. System boundary of life-cycle stages [10]

Type	Building parts
Substructure	Basement, foundation
	Beams
	Pillars
	External walls (doors)
Superstructure	Windows
	Internal walls
	Floors
	Ceilings
	Roofs
Building services	Heating system
	Cooling system
	Ventilation system
Finishes	External finishes
	Internal finishes

5.2.2 Dynamic simulation settings and HVAC strategies

Table 5-3 shows the construction and materials of the building envelope for dynamic simulations. For the boundary conditions of the building, only the exterior walls exchanged heat with the external environment. The floor, inner wall, and ceiling were set to adiabatic, representing a middle floor of the building. The U-factor of the glazing and the solar heat gain coefficient were set to 2.0 W/(m<sup>2</sup>·K) and 36%, respectively.

Table 5-3. Construction and materials of the building envelope

Construction	Material	R value	Thickness	Conductivity	Density	Specific heat capacity
		(m <sup>2</sup> ·K)/W	mm	W/(m·K)	kg/m <sup>3</sup>	J/(kg·K)
Floor/ceiling	Carpet pad	0.22	—	—	—	—
	Mortar	—	70.0	2.31	2,322	832
	Concrete	—	101.6	2.31	2,322	832
	Stucco	—	25.4	0.72	1,856	840
	Gypsum board	—	15.9	0.16	800	1,090
Outside wall	Insulation	2.37	61.5	0.03	10	1400
	Gypsum board	—	15.9	0.16	800	1,090
	Gypsum board	—	15.9	0.16	800	1,090
Inside wall	Gypsum board	—	15.9	0.16	800	1,090

Figure 5-3 shows the schedule of internal heat gain. Weather data location was obtained from Copenhagen, and the maximum values of density of occupants, lighting gain, and equipment gain were 0.05 person/m<sup>2</sup>, 6.9 W/m<sup>2</sup>, and 8.0 W/m<sup>2</sup>, respectively. As shown in Figure 5-3, the internal heat gain was varied according to a schedule.

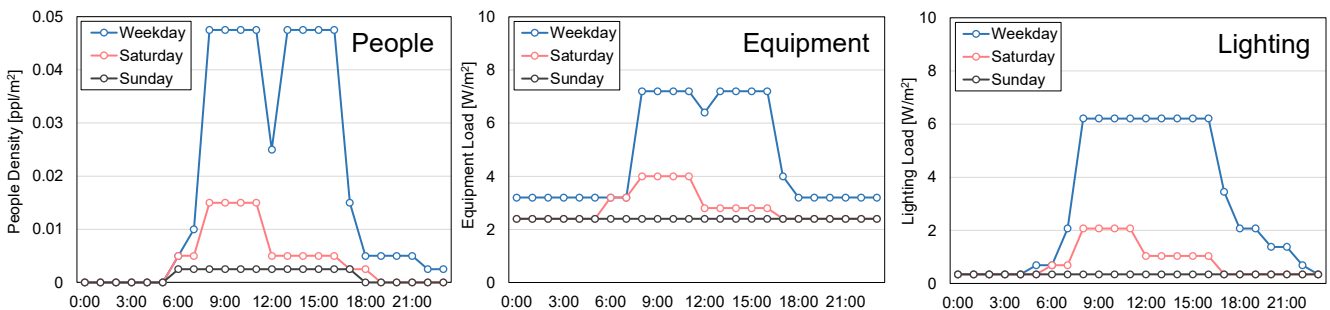


Figure 5-3. Schedule of internal heat gain

A packaged VAV system with reheat was selected as the typical all-air system, and the TABS was selected as the radiant system. In ASHRAE Standard 90.1, Appendix G [11], the baseline HVAC system was applied by building type, number of floors, conditioned floors, and climate zones. EnergyPlus Weather (EPW) data for Copenhagen (climate zone 5A) was used. The packaged VAV system was operated during the occupied hours on weekdays. A direct-expansion (DX) cooling coil was used for cooling, and the heat source for heating was a gas boiler.

The TABS was operated outside of occupancy for 12 hours per day. Cross-linked polyethylene (PEX) pipes were embedded in the middle of the mortar (70-mm thick) above the slab, which circulated water to absorb heat gain in the room or emit heat into the room from the ceiling surface. Because the TABS could not provide dehumidification or ventilation, it was coupled with a dedicated outdoor air system (DOAS) [12]. The ‘Low temperature radiant systems’ component in EnergyPlus was used to simulate the TABS [13,14]. A 70 mm mortar layer was added to the structural slabs to embed the TABS piping. For comparison under the same conditions, mortar was added to the slab for both the VAV system and TABS.

Both the VAV and DOAS systems were operated at the same cooling and heating setpoints. The required outdoor air flow rate of  $30 \text{ m}^3/(\text{h} \cdot \text{ppl})$  was supplied per person by the ventilation system [15]. The period from May to September was set as the cooling season, and the rest of the year as the heating season.

The cooling and heating setpoints for the VAV system and the DOAS during the occupied hours were  $24^\circ\text{C}$  and  $21^\circ\text{C}$ , respectively, and the room temperature dead-band for the TABS was  $20\text{--}23^\circ\text{C}$  throughout the year. The dead-band of the TABS was selected through a sensitivity analysis of several dead-bands to achieve both energy efficiency and thermal comfort. TABS was operated on/off control with the constant supply water flow rate based on the dead-band. The air flow rate of the VAV system was operated at  $0.06\text{--}0.27 \text{ m}^3/\text{s}$  during the occupied hours, and the air flow rate of the DOAS system was operated at  $0.02\text{--}0.08 \text{ m}^3/\text{s}$ . The supply water temperature and dead-band of TABS was selected within the values given in the REHVA guideline [16].

For the TABS, only the ceiling was used as the radiant surface. As the PEX tubing was embedded in the topping slab on the structural slab of the TABS building, this would lead to a heat exchange between the zones above and below the slab. To determine the validity of this modelling simplification, energy simulations were conducted using two types of models for TABS. One was a single room model used, and the other was a multiple zone model with three floors (i.e., top, middle, and bottom floors) combined. The boundary conditions for both simulation models were set adiabatic on the uppermost roof and the lowermost floor. The results showed that the difference in modelling resulted in a difference of up to 0.2 and 0.3 K for heating and cooling seasons, respectively. The differences in average heating and cooling capacities were up to 0.4 and 0.4  $\text{W}/\text{m}^2$ , respectively. Therefore, it was concluded that the modelling strategies had no significant differences for the purpose of this study, and therefore the results for the simplified model was used for analysis.

Table 5-4 shows the HVAC strategies for dynamic energy performance simulations. For the VAV system with reheat, the

supply air flow rate was adjusted based on the occupancy schedule from 7:00 to 23:00, and the supply air temperatures were 12.8°C for cooling and 40.0°C for heating. The cooling and heating operations were automatically determined based on the indoor temperature for both the VAV system and TABS. For the TABS, only the ceiling was used as the radiant surface. The water supply was constant and an on/off control, and water was supplied on weekdays for 12 hours from 6:00 p.m. to 6:00 a.m. [17]. The thermal conductivity of the tubing of the pipes was 0.35 W/(m·K) [18], and the inner and outer diameters of the pipes were 0.017 mm and 0.020 mm, respectively. The design water flow rate was calculated based on ISO11855-2 [19,20] and was set to 0.306 kg/s for both the heating and cooling modes. The DOAS was used to remove the latent heat load and any sensible heat load that could not be removed by the TABS. To dehumidify the office room, the DOAS was operated in accordance with the occupancy schedule based on occupant density, as shown in Figure 5-3.



Table 5-4. HVAC strategies for dynamic energy performance simulations

General information	Values/Inputs	Units
DNK_Copenhagen.061800_IWEC.epw	-	-
Occupant density	0.05	ppl/m <sup>2</sup>
Lighting gains (maximum value)	6.9	W/m <sup>2</sup>
Equipment gains (maximum value)	8.0	W/m <sup>2</sup>
Cooling setpoint during occupied hours	24	°C
Heating setpoint during occupied hours	21	°C
Requirement of mechanical ventilation	30	m <sup>3</sup> /(h-person)
Packaged VAV system with reheat (all-air system)		
DOAS (with radiant system)	Values/Inputs	Units
Supply air flow rate (VAV system)	0.06–0.27	m <sup>3</sup> /s
Supply air flow rate (DOAS)	0.02–0.08	m <sup>3</sup> /s
Supply air schedule	7:00–23:00	-
Supply air temperature for cooling	12.8	°C
Supply air temperature for heating	40	°C
Thermally Active Building System (TABS)	Values/Inputs	Units
Radiant surfaces	Ceiling	-
Supply water flow method	Constant	-
Supply water schedule	18:00–6:00	-
Hydronic tubing conductivity for PEX	0.35	W/(m·K)
Hydronic tubing inside diameter	0.017	m
Hydronic tubing outside diameter	0.020	m
Supply water temperature for cooling	18	°C
Design return water temperature for cooling	21	°C
Supply water temperature for heating	21	°C
Design return water temperature for heating	18	°C
Room temperature dead-bands for TABS	20-23	°C
Design supply water flow rate based on ISO11855	0.306	kg/s

5.2.3 Embodied carbon calculation

Building parts can be categorized into walls, floors, ceilings, and structural framing. Each building part was modelled in 3D to obtain its surface area and shape geometry. The embodied carbon emissions were calculated by multiplying the mass, surface, or volume by the corresponding emission factor. Embodied carbon emissions for categories A1–A3, C3, C4, and D were calculated with reference to the LCA database provided in BR18. The carbon-emission factors in the database were obtained from Ökobaudat [21], except for concrete, which was obtained from an EPD [22]. The reference values are presented in Appendix B. Because there were missing data for the carbon emission factors of certain building parts that could not be included in the LCA calculation results, the embodied carbon was estimated to be somewhat lower.

The embodied carbon emissions for category B4 (replacement) are the sum of A1–A3, C3, and C4, when the product lifespan is less than 50 years. In this study, the product lives of the ceiling panels (only for the VAV system) and carpets were assumed to be 40 and 15 years, respectively [23], and other building components were not accounted for in B4, as they were assumed to have a product lifespan of 50 years. This means that the ceiling panel was replaced once, and the carpets were replaced three times during the timeframe of this analysis. The HVAC system was assumed to be replaced once every 25 years. As shown in Figure 5-4, the boundaries of the embodied carbon calculation included building components (walls, floors, ceilings, and windows) and HVAC components (ducts, pipes, fans, pumps, ventilation units, and heat source equipment, excluding heat exchangers and coils) related to the southern office zone of the middle floor. Lighting and electrical outlets were not considered in either the embodied or operational carbon even if they were inside the room. Carbon emissions from other building parts, such as shafts and elevator components, were disregarded in the embodied carbon calculation. The embodied carbon of the basement and roof were obtained from the average values of Danish office buildings [24].

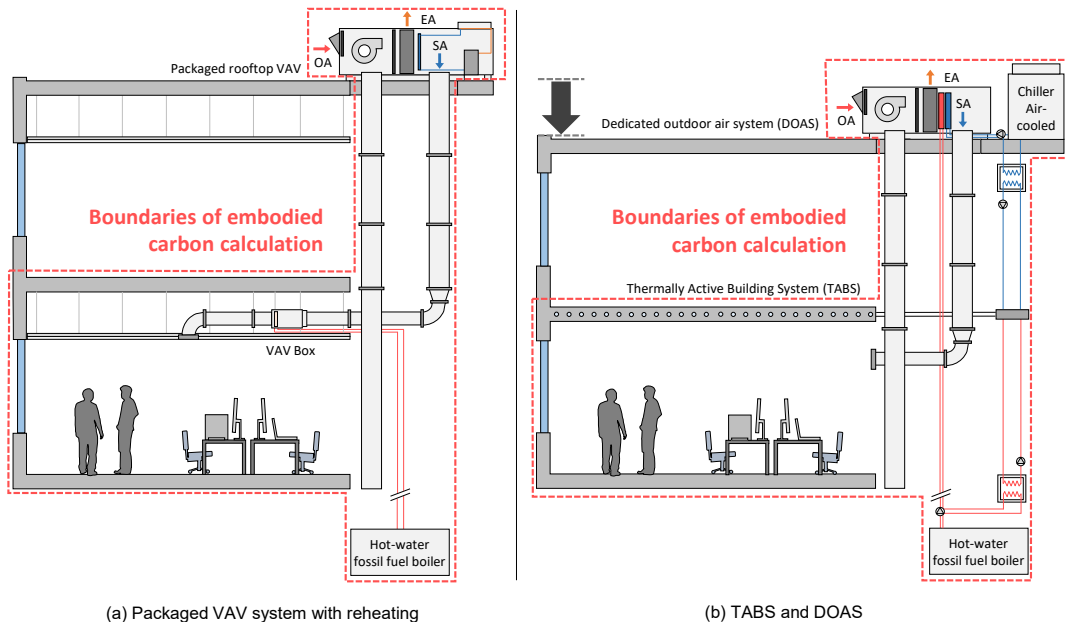


Figure 5-4. Boundaries of embodied carbon calculation

Table 5-5 shows the embodied carbon factor for each building part referenced in BR18. The embodied carbon of a building can be mainly categorized into three types: structure, surface, and MEP. A 3D modeling tool and graphical user interfaces were used to calculate the volume of each building component [25]. Structural parts included columns, beams, and floor slabs. The structure type studied was reinforced concrete, and the quantities of reinforcements in the concrete for the columns, beams, and floor slabs were set to 450 kg/m<sup>3</sup>, 350 kg/m<sup>3</sup>, and 135 kg/m<sup>3</sup>, respectively [26]. Surface parts were walls, ceilings, floor finishes, and windows in this study. Embodied carbon was calculated mainly by multiplying the surface area by the carbon emission factor. HVAC parts included ducts, pipes, heat sources, fans, pumps, and ventilation units. Based on the sizing results of the dynamic simulation, the capacity of each equipment was determined and multiplied by the carbon emission factor to estimate the embodied carbon of HVAC parts. Technical note AIVC 65 [27] was referenced for modeling the ductwork, and EN 15316-3 was referenced for modeling the piping [28].

Table 5-5 Embodied carbon factor for each building component referenced from the executive order on Building Regulations 2018 in Denmark

Category	Building part	ID <sup>a</sup>	Units	Carbon emission factor [kgCO <sub>2</sub> -eq/Units]			
				A1–A3	C3	C4	D
Building components	Reinforcing mesh (steel)	#G0148 #G0204	kg	0.7	0.0	0.0	-0.4
	Concrete	EPD	m <sup>3</sup>	261.0	6.8	5.0	-4.6
	Ceiling panel	#G1094	m <sup>2</sup>	3.5	0.0	0.0	N/A
	Carpet flooring	#G2006	m <sup>2</sup>	N/A	4.0	N/A	-1.6
	Gypsum board	#G0949	m <sup>2</sup>	1.4	N/A	0.1	N/A
	Exterior wall	#G0330	m <sup>3</sup>	242.4	13.5	N/A	-4.1
	Insulation	#G0043	m <sup>3</sup>	59.5	N/A	75.2	-39.6
	Window frame	#G0184	m	15.8	0.7	N/A	-9.5
	Glazing	#G0984	m <sup>2</sup>	13.3	N/A	0.2	N/A
HVAC system	Air duct	#G0499	kg	2.7	N/A	N/A	N/A
	Piping: Radiant system	#G0140	m <sup>2</sup>	7.7	6.7	N/A	-2.8
	Gas boiler	#G0177	PCS	446.2	9.2	0.6	-63.1
	Pump <50 W	#G0902	PCS	13.2	0.4	0.0	-2.5
	Pump 50–250 W	#G0372	PCS	26.5	0.9	0.0	-5.1
	Pump 250–1,000 W	#G0466	PCS	132.3	4.3	0.2	-25.3
	Ventilation unit 1,000 m <sup>3</sup> /h	#G0343	PCS	372.1	0.6	0.1	-212.1
Ventilation unit 60 m <sup>3</sup> /h	#G0130	PCS	25.3	4.5	0.1	-11.7	

<sup>a</sup> ID, identification number; G, generic data from Ökobaudat [21].

## 5.3 Results

### 5.3.1 Indoor thermal comfort

Figure 5-5 shows the daily operative temperature and outdoor air temperature of representative days in the heating and cooling seasons. As described in the previous section, TABS and the VAV system had different control strategies. For the radiant system, DOAS was operated during the daytime for ventilation and supplementary heating and cooling when necessary, and TABS was operated at night for pre-cooling and pre-heating the concrete slab. The VAV system was operated only during occupied hours. In the summer season, the operative temperature of the radiant system was up to 1.3°C lower at night than the operative temperature of the all-air system. In the winter season, there was little difference in the operative temperature between the two HVAC systems.

Figure 5-6 and Table 5-6 show the temperature ranges and thermal comfort category compliance during the occupied hours. In office spaces, the default indoor operative temperature ranges corresponding to Category II of EN16798-1:2019 are 20–24°C and 23–26°C for the heating season and cooling seasons, respectively [29]. The percentage of hours when the indoor temperatures were within Category II during the occupied hours was calculated. The period from May to September was set as the cooling season, and the rest of the year was set as the heating season [17]. The operative temperature during the occupied hours (8:00 to 17:00 on weekdays) was used. The results showed that the indoor operative temperature was within Category II for more than 90% of the time during the summer and winter seasons for both the VAV system and TABS. Since both systems resulted in similar indoor thermal environments, it was possible to compare them in terms of energy use and carbon emissions.

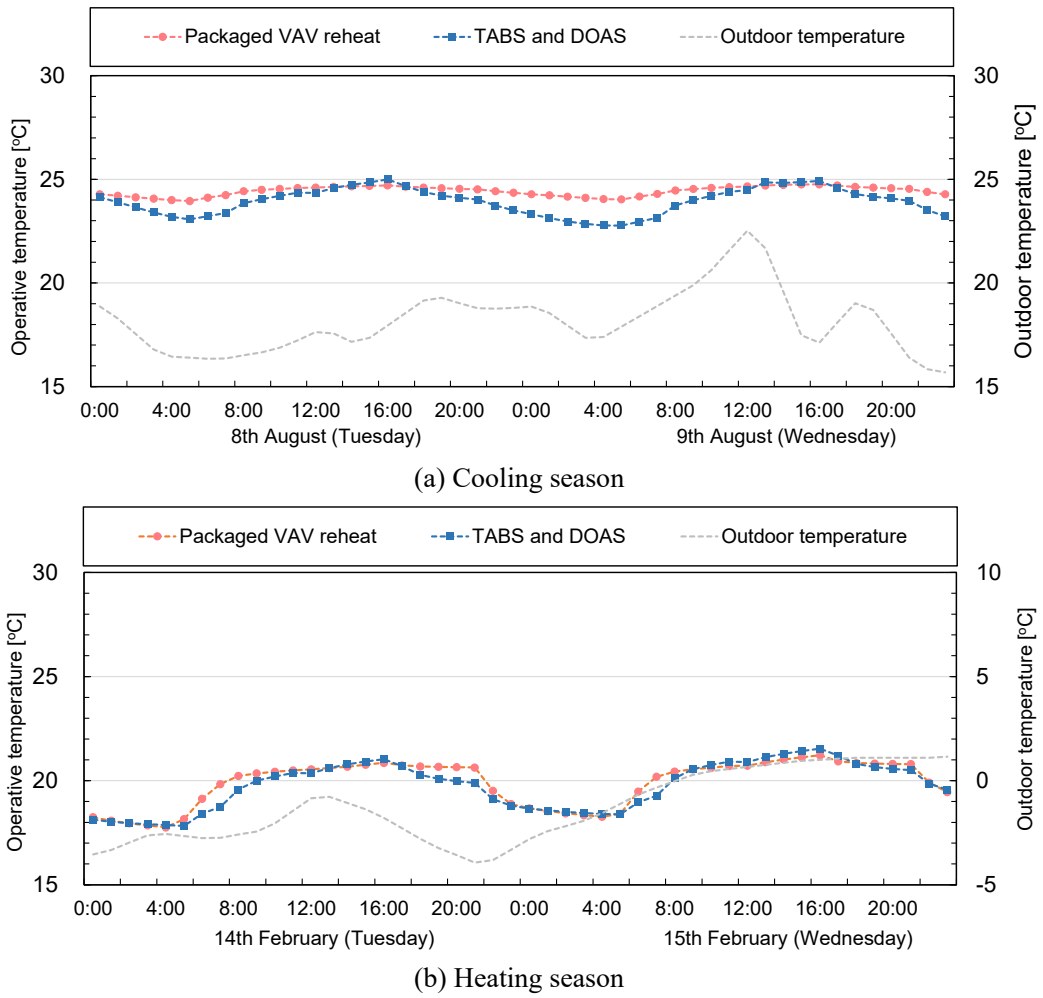


Figure 5-5. Daily operative temperature and outdoor air temperature

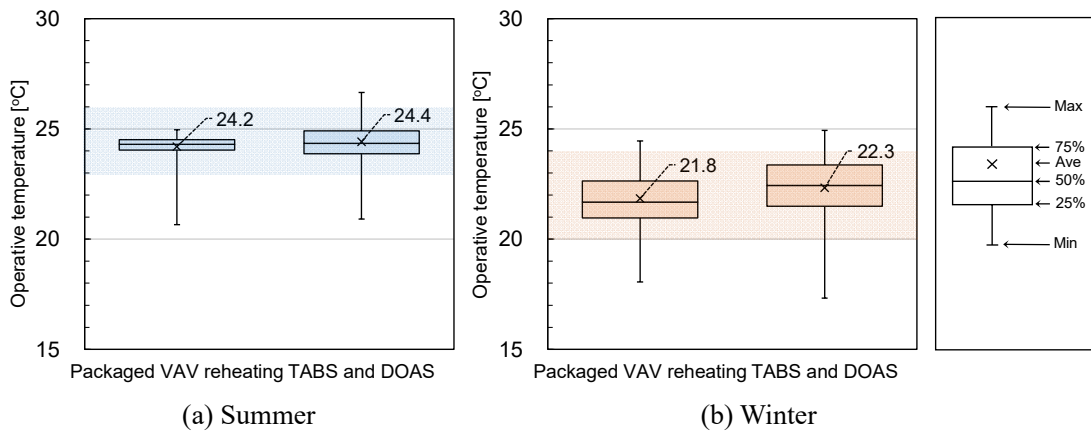


Figure 5-6. Operative temperature in the office building during occupied hours (8:00–17:00)

Table 5-6. Percentage of time in Category II of EN16798-1 [29]

Season	Packaged VAV reheat	TABS and DOAS
Summer	96%	95%
Winter	94%	92%

\* EN16798-1:2019 Category II; cooling season, 23–26°C; heating season, 20–24°C

**5.3.2 Operational energy and carbon emissions**

Figure 5-7 shows the annual total primary energy use per conditioned floor area of the HVAC system, calculated based on the primary energy conversion factor from ISO52000 [7]. As a gas boiler was used for heating, the conversion factor for gas (1.1 kWh/kWh) was used. The conversion factor for electricity (2.5 kWh/kWh) was used for the DX cooling coil, chiller, fans, and pumps. The annual primary total energy use of the HVAC systems were 19.0 kWh/m<sup>2</sup>/year and 12.6 kWh/m<sup>2</sup>/year for the VAV system and TABS, respectively. Meanwhile, the heating and cooling energy uses of the VAV system were 11.4 kWh/m<sup>2</sup>/year and 5.2 kWh/m<sup>2</sup>/year, respectively. For the TABS with a DOAS, the heating and cooling energy uses were 5.1 kWh/m<sup>2</sup>/year and 4.9 kWh/m<sup>2</sup>/year, respectively. For auxiliary equipment such as fans and pumps, fans (2.3 kWh/m<sup>2</sup>/year) accounted for most of the energy use in the VAV system, while fans (1.6 kWh/m<sup>2</sup>/year) and pumps (1.1 kWh/m<sup>2</sup>/year) yielded similar energy uses for the TABS and DOAS. The DOAS was operated in the same manner as the VAV system, with cooling and heating setpoints of 24°C and 21°C, respectively. Because the TABS handled sensible heat, the DOAS was mainly used to supply dehumidified outside air. The results showed that the primary energy saving using the TABS and DOAS was 34% relative to the VAV system. For the VAV system and DOAS, air was always supplied at the minimum flow rate for ventilation when there were no heating or cooling loads. The TABS operated 449 hours in the heating mode and 800 hours in the cooling mode.

It should be noted that the climatic conditions have a large influence on the primary energy use. For the heating season, the DOAS accounted for 60% of the heating energy for the radiant system model because the cold outside air needed to be heated. For the cooling season, due to cool and low-humidity climate in Copenhagen, 98% of the sensible cooling was handled with TABS. The VAV system also benefited from the cool summer temperature with the use of an economizer. As a reference, the use of an economizer contributes to a reduction in cooling energy use by 14.3 kWh/m<sup>2</sup>/year for the VAV system and 1.9 kWh/m<sup>2</sup>/year for the DOAS system in this study. Both systems had an economizer.

Figure 5-8 shows the annual total operational carbon emissions of the HVAC systems per conditioned floor area, calculated based on the emission factor from ISO52000. A value of 0.220 kgCO<sub>2</sub>-eq/kWh was used for natural gas and 0.420 kgCO<sub>2</sub>-eq/kWh was used for electricity. The annual total operational carbon emissions of the HVAC systems were 3.6 kgCO<sub>2</sub>-eq/m<sup>2</sup>/year and 2.3 kgCO<sub>2</sub>-eq/m<sup>2</sup>/year for the VAV system and TABS, respectively.

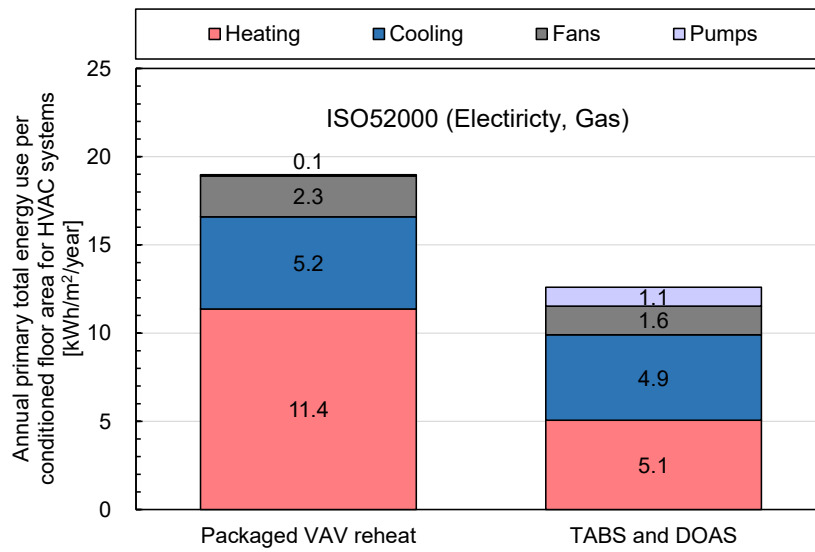


Figure 5-7. Annual primary total energy use per conditioned floor area for HVAC systems

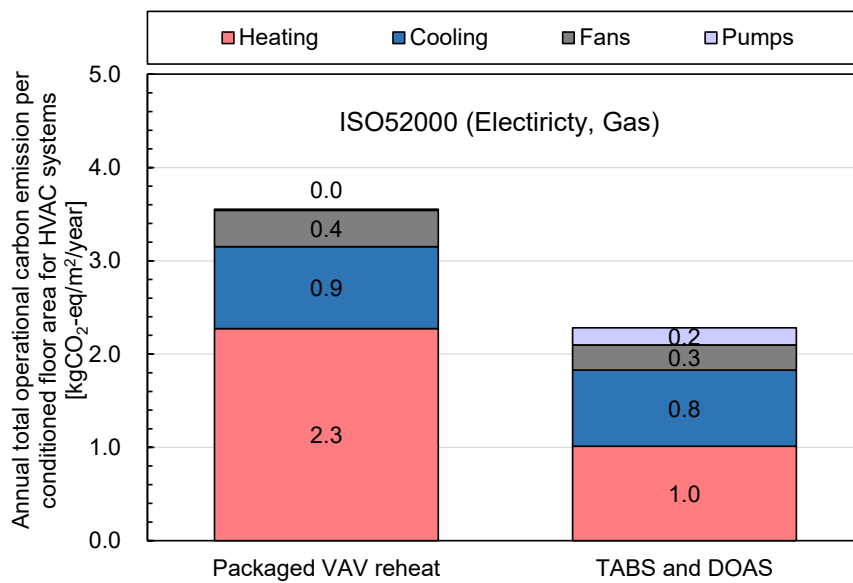


Figure 5-8. Annual total operational carbon emissions per conditioned floor area for HVAC systems

Figure 5-9 shows the annual total operational carbon emissions per conditioned floor area for the HVAC systems for different carbon emission factors and heating sources. From ISO52000 [7], 0.220 kgCO<sub>2</sub>-eq/kWh and 0.420 kgCO<sub>2</sub>-eq/kWh were used for gas and electricity, respectively. From BR18 [4], 0.225 kgCO<sub>2</sub>-eq/kWh, 0.105 kgCO<sub>2</sub>-eq/kWh, and 0.187 kgCO<sub>2</sub>-eq/kWh were used for gas, district heating, and electricity, respectively. Regarding the results of BR18 with gas as the heating source, the annual total operational carbon emissions of the HVAC systems were 2.9 kgCO<sub>2</sub>-eq/m<sup>2</sup>/year in the all-air system and 1.6 kgCO<sub>2</sub>-eq/m<sup>2</sup>/year in the TABS. Regarding the results of BR18 with district heating, the annual total operational carbon emissions of the HVAC systems were 1.7 kgCO<sub>2</sub>-eq/m<sup>2</sup>/year and 1.0 kgCO<sub>2</sub>-eq/m<sup>2</sup>/year in the all-air system and TABS, respectively. Regardless of the heating source or carbon emission factor, the operational carbon emissions of the TABS and DOAS were always lower than those of the all-air system in this case study.

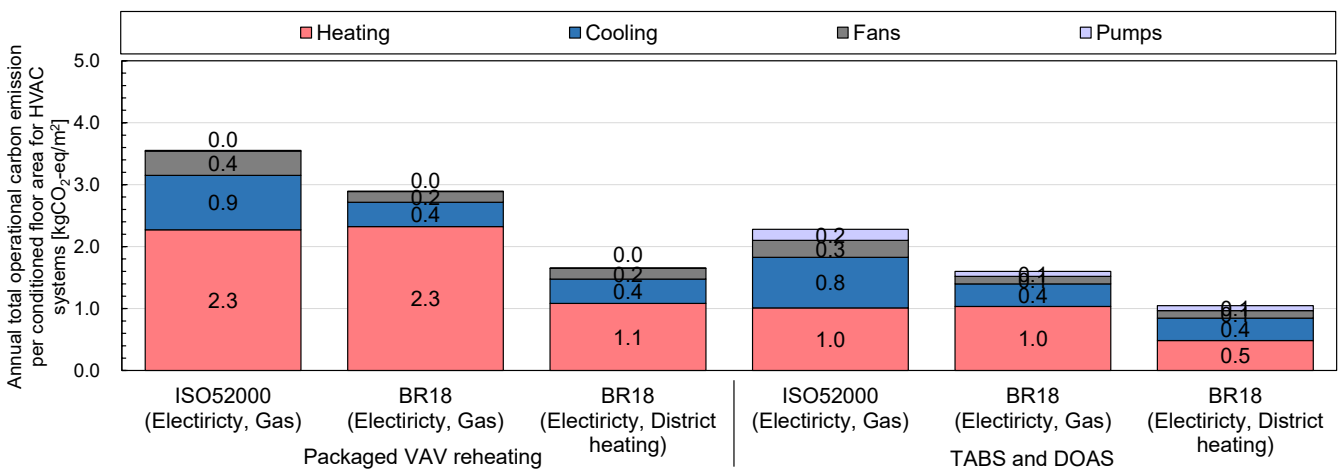


Figure 5-9. Annual total operational carbon emissions per conditioned floor area for HVAC systems for different carbon emission factors and heating sources

### 5.3.3 Whole life carbon emissions

Figure 5-10 shows the impact of the different building components on the investigated stages of whole life-cycle carbon. The whole life carbon (in kgCO<sub>2</sub>-eq/m<sup>2</sup>/year) of the concrete frame (2.7), reinforcing mesh (1.2–1.3), piping (0.0–0.6), heating (1.0–2.3), and cooling (0.4) were larger than those of other parts. In this study, the TABS was constructed differently from the VAV system in the following aspects: piping was installed, the suspended ceiling was removed, the ceiling height was reduced, and a DOAS was installed. There was little difference in the whole life carbon between the TABS and VAV system. Figure 5-11 shows the whole life carbon emissions (A1–A3, B4, B6, C3, C4, and D) for the two cases. The whole life carbon excluding D was 10.1 kgCO<sub>2</sub>-eq/m<sup>2</sup>/year and 9.0 kgCO<sub>2</sub>-eq/m<sup>2</sup>/year for the VAV system and TABS, respectively. A1–A3, especially the concrete frames and reinforcing frame, accounted for almost half of the whole life carbon, and this result is similar to those of previous studies [10,30]. For the VAV system, the percentages of embodied and operational carbon to whole life carbon (excluding D) were 71% and 29%, respectively. For the TABS, the percentages of embodied and operational carbon to whole life carbon (excluding D) were 82% and 18% (excluding D), respectively. In terms of the whole life carbon for the total floor area of the building (three floors of the medium office



building: 4980 m<sup>2</sup>) over the life span of 50 years, the whole life carbon excluding D was 2515.5 tCO<sub>2</sub>-eq and 2246.6 tCO<sub>2</sub>-eq for the VAV system and TABS, respectively. Total saving with TABS compared to the VAV system was 268.9 tCO<sub>2</sub>-eq at a building life span over 50 years.

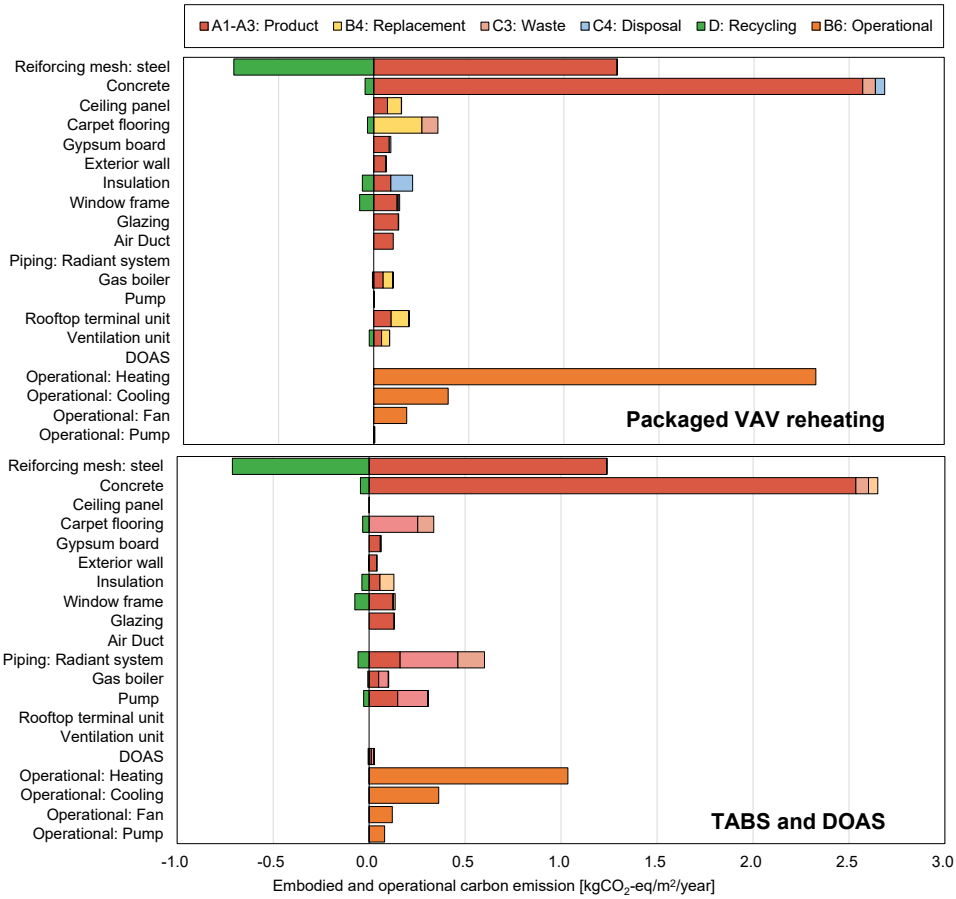


Figure 5-10. Impact of different building parts on the whole life-cycle carbon investigated

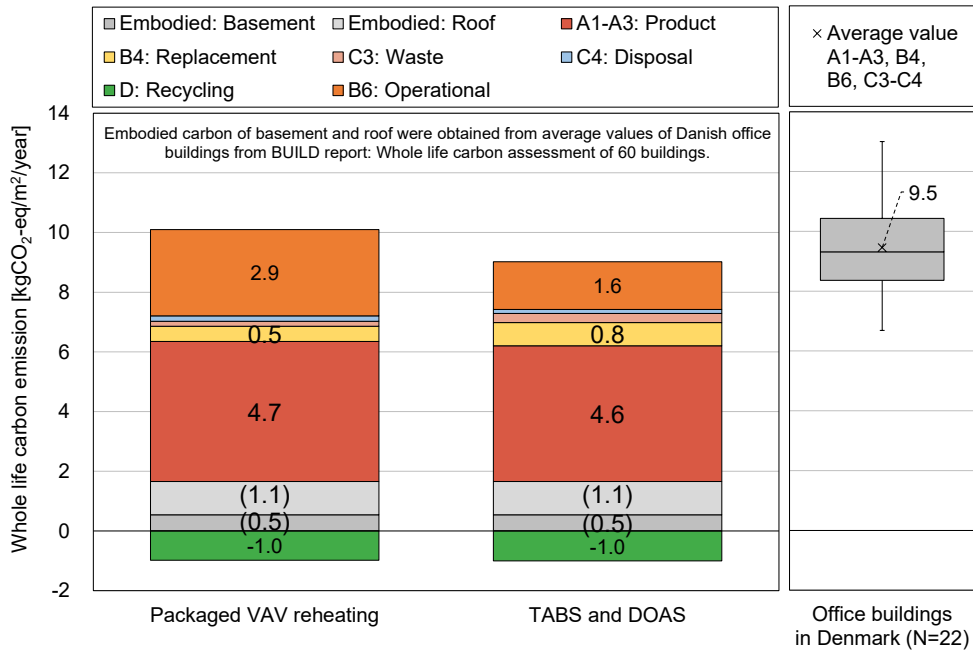


Figure 5-11. Whole life carbon (A1–A3, B4, B6, C3, C4, D)

### 5.4 Discussion

Many studies have been conducted on the LCA of buildings. However, most studies have not compared their values with benchmarks or limit values, and few have evaluated whole life carbon by encompassing building structures, façades, and MEP [31,32]. Most whole life carbon studies disregard indoor environmental quality factors, such as indoor thermal comfort, when estimating operational carbon [33]. The strength of this study is that it comprehensively examined the replacement stage (B4), use stage (B6), end-of-life stage (C3, C4), and benefits (D), in addition to the product stage (A1–A3). Operational carbon emissions were obtained from the annual calculation results of the dynamic simulations. Embodied carbon emissions were also calculated for air conditioners, pumps, ventilation units, and pipes among the HVAC components.

Figure 5-12 shows the difference in whole life carbon of the radiant system compared to that of the all-air system. Note that positive values indicate that the whole life carbon increased for the radiant system and negative values indicate that it decreased for the radiant system. It was hypothesized that the installation of a TABS would result in a reduction in the whole life carbon compared to that of the VAV system. This was because the installation of a TABS was expected to contribute to reducing both embodied and operational carbon owing to the following factors: improved plant efficiency owing to lower water temperature for heating and higher water temperature for cooling, peak-load shifting with the thermal mass of the building, lower building height, omission of ceiling panels, reduction of ducts, and downsizing of the heat source and air handling units. However, Figure 5-12 shows that the implementation of the TABS contributed to

reducing operational carbon (-1.29 kgCO<sub>2</sub>-eq/m<sup>2</sup>/year) and an increase in embodied carbon (+0.21 kgCO<sub>2</sub>-eq/m<sup>2</sup>/year). Although lowering the floor height, reducing ducting, and downsizing the HVAC equipment contributed to reducing the embodied carbon, installing a radiant system (e.g., PEX piping) resulted in an increase in the total embodied carbon. The whole life carbon for an office building was estimated in this study, and the results were 10.1 kgCO<sub>2</sub>-eq/m<sup>2</sup>/year and 9.0 kgCO<sub>2</sub>-eq/m<sup>2</sup>/year for the VAV system and TABS, respectively. Both values are close to the average whole life carbon of 9.6 kgCO<sub>2</sub>-eq/m<sup>2</sup>/year for 22 office buildings [24]. Carbon reduction by the TABS was 1.1 kgCO<sub>2</sub>-eq/m<sup>2</sup>/year. Refrigerant leakage is a major source of carbon emissions in packaged VAV systems. The impact of refrigerant leakage (B1: use) was excluded because the LCA boundary of BR18 was applied. If refrigerant leakage was taken into account, the embodied carbon emission of the VAV system would be larger, resulting in a larger difference with the TABS and DOAS. It should also be noted that the value of whole life carbon is highly dependent on the region owing to factors such as climate conditions, carbon intensity for electricity and gas, and LCA boundaries. Hence, the impact of each aspect on the whole life carbon of the building was discussed. Note that + means it increased for the radiant system and - means it decreased for the radiant system in the Figure 5-12.

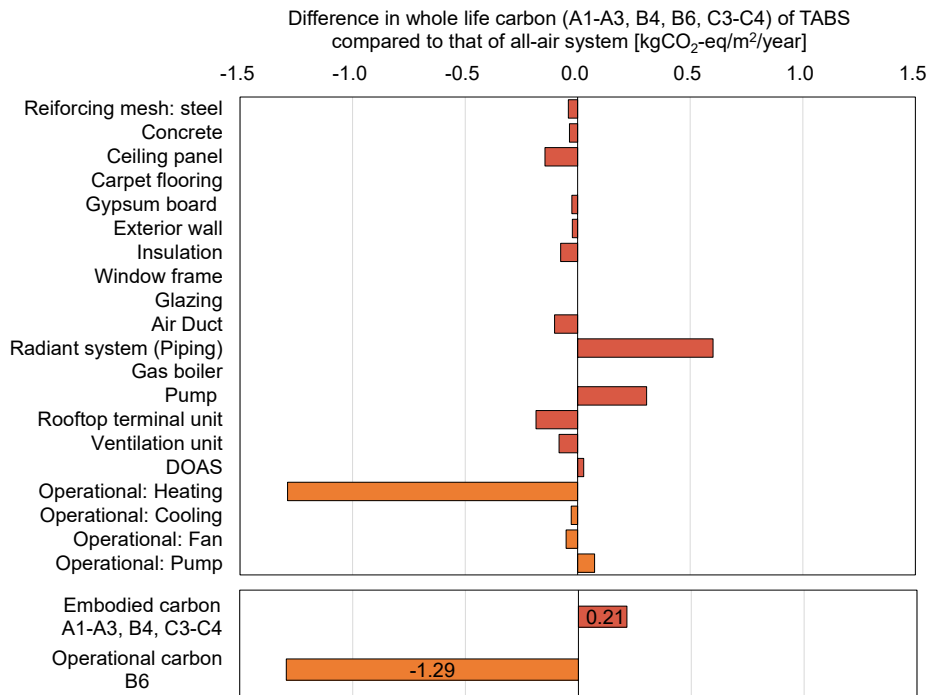


Figure 5-12. Difference in whole life carbon of the radiant system compared to that of the all-air system

In the future, when the carbon emission factor of electricity becomes even lower because of the large share of renewable sources, it is expected that the ratio of embodied carbon to whole life carbon in new construction will increase as the ratio of operational carbon decreases. In this study, the reduction in whole life carbon owing to the installation of the TABS was mainly the result of reduced operational carbon. If future carbon emission factors for electricity from renewable resources are also considered, the reduction in operational carbon owing to the implementation of TABS is expected to

be smaller. In this study, operational carbon was estimated assuming electricity supply from the grid, and on-site renewables such as solar photovoltaic were excluded. If dynamically varying carbon emission factors for electricity [34,35] would be considered in the future, TABS may contribute to a larger reduction of operational carbon emissions, as it can be operated more flexibly compared to an all-air system, owing to the activation of thermal mass. Furthermore, the reduction of the carbon emission factors from the grid would also contribute to the reduction of the embodied carbon, as the emissions in other stages e.g. material production would decrease as well.

Owing to global warming, new installations of cooling systems in areas where cooling demand has not existed before are expected to result in additional increases in embodied and operational carbon emissions from the building sector. In addition, future cooling demand increases could offset reductions in operational carbon owing to lower carbon emission factors from renewable resources. A previous case study compared the performance of a TABS and VAV system using future weather data for Copenhagen [36]. The simulation results showed a decrease in the heating demand and an increase in the cooling demand. Total primary energy use and operational carbon are expected to increase with future increases in outdoor temperatures.

In the present study, the LCA boundary from BR18 was applied, and the resulting whole life carbon emissions were 505 kgCO<sub>2</sub>-eq/m<sup>2</sup> for the VAV system and 450 kgCO<sub>2</sub>-eq/m<sup>2</sup> for TABS (assessment period: 50 years; A1–A3, B4, B6, C3–C4). Embodied carbon emissions were 360–370 kgCO<sub>2</sub>-eq/m<sup>2</sup> for both the VAV system and TABS (assessment period: 50 years; A1–A3, B4, C3–C4). From the report by Ramboll [37], the mean value of embodied carbon for Danish non-residential buildings was 348 kgCO<sub>2</sub>-eq/m<sup>2</sup>, which was close to the results of this study. Compared with the London Plan's benchmark of less than 1,400 kgCO<sub>2</sub>-eq/m<sup>2</sup> [38] and the LETI/RIBA's 2030s target of 750 kgCO<sub>2</sub>-eq/m<sup>2</sup> [39,40] for embodied carbon (A1–A5, B–C excluding B6 and B7) in office buildings, the embodied carbon of 360–370 kgCO<sub>2</sub>-eq/m<sup>2</sup> in this study is a considerably small value. The electricity conversion factors were not considerably different between Denmark and the UK, and the difference in the life-cycle stages was expected to be one of the reasons for this. It should be noted that it is difficult to compare whole life carbon emissions between countries. The LCA of BR18 does not include all stages because it focuses on a particularly environmentally important stage of the life cycle, and there is a lack of experience and routines to document other life cycle stages [24].

Another strength of the present study is the comparison of the two HVAC systems under very similar indoor thermal comfort conditions. In this case study, the operative temperature was shown to be a prerequisite for estimating whole life carbon emissions from the two HVAC systems. Consequently, both the all-air system and TABS were within the comfort zone for more than 90% of the occupied hours. Because the indoor temperature and the setpoints or dead-bands of heating and cooling have a significant impact on the results of operational carbon, indoor thermal comfort should be evaluated as a key indicator when estimating the whole life carbon of a building, especially when using dynamic simulations.

In this study, some architectural components were excluded from the LCA calculations. One example is the piles for

special soil conditions below a building. Soil conditions at a building site considerably impact the quantity of materials below the ground. Such circumstances include cases where a building is to be constructed on piles as a result of special soil conditions, such as a poor bearing capacity of the soil under the building, or if a building is built on a sloping site. In such cases, piles are excluded from the LCA calculation in accordance with BR18 [4]. To further reduce whole life carbon emissions, it is necessary to consider switching to materials with lower carbon emissions, optimize the operation of HVAC systems, and use more renewable energy sources.

## 5.5 Conclusions

The objective of this study was to quantify the effect of two different HVAC systems on whole life carbon emissions. A methodology to compare the whole life carbon of different HVAC systems was developed. Two types of models, one for dynamic building simulation and the other for measuring the mass of materials, were adopted in this novel approach. A Thermally Active Building System (TABS) and a packaged variable air volume (VAV) system with reheat were compared as a case study using the presented methodology with boundary conditions in Denmark. The comparison of the two HVAC systems were made under very similar indoor thermal conditions. The conclusions are as follows:

- Prior to comparing the whole life carbon emissions of the two HVAC systems, it was confirmed that both systems could provide very similar indoor thermal conditions. Both the VAV system and TABS yielded operative temperatures within the comfort ranges of EN16798-1:2019 for more than 90% of the occupied hours; therefore, a comparison could be made. It is critical to ensure similar indoor thermal environments when comparing systems and carrying out LCA studies.
- The annual primary total energy use of the HVAC systems were 19.0 kWh/m<sup>2</sup>/year and 12.6 kWh/m<sup>2</sup>/year for the VAV system and TABS, respectively. The result showed that TABS had 34% lower primary total energy use than the VAV system.
- The whole life carbon excluding D (recycling) was 10.1 kgCO<sub>2</sub>-eq/m<sup>2</sup>/year for the VAV system and 9.0 kgCO<sub>2</sub>-eq/m<sup>2</sup>/year for TABS. These values are close to the average whole life carbon of 9.6 kgCO<sub>2</sub>-eq/m<sup>2</sup>/year for 22 office buildings in Denmark. The result showed that TABS had 11% lower whole life carbon than the VAV system.
- The percentages of operational carbon to whole life carbon were 29% and 18% for the VAV system and TABS, respectively.
- The implementation of the TABS contributed to the reduction of operational carbon (-1.29 kgCO<sub>2</sub>-eq/m<sup>2</sup>/year) and a slight increase in embodied carbon (+0.21 kgCO<sub>2</sub>-eq/m<sup>2</sup>/year) compared to the VAV system.

This study was a case study evaluating a VAV system and TABS from an LCA perspective. The methodology presented in this study can be used for comparing different HVAC systems.

## References

- [1] O.B. Kazanci, *Low Temperature Heating and High Temperature Cooling in Buildings*, PhD Thesis, Kgs. Lyngby: Technical University of Denmark, 2016.
- [2] J. Babiak, B.W. Olesen, Dusan Petras, *Low temperature heating and high temperature cooling*, REHVA guidebook, 2007.
- [3] B.W. Olesen, *Thermo Active Building Systems Using Building Mass to Heat and Cool*, ASHRAE Journal, 2012.
- [4] *Building regulation 2018 (BR18)*, 2018. <https://byggningsreglementet.dk/> (accessed July 20, 2023)
- [5] EN 15978:2011, *Sustainability of construction works – Assessment of environmental performance of buildings – Calculation method*, CEN, 2011.
- [6] EnergyPlus, National Renewable Energy Laboratory (NREL). <https://energyplus.net/> (accessed July 20, 2023)
- [7] ISO 52000-1:2017, *Energy performance of buildings — Overarching EPB assessment — Part 1: General framework and procedures*, International Organization for Standardization, 2017.
- [8] National Renewable Energy Laboratory (NREL), *Commercial Reference Buildings*, 2022. <https://www.energy.gov/eere/buildings/commercial-reference-buildings> (accessed July 20, 2023)
- [9] P. Im, J.R. New, Y. Bae, *Updated OpenStudio Small and Medium Office Prototype Models*, 16th IBPSA International Conference & Exhibition on Building Simulation 2019 - Rome, 2019.
- [10] International Energy Agency, *Guideline for Design Professionals and Consultants Part 1: Basics for the Assessment of Embodied Energy and Embodied GHG Emissions*, IEA EBC Annex 57, 2016.
- [11] ANSI/ASHRAE/IES Standard 90.1-2019, *Energy Standard for Buildings Except Low-Rise Residential Buildings*, ASHRAE, 2019.
- [12] J. Murphy, *Common pitfalls in design and operation of a DOAS*, ASHRAE Journal, 2018.
- [13] R.K. Strand, K.T. Baumgartner, *Modeling radiant heating and cooling systems: Integration with a whole-building simulation program*, *Energy and Buildings*, 37, 389–397, 2005. <https://doi.org/10.1016/j.enbuild.2004.07.009>.
- [14] R.K. Strand, *Recent energy simulation model enhancements for radiant systems*, *Energy and Buildings*, 268, 112237, 2022. <https://doi.org/10.1016/j.enbuild.2022.112237>.
- [15] ANSI/ASHRAE/IES Standard 62.1-2022, *Ventilation and Acceptable Indoor Air Quality*, ASHRAE, 2022.
- [16] F. Bockelmann, S. Plessner, H. Soldaty, *Advanced system design and operation of GEOTABS buildings*, REHVA guidebook, 2013.
- [17] B.W. Olesen, F.C. Dossi, *Operation and control of activated slab heating and cooling systems*, CIB World Buildings Congress, 2004.
- [18] M. Achermann, G. Zweifel, *RADTEST – Radiant heating and cooling test cases*, International Energy Agency, 2003.
- [19] ISO 11855-2:2021, *Building environment design — Embedded radiant heating and cooling systems — Part 2: Determination of the design heating and cooling capacity*, International Organization for Standardization, 2021.
- [20] ISO 11855-1:2021, *Building environment design — Embedded radiant heating and cooling systems — Part 1:*

Definitions, symbols, and comfort criteria, International Organization for Standardization, 2021.

- [21] Ökobaudat. <https://www.oekobaudat.de/en.html> (accessed July 20, 2023)
- [22] EN 15804:2012+A2:2019, Sustainability of construction works. Environmental product declarations. Core rules for the product category of construction products, CEN, 2019.
- [23] BUILD, BUILD Lifetime table, Aalborg university, 2021.
- [24] R.K. Zimmermann, C.M. Ernst Andersen, K. Kanafani, H. Birgisdottir, Whole life carbon assessment of 60 buildings – possibilities to develop benchmark values for LCA of buildings, BUILD, Aalborg university, 2021
- [25] Rhinoceros. <https://www.rhino3d.co.jp/> (accessed July 20, 2023)
- [26] One Click LCA, Average Quantities of Reinforcement in Concrete, 2021.
- [27] P.G. Schild, M. Mysen, Recommendations on Specific Fan Power and Fan System, Technical Note AIVC 65, AIVC, 2009.
- [28] EN 15316-3: 2017, Energy performance of buildings - Method for calculation of system energy requirements and system efficiencies - Part 3: Space distribution systems (DHW, heating and cooling), European Committee for Standardization, CEN, 2017.
- [29] EN16798: 2019, Energy performance of buildings – Ventilation for buildings – Part 1: Indoor environmental input parameters for design and assessment of energy performance of buildings addressing indoor air quality, thermal environment, lighting and acoustics – Module M1-6, European Committee for Standardization, CEN, 2019.
- [30] P. Ylmén, D. Peñaloza, K. Mjörnell, Life cycle assessment of an office building based on site-specific data, *Energies*, 12, 1–11, 2019. <https://doi.org/10.3390/en12132588>.
- [31] M. Rabani, H.B. Madessa, M. Ljungstrom, L. Aamodt, S. Løvvold, N. Nord, Life cycle analysis of GHG emissions from the building retrofitting: The case of a Norwegian office building, *Building and Environment*, 204, 108159, 2021. <https://doi.org/10.1016/j.buildenv.2021.108159>
- [32] H. Zhang, J. Cai, James E. Braun, A whole building life-cycle assessment methodology and its application for carbon footprint analysis of U.S. commercial buildings, *Journal of Building Performance Simulation*, 16, 1, 38–56, 2023. <https://doi.org/10.1080/19401493.2022.2107071>
- [33] Á. Menacho, A. Marvuglia, E. Benetto, Occupant's health and energy use in an office building: A sensor-enabled life cycle assessment, *Building and Environment*, 236, 110274, 2023. <https://doi.org/10.1016/j.buildenv.2023.110274>
- [34] M. Frapin, C. Roux, E. Assoumou, B. Peuportier, Modelling long-term and short-term temporal variation and uncertainty of electricity production in the life cycle assessment of buildings, *Applied Energy*, 307, 118141, 2022. <https://doi.org/10.1016/j.apenergy.2021.118141>
- [35] B. Tranberg, O. Corradi, B. Lajoie, T. Gibon, I. Staffell, G.B. Andresen, Real-time carbon accounting method for the European electricity markets, *Energy Strategy Reviews*, 26, 100367, 2019. <https://doi.org/10.1016/j.esr.2019.100367>
- [36] K. Shindo, J. Shinoda, O.B. Kazanci, D.I. Bogatu, S. Tanabe, B.W. Olesen, Resiliency comparison of radiant cooling systems and all-air systems, *The 11th International Conference on Indoor Air Quality, Ventilation & Energy Conservation in Buildings (IAQVEC2023)*, E3S Web of Conf, Volume 396, 2023.

<https://doi.org/10.1051/e3sconf/202339601089>

- [37] M. Röck, A. Sørensen, Towards embodied carbon benchmarks for buildings in Europe #2 Setting the baseline: A bottom-up approach, RAMBOLL, 2022.
- [38] Mayor of London, London plan guideline – Whole Life-Cycle Carbon Assessments, 2022. <https://www.london.gov.uk/programmes-strategies/planning/implementing-london-plan/london-plan-guidance/whole-life-cycle-carbon-assessments-guidance> (accessed July 20, 2023).
- [39] RIBA 2030 Climate Challenge version 2, Royal Institute of British Architects (RIBA), 2021. <https://www.architecture.com/-/media/files/Climate-action/RIBA-2030-Climate-Challenge.pdf> (accessed Sep 14, 2023)
- [40] Embodied Carbon Target Alignment, London Energy Transformation Initiative (LETI), 2021. [https://www.leti.uk/\\_files/ugd/252d09\\_25fc266f7fe44a24b55cce95a92a3878.pdf](https://www.leti.uk/_files/ugd/252d09_25fc266f7fe44a24b55cce95a92a3878.pdf) (accessed Sep 14, 2023)



## Chapter 6:

# A full-scale study of the upfront and operational carbon of an all-air system and a radiant system in Japan

### Abstract

Climate change is a severe problem, with natural disasters causing extensive damage to buildings and urban scale. Global greenhouse gas (GHG) emissions should be reduced to prevent further acceleration of global warming. Whole life carbon emissions are the total GHG emissions, including operational and embodied carbon emissions, over the life cycle of buildings. Upfront carbon is sum of A1-A3: products and A4-A5: construction. Although the life cycle assessment guidelines of the Architectural Institute of Japan recommended that all categories be calculated, this study focused on the upfront carbon of a non-residential building. Inventory Database for Environmental Analysis (IDEA) and Environmental Product Declaration (EPD) were used for calculating upfront carbon. The results indicated that the upfront carbon was 783 kgCO<sub>2</sub>-eq/m<sup>2</sup> of the total. Concrete (264 kgCO<sub>2</sub>-eq/m<sup>2</sup>) and Steel (221 kgCO<sub>2</sub>-eq/m<sup>2</sup>) were the main sources of emissions compared to the other materials. The upfront carbon of the HVAC system was shown to be 26 kgCO<sub>2</sub>-eq/m<sup>2</sup> of the packaged system and 62 kgCO<sub>2</sub>-eq/m<sup>2</sup> of the radiant system, respectively. The findings of this study are expected to fill a gap in the knowledge base for building decarbonization.

### KEYWORDS:

Building energy, Embodied carbon, Upfront carbon, Radiant ceiling panel system (RCP), All-air system, Circular economy

## 6.1 Introduction

### 6.1.1 Net zero energy and net zero carbon building

Climate change is a severe problem, with natural disasters causing extensive damage to buildings and urban scale. Global greenhouse gas (GHG) emissions should be reduced to prevent further acceleration of global warming [1]. Since, the building sector accounted for 75% of the total GHG emissions in Tokyo [2], it is an urgent need to reduce carbon emissions in the building sector drastically. Based on the net Zero Energy Building (nZEB) concept, energy efficient buildings have been built in the past ten years [3][4]. It is very relevant to reduce the carbon emissions of building use stage by reducing energy use and utilizing renewable resources, such as photovoltaics and geothermal energy. In addition to operational carbon emissions, it is also essential to reduce carbon emissions over the entire building lifecycle. Embodied carbon emissions are the sum associated with materials, construction, and demolition processes throughout the whole lifecycle of a building [5]. Whole life carbon emissions are sum of operational carbon and embodied carbon [6]. In Japan, Zero Carbon Building (LCCO<sub>2</sub> net zero) Initiative committees have been set up for tackling for building decarbonization [7]. Based on the ISO21930:2022 [8] and EN15978:2011 [9], it comprises several stages, namely A1–A3: products, A4–A5: construction, B1–B7: use, C1–C4: end of life, and D: benefits and loads beyond the system boundary (reuse, recovery, and recycling potential). The World Business Council for Sustainable Development (WBCSD) [10] and ASHRAE Task Force for Building Decarbonization (TFBD) [11] have provided definitions of the scope of life cycle assessments (LCA). According to the definition, whole life carbon emissions are the total GHG emissions, including operational and embodied carbon emissions, over the life cycle of buildings. Embodied carbon emissions are the total GHG emissions based on the manufacturing, transportation, maintenance, and disposal of buildings. Upfront carbon is sum of A1-A3: products and A4-A5: construction. Operational carbon emissions are the total GHG emissions related to the operation of a building during the use stage.

### 6.1.2 Electrical grid

Figure 6-1 shows the annual average carbon intensity of electricity generation in Japan, 2009 to 2021 [12]. After 2011, carbon intensities in Japan have been increased as the share of thermal power generation increased in place of nuclear power generation. From the late 2010s to the present, carbon intensities were likely to be declined due to the high efficiency of thermal power generation and the installation of renewable energy sources. In 2021, adjusted value of annual average carbon intensities of electricity was 451 gCO<sub>2</sub>/kWh in Tokyo electric power company holdings (TEPCO). Compared to European countries, such as 187 gCO<sub>2</sub>/kWh in Denmark for 2023 [13], 190 gCO<sub>2</sub>/kWh in United Kingdom (UK) for 2023 [14], the carbon intensity of electricity in Japan was higher, resulting in whole life carbon of buildings are also expected to be higher. Since buildings used electricity for heating, cooling, ventilation, lighting and equipment, operational carbon is significantly affected by the value of the carbon intensity of electricity in the region. Embodied carbon is also affected by carbon intensity of electricity, since some components of a building, such as piles and steel frames made in electric furnaces and the equipment, were consumed electricity at the material production stage. As a part

of the upfront carbon (A1-A5) [15] reduction approach in one of the Japanese construction companies [16], electricity for Renewable Energy 100% (RE100) [17] was used to reduce carbon emissions at construction site (A5). There are three ways to achieve 100% renewable energy of buildings: installation of new onsite generation facilities, offsite renewable energy procurement contracts, and purchase of environmental value certificates.

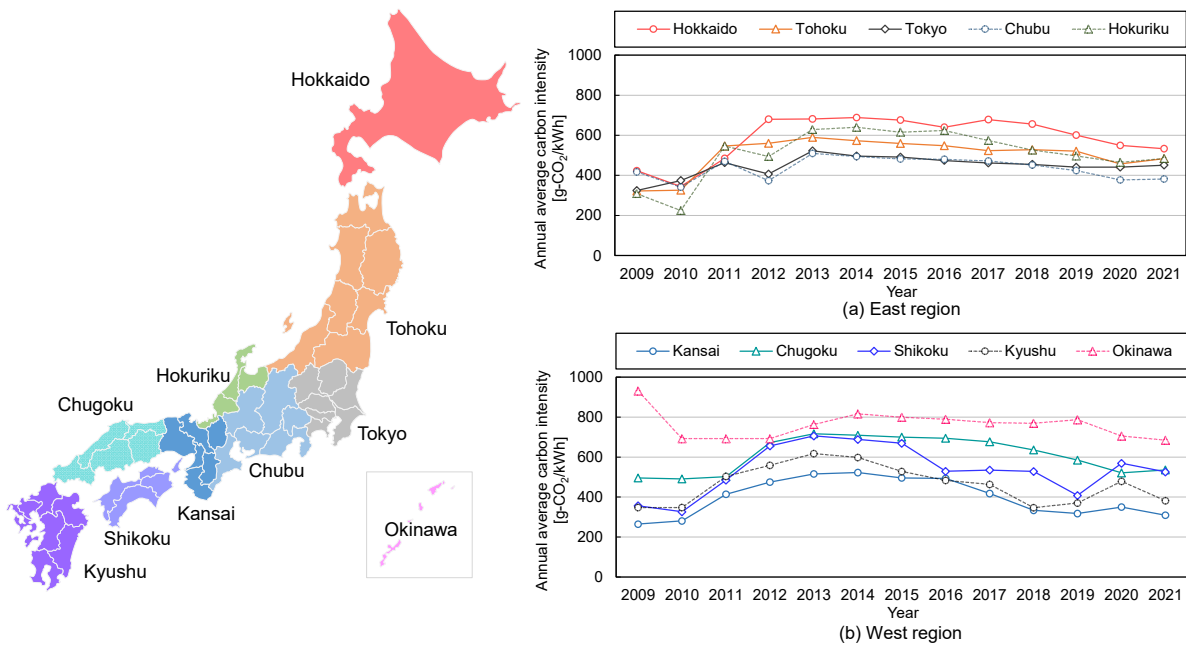


Figure 6-1. Annual average carbon intensity of electricity generation in Japan, 2009 to 2021 [12]

### 6.1.3 Life cycle assessment study in Japan

Studies on building Life Cycle Assessment (LCA) have been conducted in Japan for more than 20 years. Ikaga et al. summarized the Life Cycle Inventory (LCI) data on electrical and mechanical facilities of office and various kinds of buildings in Japan [18][19]. Figure 6-2 and Figure 6-3 show the upfront carbon of electrical facility, HVAC system, and sanitary system. Results indicated that Upfront carbon of the electrical facility ranged from 76-160 kgCO<sub>2</sub>-eq/m<sup>2</sup>, HVAC systems from 65-179 kgCO<sub>2</sub>-eq/m<sup>2</sup> and sanitary systems from 55-79 kgCO<sub>2</sub>-eq/m<sup>2</sup>, respectively. The upfront carbon for electrical and sanitation equipment was higher for buildings less than 1000 m<sup>2</sup>. The reason for this is that electrical and sanitary installations, which must be equipped even if the size of the building is small, are more numerous than HVAC installations. Another study investigated comparison of new construction project and renovated project on embodied carbon in Japan [20]. This study focused on embodied carbon, especially upfront carbon (A1-A3, A5), Demolition, transport, and waste processing (C1-C3). A renovated building was a logistics warehouse that has been converted to an office building. Compared to the new construction building, carbon emission from the renovated building was reduced to 43%, and the amount of waste was also reduced to 30%. One of the research projects clarified the resource circulation for 12 building materials used in non-structural parts, such as façade materials, interior material, fixtures, and fittings [21]. The results suggested that key factors for determining the resource circulation of the building material were reversibility of the composite material and recovery system that recycle the material. To reduce the burden of unit conversion between

foreground (material weight, area, and volume) and background (carbon intensity of material) data, Kobayashi et al. analyzed the current unit conversion by examining the 11 building LCA databases and proposed a method for constructing a unit conversion database [22].

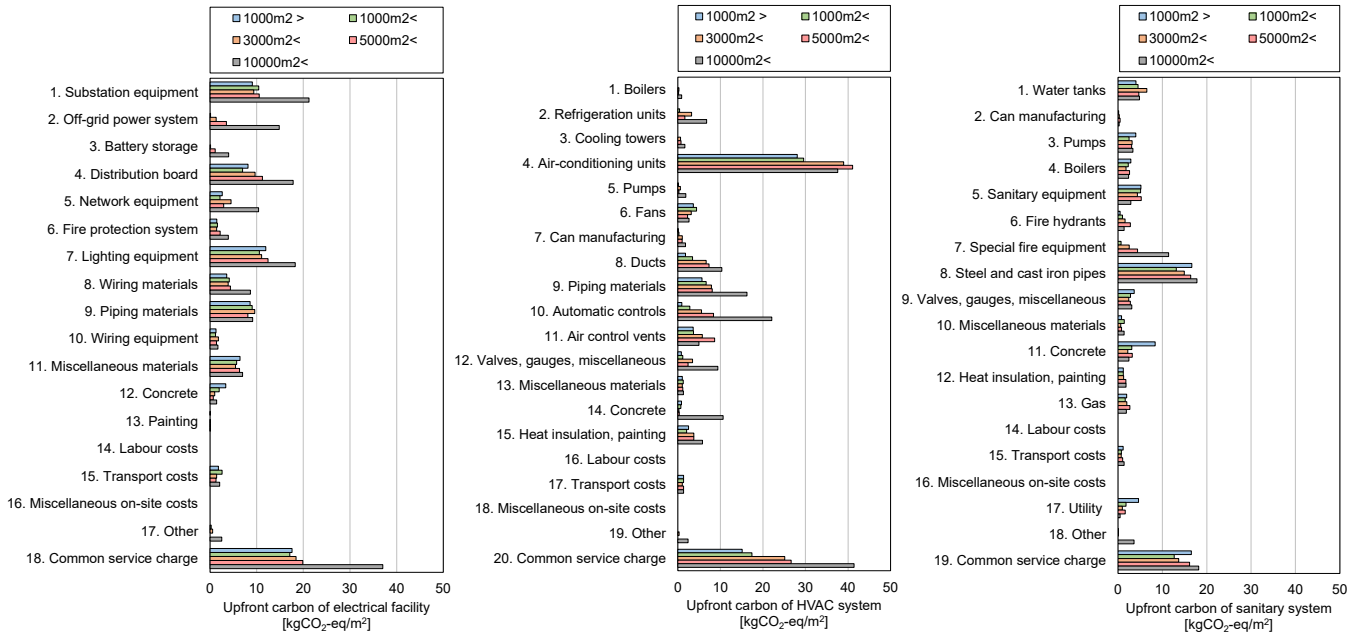


Figure 6-2. Upfront carbon of electrical facility, HVAC, and Sanitary equipment [18]

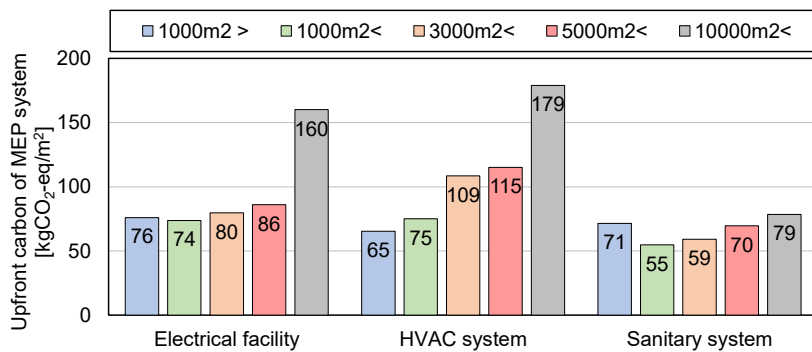


Figure 6-3. Upfront carbon of electrical facility, HVAC system, and Sanitary system [18]

### 6.1.4 Objective

Studies on the most LCA of buildings have focused on the shell and core. In general, there is a lack of embodied and whole life cycle carbon studies that explore the impact of different MEP systems. Previous chapter has highlighted that the whole life carbon of TABS with DOAS was 11% lower than that of a packaged VAV system in Denmark [23]. Therefore, in the present study, the selection of the HVAC system for the whole life carbon in Japan was also investigated, as different HVAC systems have different working principles and the potential for differences in both embodied and operational carbon. Different LCA databases, heating and cooling systems and carbon intensities of electricity in different regions - Europe and Japan - are expected to be a difference for the whole life carbon. As a simplified case study of

different HVAC systems, all-air and radiant systems were compared. Radiant systems are energy-efficient and resource-effective heating and cooling solutions for buildings [24]. A Radiant Ceiling Panel System (RCP) is a radiant system that combines water pipes for heating and cooling with ceiling panels [25]. A comparative study of variable air volume (VAV) system and radiant cooling with dedicated outdoor air system (DOAS) [26] concluded that the radiant system has used 34% less energy as compared to the VAV system after two years of operation [27]. If supply water temperature is close to room temperature like radiant system, the efficiencies of the chiller and heat pump will increase. Another feature of RCP is that it reduces duct and fan sizes compared to the all-air system. Given these features, it was hypothesized that radiant systems would perform better than all-air systems in terms of whole life carbon emissions.

The objective of this study is to quantify the effect of HVAC systems on whole life carbon emissions in Japanese case study. An all-air system, that is, a packaged variable refrigerant flow (VRF) system [28], was used as the reference system for comparison with a RCP. Two models were used: one for dynamic building simulation and the other for calculating the mass of materials (e.g., concrete). Dynamic building simulations were conducted to evaluate the indoor operative temperature and operational carbon emissions related to the HVAC systems. The embodied carbon emissions of the building were calculated based on the LCA guidelines for buildings published by Architectural Institute of Japan [29]. The entire life-cycle stages of a building were classified according to ISO 21931-1:2022 [8], ISO14044 [30], and ISO14040 [31].

### 6.2 Methods

The aim of this study is to analysis the embodied and operational carbon for two selected HVAC systems for a typical office and classroom building in Waseda university, Tokyo, Japan. Figure 6-4 shows the methodology for calculating operational and embodied carbon emissions in this study. The following are the detail explanation of this study.

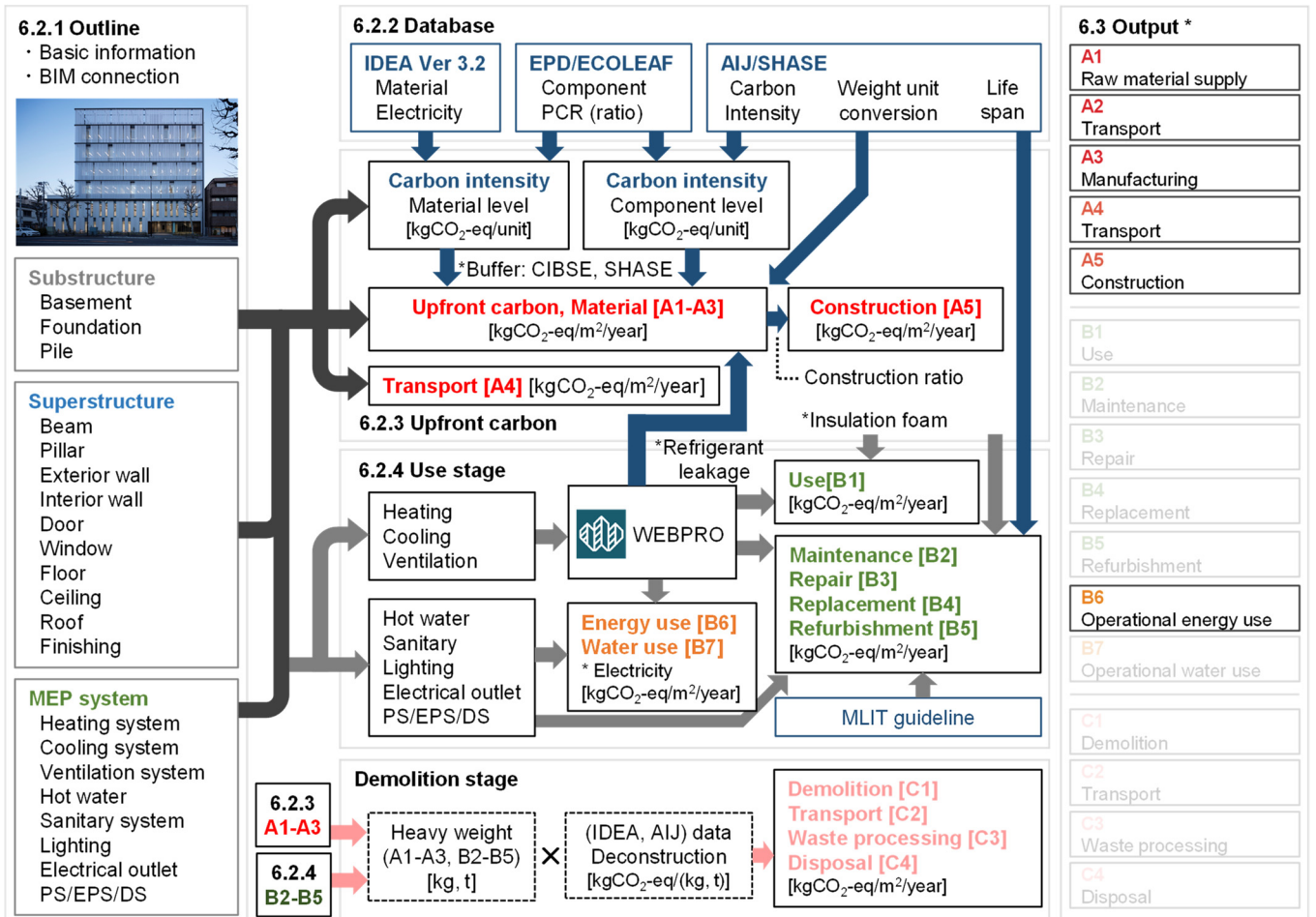


Figure 6-4. Methodology for calculating operational and embodied carbon emissions in this study



6.2.1 Outline of the building model

Figure 6-5 shows the interior and exterior view of the case study building [32][33]. This building was built in 2017 and was mainly used as a language classroom. The site area was 1,176 m<sup>2</sup>, the building area 881 m<sup>2</sup> and the total floor area was 3,974 m<sup>2</sup>. The building consists of six floors above ground and one basement floor. The main floor height was 3.75 m, and the ceiling height was 2.75 m. The building was constructed using pre-existing piles, with Reinforced Concrete (RC) structure in the basement and Steel based structure above ground floor.



(a) Exterior 1 [32]



(b) Exterior 2 [33]



(c) 1F Entrance



(d) 1F Lounge



(e) Classroom A



(f) Classroom B

Figure 6-5. Interior and exterior view of the case study building

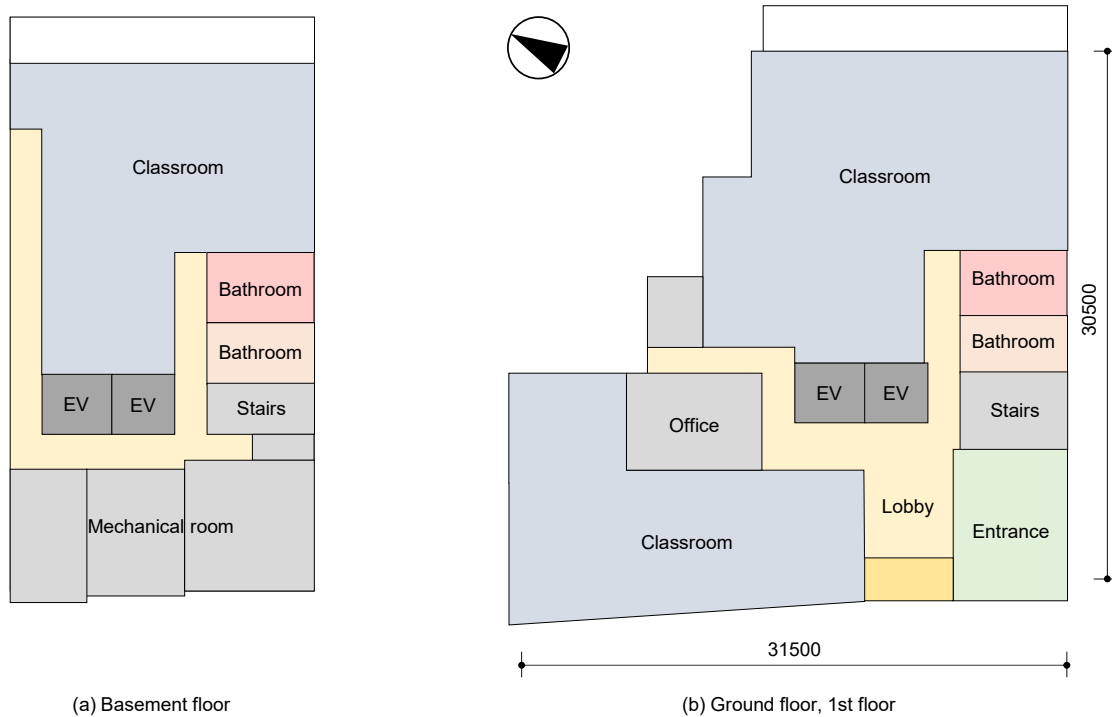


Figure 6-6. Zone layout of the basement and ground floor

The boundary for LCA study of the building was classified into three categories: Substructure, Superstructure, and MEP system. A substructure was categorized into basement, foundation, and piles. A superstructure consisted of structural components, such as beams and pillars, exterior and interior wall, doors, windows, floor, ceiling, roof, and finishing. The MEP system was divided into electrical facilities, HVAC systems, and sanitary systems. For the HVAC system of this building, heat source and air conditioning were packaged based VRF system with total heat exchanger for outdoor air. Results of whole life carbon was annual carbon emissions per unit floor area [ $\text{kgCO}_2\text{-eq/m}^2\text{/year}$ ].

### 6.2.2 Database

Two main methods of Life Cycle Inventory (LCI) analysis have been used in many studies. The first method is the process-based method, which is a basic method of inventory analysis that accumulates the environmental impacts of each material one by one. While the advantage of the process-based method is to be able to carry out detailed analysis, its disadvantage is that it requires a lot of time to collect the data. In Japan, there is a LCI database named Inventory Database for Environmental Analysis (IDEA) [34], which can quantify the environmental impact of Japanese products and services, including about 4,700 databases. In addition to these process-based databases, there is a growing number of Environmental Product Declaration (EPD) [35][36] in which manufacturers disclose the carbon emission intensity from materials in their own products (in buildings, this refers to building materials). In Japan, Sustainable Management Promotion Organization (SuMPO) [37] certifies EPDs, but the number of EPD registrations was still few compared to that in other countries. Another inventory method is the Input-Output (I-O) method. Input-output analysis is to quantify



the spillover effects of a particular product industry on other industries and incorporating them into environmental impacts. The advantage of this method is that it can be calculated on a monetary basis, such as construction costs, thereby reducing the time required for LCA analysis. On the other hand, the wide scope covered by one sector makes it difficult to carry out detailed LCA analyses. Therefore, due to the problems with both the process-based method and the I-O method, a hybrid method [38] was used in this study.

6.2.3 Upfront carbon

Figure 6-7 shows the classification for Upfront carbon calculations. Based on the IDEA calculation tools developed by Architectural Institute of Japan (Kensuke Kobayashi laboratory, Prefectural University of Hiroshima) [39], Building model was separated by each component. Figure 6-8 shows the upfront carbon calculation of process-based analysis. After 3D Aided Design (3D-CAD) modelling has been done, the weight of the building materials was calculated using the AIJ-LCA unit conversion database. Based on the calculated weights of the building, the upfront carbon was finally estimated by coupling it with the IDEA database and EPD data. Some of the minor building materials were cut off, such as joint of steel, doorknob, and metal fittings. As the IDEA database basically only lists greenhouse gas emissions per unit of material production stage (A1-A3), additional calculations were made for the transport stage (A4) and the construction stage (A5).

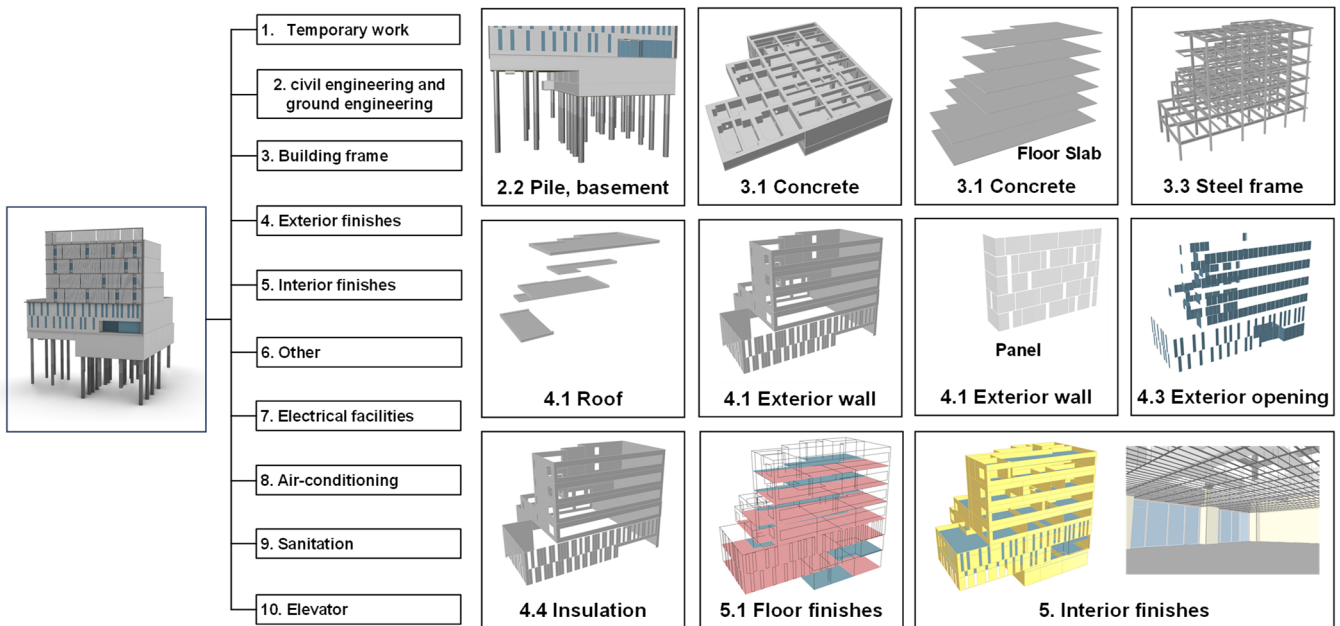
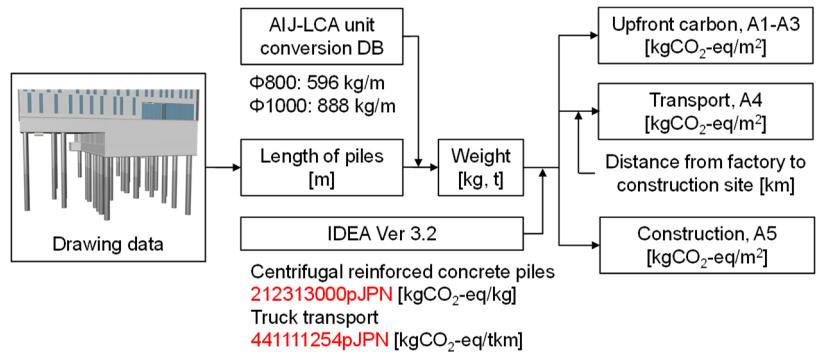
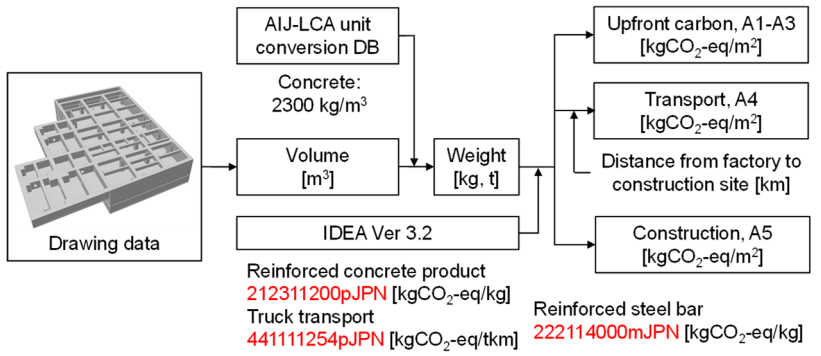


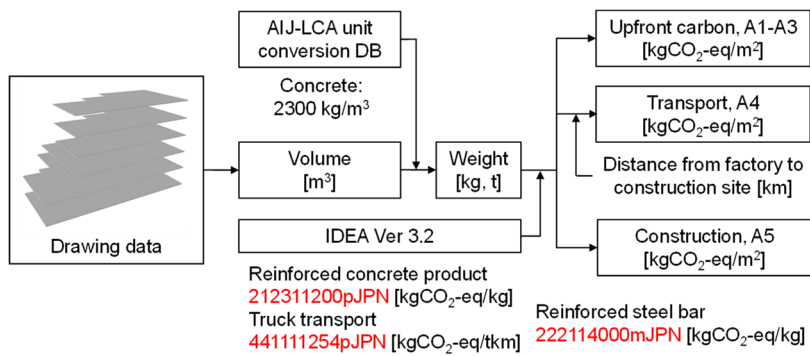
Figure 6-7. Classification for Upfront carbon calculations



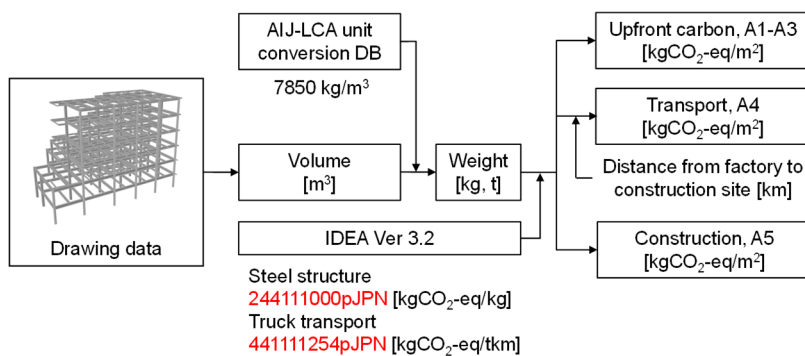
(a) Piles and foundations



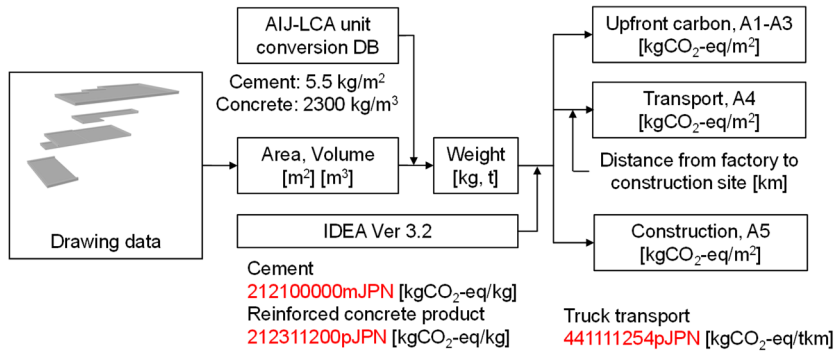
(b) Basement



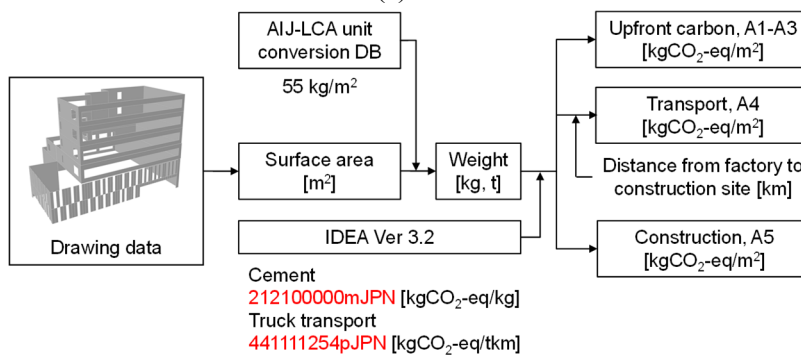
(c) Floor slab



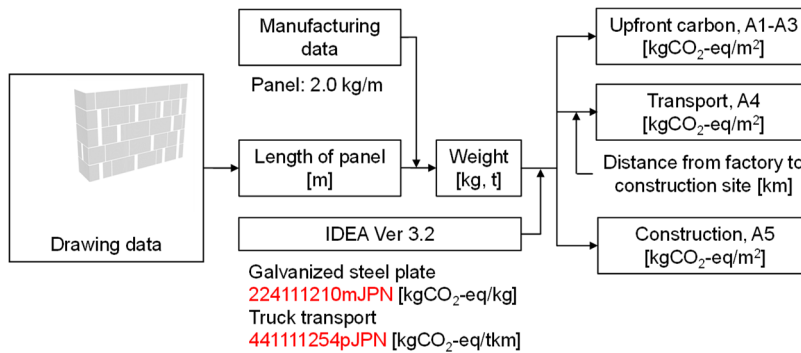
(d) Steel frame



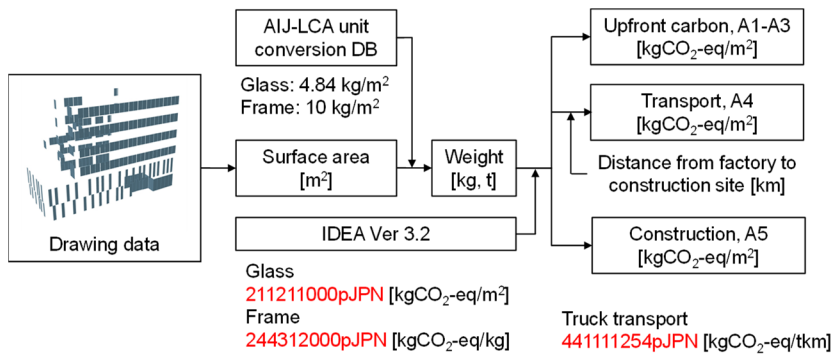
(e) Roof



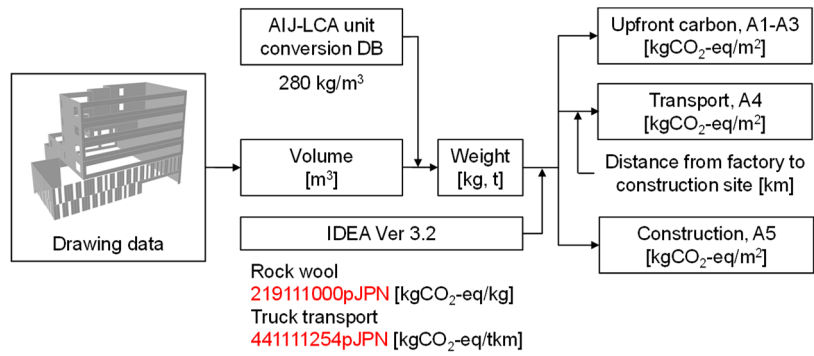
(f) Exterior wall



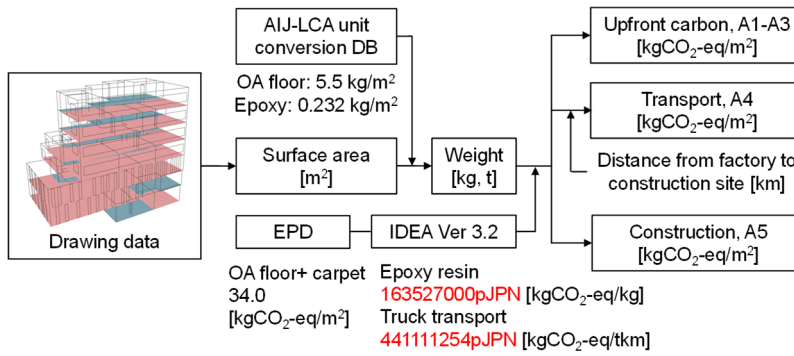
(g) Punching panel



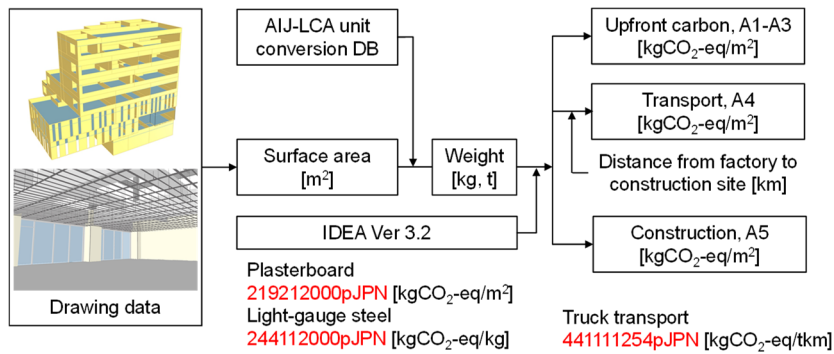
(h) Exterior opening



(i) Insulation



(j) Interior floor finishes



(k) Interior wall finishes

Figure 6-8. Upfront carbon calculation of process-based analysis

Figure 6-9 shows the diagram of packaged air conditioning system and radiant ceiling panel system. An all-air system and a radiant system were compared in terms of upfront carbon emissions. For the case study building, the packaged air conditioning system was installed, and total heat changer was also adopted for outdoor ventilation unit. Total cooling capacity of the packaged system in the 1<sup>st</sup> to 6<sup>th</sup> floor was 545 kW. As a comparison for the packaged air conditioning system, the upfront carbon of the radiant ceiling panel system was also calculated. In this study, the radiant system was assumed to be installed in the main classrooms and the office rooms (2,143 m<sup>2</sup>, 1<sup>st</sup> to 6<sup>th</sup> floor). For the ventilation requirement, an outdoor air handling unit system with direct expansion was adopted. In general, there is a lack of LCI and EPD data for HVAC equipment. To calculate the upfront carbon of HVAC system, SHASE-LCA guidebook [40] and IDEA database [34] were used. The information on the weight ratio of materials for HVAC equipment was obtained from the SHASE guidebook, and the carbon emission factor of materials was obtained from IDEA Ver 3.0. Note that this method usually does not include the process stages of the materials and equipment. Therefore, in accordance with the SHASE guidelines, the emission factor for simple HVAC equipment was added by 30% for the material manufacturing stage, and 50% for heat source equipment such as a chiller.

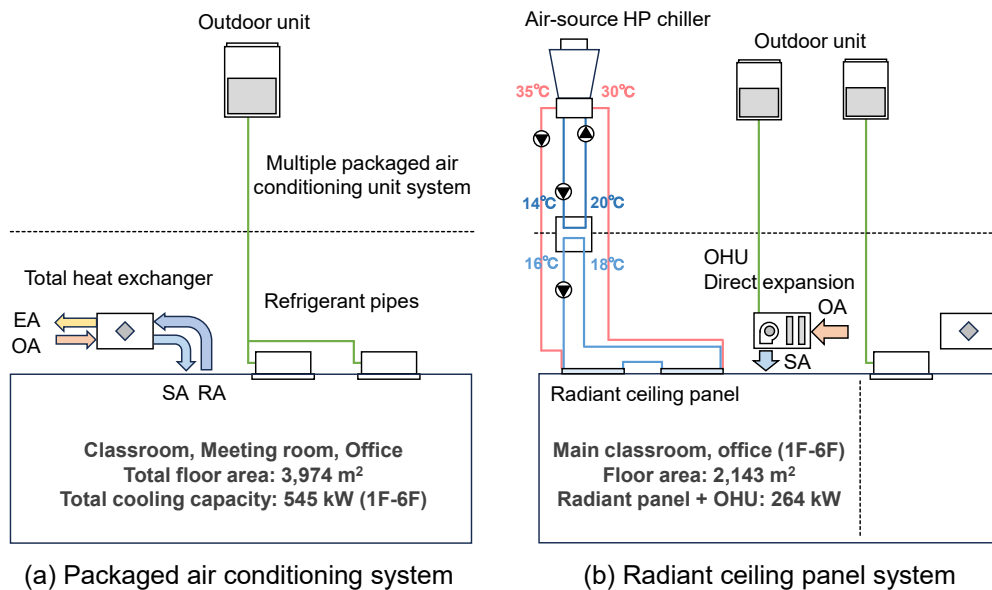


Figure 6-9. Diagram of packaged air conditioning system and radiant ceiling panel system



### 6.3 Results and Discussions

#### Upfront carbon of the full-scale case study

Figure 6-11 shows the upfront carbon emissions of the case study building and Figure 6-12 shows the upfront carbon emissions of the building materials. Upfront carbon was shown to be 783 kgCO<sub>2</sub>-eq/m<sup>2</sup> of the total. For this calculation, upfront carbon of the electrical, HVAC, and sanitation system were obtained from average values of Japanese university buildings from Ikaga et al. [19]. In the upfront carbon stage, it was found that the building frame accounted for a larger share of emissions than the mechanical, electrical, and plumbing (MEP) system. It should be noted that the embodied carbon of the MEP system increases substantially due to B4: replacement and B5: refurbishment. As shown in (b) the building material of the Figure 3, concrete (264 kgCO<sub>2</sub>-eq/m<sup>2</sup>) and steel (221 kgCO<sub>2</sub>-eq/m<sup>2</sup>) were the main sources of emissions compared to the other materials.

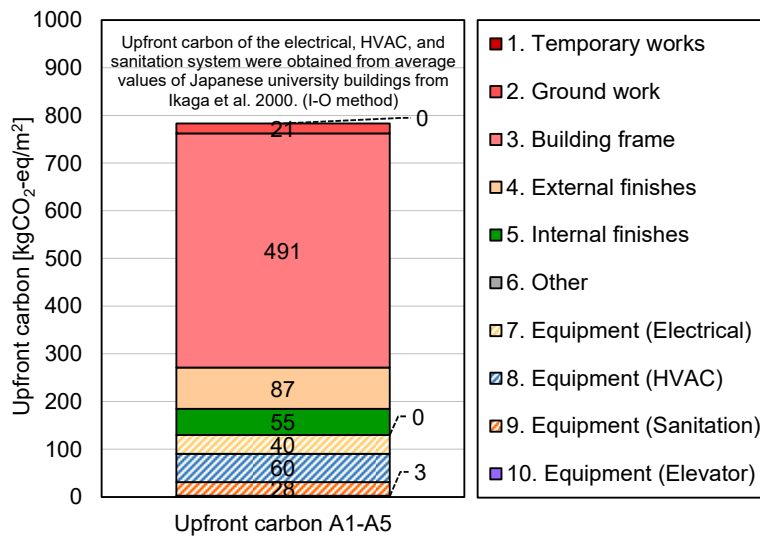


Figure 6-11. Upfront carbon emissions of the case study building

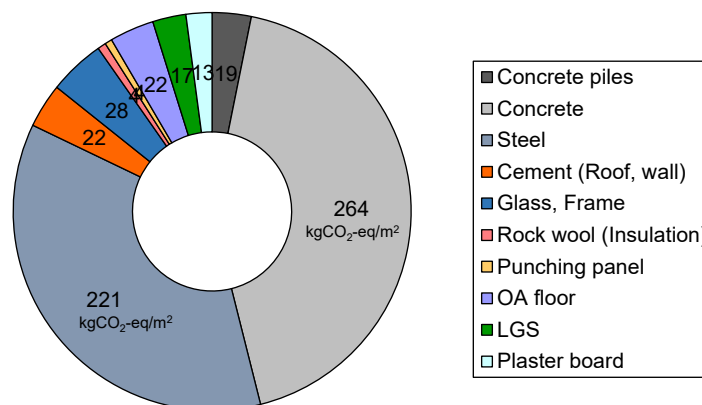


Figure 6-12. Upfront carbon emissions of the building materials

**Upfront carbon of the all-air system and the radiant system**

Figure 6-13 shows the upfront carbon emissions of the building HVAC materials. Upfront carbon of the HVAC system was shown to be 25.9 kgCO<sub>2</sub>-eq/m<sup>2</sup> of the packaged system and 62.0 kgCO<sub>2</sub>-eq/m<sup>2</sup> of the radiant system, respectively. It was found that the aluminum punching panels accounted for a larger share of emissions of the HVAC system. Upfront carbon of radiant systems was 8% of upfront carbon of the full-scale building materials. If the installation of a radiant system significantly reduces operational carbon, the increase in upfront carbon would not have such a negative impact. The use of recycled materials is another option to reduce the upfront carbon derived by aluminum of panels.

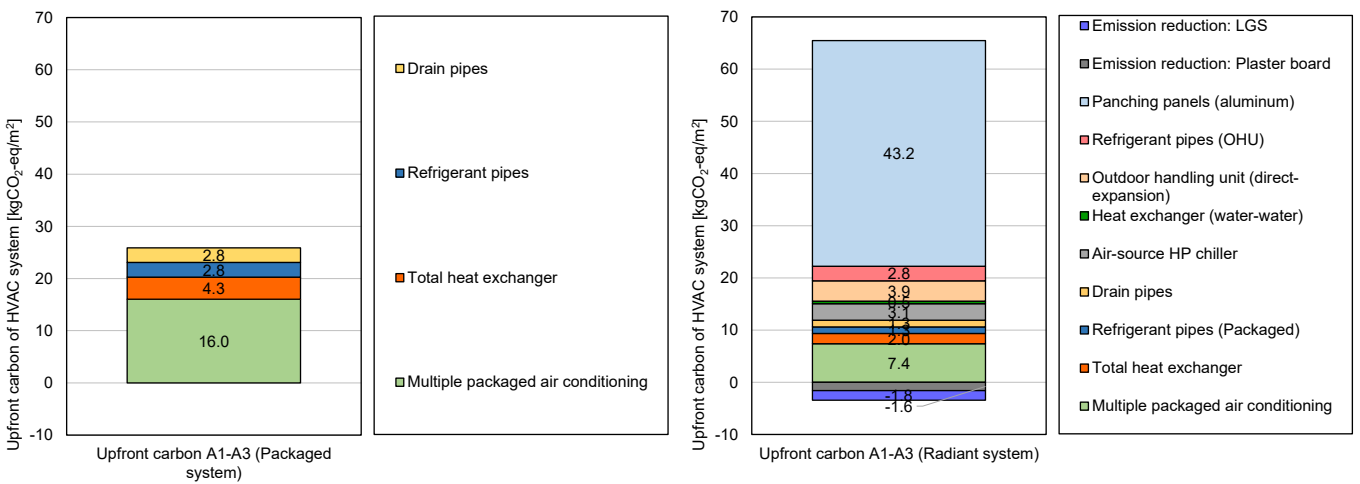


Figure 6-13. Upfront carbon emissions of the building HVAC materials



**Operational carbon of the packaged air conditioning system**

Figure 6-14 shows the operational carbon emissions of the case study building. Results indicated that operational carbon emissions were 39.0 kgCO<sub>2</sub>-eq/m<sup>2</sup>/year for the standard value and 28.2 kgCO<sub>2</sub>-eq/m<sup>2</sup>/year for the design value. It was found that the reductions were superior to the standard, especially in the lighting and ventilation.

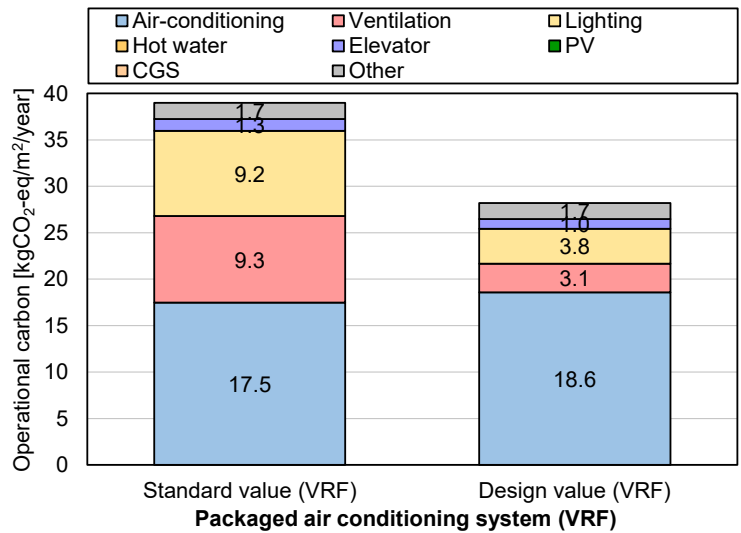


Figure 6-14. Operational carbon emissions of the case study building

**Comparison of upfront carbon and operational carbon between this full-scale case study and foreign case study**

According to the LETI embodied carbon primer [41], the upfront carbon target (A1-A5, including substructure, superstructure, MEP, façade, and internal finishes) for school and commercial office are 1000 kgCO<sub>2</sub>-eq/m<sup>2</sup> for business as usual, 600 kgCO<sub>2</sub>-eq/m<sup>2</sup> for 2020, and 350 kgCO<sub>2</sub>-eq/m<sup>2</sup> for 2030. Embodied carbon targets of RIBA 2030 Climate Challenge [42] for non-residential building (new build schools) were 1000 kgCO<sub>2</sub>-eq/m<sup>2</sup> for business as usual, 675 kgCO<sub>2</sub>-eq/m<sup>2</sup> in 2025, and 540 kgCO<sub>2</sub>-eq/m<sup>2</sup> in 2030. The team of Ramboll reported that embodied carbon benchmarks for buildings in Europe [43]. The team has collected building-level embodied carbon data from LCA case studies already done in five European Union members states. In this report, mean value of product stage upfront carbon (A1-A3) was around 300 kgCO<sub>2</sub>-eq/m<sup>2</sup> and ranging from 70 to 520 kgCO<sub>2</sub>-eq/m<sup>2</sup>. Hence, the upfront carbon in this study (783 kgCO<sub>2</sub>-eq/m<sup>2</sup>) was relatively larger than these target values and benchmark values. One reason is expected to be that Japanese building structures are relatively massive to cope with earthquakes and other natural disasters.

## 6.4 Conclusions

This study focused on the whole-life carbon emissions of a building's heating, ventilation, and air-conditioning systems. The studied radiant system was a radiant ceiling panel system, and the all-air system was a packaged variable refrigerant flow system. The building model was based on that of a medium-sized classroom building at Waseda University, Tokyo, Japan. Results showed that upfront carbon was shown to be 783 kgCO<sub>2</sub>-eq/m<sup>2</sup> of the total and operational carbon was 28.2 kgCO<sub>2</sub>-eq/m<sup>2</sup>/year, respectively. Concrete (264 kgCO<sub>2</sub>-eq/m<sup>2</sup>) and steel (221 kgCO<sub>2</sub>-eq/m<sup>2</sup>) were the superior to other materials in terms of upfront carbon emissions. Upfront carbon of the HVAC system was shown to be 26 kgCO<sub>2</sub>-eq/m<sup>2</sup> of the packaged system and 62 kgCO<sub>2</sub>-eq/m<sup>2</sup> of the radiant system, respectively.

## References

- [1] IPCC DDC Glossary, Intergovernmental Panel on Climate Change, 2020. [https://www.ipcc-data.org/guidelines/pages/glossary/glossary\\_c.html](https://www.ipcc-data.org/guidelines/pages/glossary/glossary_c.html) (accessed July 20, 2023)
- [2] Greenhouse gas emissions in Tokyo, [https://www.kankyo.metro.tokyo.lg.jp/climate/zenpan/emissions\\_tokyo.html](https://www.kankyo.metro.tokyo.lg.jp/climate/zenpan/emissions_tokyo.html) (accessed December 6, 2023)
- [3] ASHRAE Standard 90.1-2022—Energy Standard for Sites and Buildings Except Low-Rise Residential Buildings, ASHRAE, 2022.
- [4] ISO/TS 23764:2021, Methodology for achieving non-residential zero-energy buildings (ZEBs), International Organization for Standardization, 2021.
- [5] World Business Council For Sustainable Development (WBCSD), Decarbonizing construction Guideline for investors and developers to reduce embodied carbon, Arup, 2021.
- [6] World Business Council For Sustainable Development (WBCSD), Net-zero buildings Where do we stand?, Arup, 2021.
- [7] Institute for Built Environment and Carbon Neutral for SDGs (IBECs), Zero carbon building (LCCO2 net zero) meeting, [https://www.ibec.or.jp/zero-carbon\\_building/](https://www.ibec.or.jp/zero-carbon_building/) (accessed December 6, 2023)
- [8] ISO 21930:2022, Sustainability in buildings and civil engineering works — Core rules for environmental product declarations of construction products and services, International Organization for Standardization, 2022.
- [9] EN 15978:2011, Sustainability of construction works – Assessment of environmental performance of buildings – Calculation method, CEN, 2011.
- [10] World Business Council For Sustainable Development (WBCSD), The Building System Carbon Framework – A common language for the building and construction value chain, Arup, 2021.
- [11] ASHRAE, ASHRAE task force for building decarbonization (TFBD). <https://www.ashrae.org/about/ashrae-task-force-for-building-decarbonization> (accessed December 6, 2023)
- [12] Ministry of the Environment, Greenhouse Gas Emissions Calculation, Reporting and Publication System in Japan, <https://ghg-santeikohyo.env.go.jp/calc> (accessed December 6, 2023)

- [13] Building regulation (BR18), 2018. <https://byggningsreglementet.dk/> (accessed December 6, 2023)
- [14] Ministry of the Environment in its “Draft Approach to Contracts for Electricity Supply. <https://www.env.go.jp/content/000081247.pdf> (accessed July 20, 2023).
- [15] World Green Building Council, Bringing Embodied Carbon Upfront, <https://worldgbc.org/article/bringing-embodied-carbon-upfront/> (accessed December 6, 2023)
- [16] Toda Corporation, Japanese high-rise construction worksite to use 100% renewable electricity, <https://www.toda.co.jp/assets/pdf/20190902.pdf> (accessed December 6, 2023)
- [17] Renewable Energy 100% (RE100), <https://www.there100.org/> (accessed December 6, 2023)
- [18] T. Ikaga, Y. Tonooka, LCI data on electrical and mechanical facilities of office building, Architectural Institute of Japan’s Journal of Architecture Planning, Volume 65, No.529, 117-123, 2000. [https://doi.org/10.3130/aija.65.117\\_1](https://doi.org/10.3130/aija.65.117_1)
- [19] T. Ikaga, Y. Tonooka, LCI data on electrical and mechanical facilities for various kind of buildings, Architectural Institute of Japan’s Journal of Architecture Planning, Volume 65, No.533, 51-58, 2000. [https://doi.org/10.3130/aija.65.51\\_3](https://doi.org/10.3130/aija.65.51_3)
- [20] K. Asabuki, T. Seike, R. Sakurano, A study on environmental load of the renovation project which reused building frames – Estimation by process analysis, Architectural Institute of Japan’s Journal of technology and design, Volume 22, No.44, 429-434, 2014. <https://doi.org/10.3130/aijt.20.429>
- [21] M. Shimura, T. Seike, Y. Kim, Study on resource circulation of non-structural building materials focusing on lifecycle, Architectural Institute of Japan’s Journal of technology and design, Volume 26, No.62, 55-60, 2020. <https://doi.org/10.3130/aijt.26.55>
- [22] K. Kobayashi, K. Shimokawa, R. Matsuzaki, Y. Suzuki, T. Isobe, Development of a background database for building LCA -Analysis based on field survey and development of a unit-conversion database-, Architectural Institute of Japan’s Journal of Environmental Engineering, Volume 86, No.782, 388-398, 2021. <https://doi.org/10.3130/aije.86.388>
- [23] K. Shindo, J. Shinoda, O. B. Kazanci, D. Bogatu, S. Tanabe, B. W. Olesen, A comparative study of the whole life carbon of a radiant system and an all-air system in a non-residential building, Energy and Buildings, Volume 300, 113668, 2023. <https://doi.org/10.1016/j.enbuild.2023.113668>
- [24] O.B. Kazanci, Low Temperature Heating and High Temperature Cooling in Buildings, PhD Thesis, Technical University of Denmark, 2016.
- [25] EN 14037-1:2003, Ceiling mounted radiant panels supplied with water at temperature below 120°C Part 1: Technical specifications and requirements, European Standard, 2003.
- [26] J. Murphy, Common pitfalls in design and operation of a DOAS, ASHRAE Journal, 2018.
- [27] G. Sastry, Peter H Rumsey, VAV vs. radiant: Side-by-side comparison, ASHRAE Journal, 56, 16-24, 2014.
- [28] ASHRAE Guideline 41-2020, Design, Installation and Commissioning of Variable Refrigerant Flow (VRF) Systems, ASHRAE, 2020.
- [29] Global Environment Committee, LCA Sub-Committee, Guidelines for building LCA, Architectural Institute of Japan, 2013.
- [30] ISO 14044:2006, Environmental management Life cycle assessment Requirements and guidelines, International

Organization for Standardization, 2006.

- [31] ISO 14040:2006, Environmental management Life cycle assessment Principles and framework, International Organization for Standardization, 2006.
- [32] Waseda University, Building 29, 2017. <https://www.waseda.jp/top/news/49172> (accessed December 6, 2023)
- [33] Waseda University, Building 29, 2017. <https://www.waseda.jp/top/news/49639> (accessed December 6, 2023)
- [34] SuMPO, LCI database IDEA Ver. 3, <https://sumpo.or.jp/consulting/lca/idea/> (accessed December 6, 2023)
- [35] EN 15804:2012, Sustainability of construction works. Environmental product declarations. Core rules for the product category of construction products, CEN, 2012.
- [36] EN 15804:2012+A2:2019, Sustainability of construction works. Environmental product declarations. Core rules for the product category of construction products, CEN, 2019.
- [37] SuMPO, Japan EPD program by SuMPO, <https://ecoleaf-label.jp/> (accessed December 6, 2023)
- [38] S. Suh, G. Huppes, Methods for Life Cycle Inventory of a product, Journal of Cleaner Production, Volume 13, Issue 7, 687-697, 2005. <https://doi.org/10.1016/j.jclepro.2003.04.001>
- [39] K. Kobayashi, IDEA v3 Tool for LCA guideline of AIJ, Prefectural University of Hiroshima, 2022. [https://www.pu-hiroshima.ac.jp/p/kensuke/Data/IDEA%20v3%20Tool%20for%20Building%20Manual%20ver\\_0\\_1.pdf](https://www.pu-hiroshima.ac.jp/p/kensuke/Data/IDEA%20v3%20Tool%20for%20Building%20Manual%20ver_0_1.pdf) (accessed December 6, 2023)
- [40] SHASE, All Environmental Technologies for Buildings and Facilities -from elemental technologies to smart cities-, 2015.
- [41] Embodied Carbon Target Alignment, London Energy Transformation Initiative (LETI), 2021. [https://www.leti.uk/\\_files/ugd/252d09\\_25fc266f7fe44a24b55cce95a92a3878.pdf](https://www.leti.uk/_files/ugd/252d09_25fc266f7fe44a24b55cce95a92a3878.pdf) (accessed Sep 14, 2023)
- [42] RIBA 2030 Climate Challenge version 2, Royal Institute of British Architects (RIBA), 2021. <https://www.architecture.com/-/media/files/Climate-action/RIBA-2030-Climate-Challenge.pdf> (accessed Sep 14, 2023)
- [43] M. Röck, A. Sørensen, Towards embodied carbon benchmarks for buildings in Europe, RAMBOLL, 2022.

# **Chapter 7:**

# **Conclusions**

## 7 Conclusions

In response to climate change, it is important to reduce carbon emissions from the building sector and avoid dependence on fossil fuels. Typified by net zero-energy buildings, the building sector has attempted to reduce carbon emissions, especially during the operational use stage. Furthermore, an urgent necessity exists to mitigate carbon emissions throughout the building life cycle, including the material production, construction, demolition, and reuse stages. This study focused on (i) resilience, (ii) energy efficiency, and (iii) embodied carbon, which constitute the environmental performance of zero-carbon buildings. Although the radiant heating and cooling system focused on in this study has been reported to provide energy efficiency and thermal comfort, few studies exist on whether radiant systems are beneficial in terms of whole-life carbon emissions. The findings on radiant systems contributing to zero-carbon buildings were summarized through interviews, field surveys, and simulation case studies.

Chapter 1 provides the research background, aims of this study, and a summary of the relevant research.

Chapter 2 presents the installation surveys and expert interviews conducted between 2021 and 2022. The participants included manufacturers and mechanical, electrical, and plumbing (MEP) engineers in Japan who had experience in designing radiant heating and cooling systems. Fifty-six respondents from 15 companies were interviewed. The results indicated that radiant ceilings and floors were installed in 69% and 30% of the total cases, respectively. Water-based radiant systems were installed in 56% of the cases, and air-based radiant systems were installed in 43%. Notably, 79% of all respondents in expert interview foresaw an increasing use of radiant systems, with 54% stating that designing such systems is presently easier than in the 2010s. Many MEP engineers emphasized that radiant systems could provide energy savings and thermal comfort for buildings. Regarding the impact of building decarbonization on the installation of radiant systems, 53% of the respondents answered that it would impact the installation of radiant systems. Those who answered “high impact” asserted that radiant systems were becoming a powerful tool for building decarbonization, specifically in reducing operational energy and carbon emissions. Additionally, other respondents pointed out that radiant system would be beneficial or not in terms of whole-life carbon emissions. The survey identified the actual status of radiant heating and cooling systems in Japan, which is useful information for the industry.

Chapter 3 details the results of field measurement studies investigating the effects of solar heat removal on radiant-cooled surfaces. This chapter focuses on solar radiation, a significant contributor to a building’s internal heat gain. The integration of radiant cooling for daylighting, ensuring energy efficiency and indoor thermal comfort, has recently attracted considerable attention. Previous studies have reviewed the substantial increase in radiant cooling capacity owing to solar absorption on the cooled surface. A literature review indicated that widely varying peak cooling capacity values across studies, affecting equipment selection and majorly contributing to a lack of established design methodologies. During the midterm and summer periods, field measurements were conducted to measure the solar heat removal performance of cooled surfaces and thermal environment of office spaces. Surface heat flux and heat extraction rate were calculated to

validate the solar heat removal performance of slit ceilings. Under solar radiation influence, the maximum surface heat flux was  $190 \text{ W/m}^2$  and the maximum heat extraction rate was  $126 \text{ W/m}^2$ . The field measurement results confirmed that radiant cooling capacity was considerably enhanced when the building absorbed solar radiation. During working hours on August 27 and 28, 2020, the operative temperature (OT) of the 3F office space was generally within category A (OT =  $25.8 \pm 1.0 \text{ }^\circ\text{C}$ ), affirming that a comfortable thermal environment was ensured. The results confirmed the establishment of an energy-saving and thermally comfortable office space. This study is evaluated for its detailed analysis of the variation in radiant cooling capacity under solar radiation, which has been reported in previous studies, by measuring the surface heat flux and heat extraction rate by radiant systems.

Chapter 4 presents simulated results aimed at quantifying the resilience of a thermally active building system (TABS) to heatwaves. The previous section focused on solar radiation, which causes indoor overheating. In this chapter, the concept of overheating risk is broadened to assess the resilience of cooling systems to indoor overheating during heatwaves. A distinctive feature of TABS, a type of radiant system, is its ability to activate and control the thermal mass of the building structure. The notable advantage of this feature is the peak load-shifting effect of the thermal mass, resulting in energy savings compared with a conventional system (such as an all-air system). An all-air system (air-conditioning) was used as the reference cooling system. Further, dynamic simulations were performed using the EnergyPlus software. Future weather files (typical meteorological years and heatwave weather years) developed in IEA EBC Annex 80, were used for the simulations. The results revealed that, for typical meteorological and heatwave weather years, the TABS and variable air volume (VAV) systems could maintain indoor temperatures within a comfortable range for both heating, ventilation, and air-conditioning (HVAC) systems. Additionally, simulation results using future weather data indicated a decrease in heating demand and an increase in cooling demand in Copenhagen.

Chapter 5 presents a comparative study of the whole-life carbon emissions of radiant and all-air systems within a nonresidential building. Specifically, this study focused on the whole-life carbon footprint of the building's HVAC system. A methodology for comparing the entire carbon life of different HVAC systems was proposed and used in a case study with boundary conditions set in Denmark. All-air and radiant systems were compared because they have different working principles and the potential variations in their embodied and operational carbon. The studied radiant system was a TABS, and the all-air system was a packaged variable air volume system with reheating. The building model was based on that of medium-sized offices from prototype buildings developed by the U.S. Department of Energy. The lifecycle stages of the building were classified based on EN15978:2011. A novel approach adapted two models, one for dynamic building simulation and another for measuring the mass of materials (such as concrete). The operational carbon emissions of HVAC systems were calculated under comparable indoor thermal comfort conditions. The calculated whole-life carbon values were  $10.1 \text{ kgCO}_2\text{-eq/m}^2\text{/year}$  and  $9.0 \text{ kgCO}_2\text{-eq/m}^2\text{/year}$  for the all-air system and TABS, respectively. Compared with the all-air system, TABS showed a 34% reduction in annual total primary energy use and 11% decrease in whole-life carbon. Furthermore, the implementation of dynamic carbon intensity in the grid could lead to further reduction in carbon emissions in TABS, owing to its operational flexibility with the activated thermal mass. This study is evaluated in that it focused on building HVAC systems, which have been rarely discussed, and proposed a method to compare them

from the whole life carbon perspective. Furthermore, it is significant that this study comprehensively shows that radiant systems have the potential to contribute to the reduction of whole life carbon compared to conventional all-air systems.

Chapter 6 presents a comparative study of the whole-life carbon footprint of radiant and all-air systems within a university building in Japan. This study focused on the whole-life carbon emissions of a building's heating, ventilation, and air-conditioning systems. The studied radiant system was a radiant ceiling panel system, and the all-air system was a packaged variable refrigerant flow system. The building model was based on that of a medium-sized classroom building at Waseda University, Tokyo, Japan. The life-cycle stages of the building were classified based on ISO 21931-1:2022. Results showed that upfront carbon was shown to be 783 kgCO<sub>2</sub>-eq/m<sup>2</sup> of the total and operational carbon was 28.2 kgCO<sub>2</sub>-eq/m<sup>2</sup>/year, respectively. Concrete (264 kgCO<sub>2</sub>-eq/m<sup>2</sup>) and steel (221 kgCO<sub>2</sub>-eq/m<sup>2</sup>) were the superior to other materials in terms of upfront carbon emissions. Upfront carbon of the HVAC system was shown to be 25.9 kgCO<sub>2</sub>-eq/m<sup>2</sup> of the packaged system and 62.0 kgCO<sub>2</sub>-eq/m<sup>2</sup> of the radiant system, respectively. This study is evaluated in that the upfront carbon of the HVAC systems in addition to the building frame and finishes was calculated by the process analysis of building LCA.

Chapter 7 summarizes the main findings of each chapter. The thesis indicated the potential of radiant systems to reduce energy and operational carbon compared to all -air systems while ensuring thermal comfort in the room. The study of radiant systems in terms of carbon emissions over the entire building life cycle is highly evaluated from an academic perspective.



## List of research achievements for application of Doctor of Engineering, Waseda University

Full Name : 新藤 幹

seal or signature

Date Submitted(yyyy/mm/dd): 2023/12/07

種別 (By Type)	題名、発表・発行掲載誌名、 (theme, journal name, date & year of publication, name of authors inc. yourself)
Journal paper	A comparative study of the whole life carbon of a radiant system and an all-air system in a non-residential building, Energy and Buildings, Volume 300, 113668, December 2023, <b>Kan Shindo</b> , Jun Shinoda, Ongun B. Kazanci, Dragos-Ioan Bogatu, Shin-ichi Tanabe, Bjarne W. Olesen.
Journal paper	Analysis of energy consumption in net zero energy houses, The Architectural Institute of Japan's Journal of Environmental Engineering, Vol.87, No.802, pp.877-887, December 2022, Yohei Sato, <b>Kan Shindo</b> , Manae Inaba, Kanako Fujii, Haruka Arai, Jun Nakagawa, Shin-ichi Tanabe.
Journal paper	Application of a slit ceiling based on thermally activated building systems in a daylight-harvesting office space with direct solar radiation, Japan Architectural Review, Vol.5, Issue 4, pp.548-559, September 2022, <b>Kan Shindo</b> , Jun Shinoda, Ken Ikai, Takeshi Takenaka, Shuichi Tamura, Tetsuo Kobori, Shin-ichi Tanabe.
Journal paper	Radiant cooling effect of ceiling slit capable of both daylight harvesting and solar heat removal, The Architectural Institute of Japan's Journal of Environmental Engineering, Vol.86, No.787, pp.788-796, September 2021, <b>Kan Shindo</b> , Jun Shinoda, Ken Ikai, Takeshi Takenaka, Shuichi Tamura, Tetsuo Kobori, Shin-ichi Tanabe.
Journal paper	Spectral irradiance simulation for evaluating light environments for indoor plants, Japan Architectural Review, Vol.4, Issue 4, pp.649-659, September 2021, Soma Sugano, Ryo Nitta, <b>Kan Shindo</b> , Akihisa Nomoto, Shu Yoda, Tamaho Shigemura, Masahisa Ishii, Shin-ichi Tanabe.
Journal paper	Spectral irradiance simulation for evaluating light environments for indoor plants, The Architectural Institute of Japan's Journal of Environmental Engineering, Vol.86, No.781, pp.337-346, March 2021, Soma Sugano, Ryo Nitta, <b>Kan Shindo</b> , Akihisa Nomoto, Shu Yoda, Tamaho Shigemura, Masahisa Ishii, Shin-ichi Tanabe.
Conference paper	Estimating CO <sub>2</sub> emissions from product and operational stages of a low-rise office building using 3D models, Annual meeting of Architectural Institute of Japan, pp.2431-2432, September 2023, Ryota Matsumura, <b>Kan Shindo</b> , Shin-ichi Tanabe.
Conference paper	Comparison of Environmental Product Declaration (EPD) in the building sector between Japan and Denmark, Annual meeting of Architectural Institute of Japan, pp.2433-2434, September 2023, <b>Kan Shindo</b> , Jun Shinoda, Ongun B. Kazanci, Shin-ichi Tanabe, Bjarne W. Olesen.
Conference paper	Estimating CO <sub>2</sub> emissions from product and operational stages of a low-rise office building through integration of a 3D model and a LCA database, Annual meeting of Society of Heating, Air-Conditioning and Sanitary Engineers of Japan, pp.193-196, September 2023, Ryota Matsumura, <b>Kan Shindo</b> , Shin-ichi Tanabe.
Conference paper	State-of-the-art of building decarbonization in European countries, Annual meeting of Society of Heating, Air-Conditioning and Sanitary Engineers of Japan, pp.205-208, September 2023, <b>Kan Shindo</b> , Jun Shinoda, Ongun B. Kazanci, Shin-ichi Tanabe, Bjarne W. Olesen.
Conference paper	Using 3D City Models to Simulate the Possibility of Carbon Neutral Districts in 2050 (Part 1) Overview of the research and visualization of CO <sub>2</sub> emissions for large-scale emitters, Annual meeting of Architectural Institute of Japan, pp.685-688, September 2022, <b>Kan Shindo</b> , Ryota Matsumura, Ken Ikai, Yutaro Ogawa, Yuki Saito, Miku Tazaki, Tamaho Shigemura, Shin-ichi Tanabe.
Conference paper	Using 3D City Models to Simulate the Possibility of Carbon Neutral Districts in 2050 (Part 2) Estimation of CO <sub>2</sub> Emission Reduction by solar power generation on the Walls of Buildings in Urban Areas, Annual meeting of Architectural Institute of Japan, pp689-692, September 2022, Ryota Matsumura, <b>Kan Shindo</b> , Ken Ikai, Yutaro Ogawa, Yuki Saito, Miku Tazaki, Tamaho Shigemura,

## List of research achievements for application of Doctor of Engineering, Waseda University

Full Name : 新藤 幹

seal or signature

Date Submitted(yyyy/mm/dd): 2023/12/07

種類別 (By Type)	題名、発表・発行掲載誌名、 (theme, journal name, date & year of publication, name of authors inc. yourself)
Conference paper	Evaluation of an Open-air Sub-tropical Airport for Energy and Comfort Part 8: Outline of Questionnaire Survey and Effect of Window Opening on Environmental Satisfaction, Annual meeting of Architectural Institute of Japan, pp.833-834, September 2022, Ryosuke Onoda, Yutaro Ogawa, Yuki Saito, Miku Tazaki, Kazuya Matsuo, <b><u>Kan Shindo</u></b> , Takuya Asagawa, Osamu Nagase, Naoyuki Harada, Kikka Uchida, Shin-ichi Tanabe.
Conference paper	Evaluation of an Open-air Sub-tropical Airport for Energy and Comfort Part 9: Effects of Window Opening and Closing on Thermal Environment and Thermal Comfort, Annual meeting of Architectural Institute of Japan, pp.835-836, September 2022, Yutaro Ogawa, Ryosuke Onoda, Miku Tazaki, Yuki Saito, Kazuya Matsuo, <b><u>Kan Shindo</u></b> , Takuya Asagawa, Osamu Nagase, Naoyuki Harada,
Conference paper	Evaluation of an Open-air Sub-tropical Airport for Energy and Comfort Part 10: The influence of opening and closing windows for connection with nature and psychological evaluation, Annual meeting of Architectural Institute of Japan, pp.837-838, September 2022, Miku Tazaki, Yutaro Ogawa, Ryosuke Onoda, Yuki Saito, Kazuya Matsuo, <b><u>Kan Shindo</u></b> , Takuya Asagawa, Osamu Nagase, Naoyuki Harada, Kikka Uchida, Shin-ichi Tanabe.
Conference paper	Evaluation of an Open-air Sub-tropical Airport for Energy and Comfort Part 11: Effect of Window Opening and Closing on Airflow Environment, Annual meeting of Architectural Institute of Japan, pp.839-840, September 2022, Naoyuki Harada, Yutaro Ogawa, Ryosuke Onoda, Miku Tazaki, Yuki Saito, Kazuya Matsuo, <b><u>Kan Shindo</u></b> , Takuya Asagawa, Osamu Nagase, Kikka Uchida, Shin-ichi
Conference paper	Qualitative Research of the Implementation of Radiant Cooling and Heating System in Japan. (Part 1) Analysis of Case Studies in Literature, Annual meeting of Architectural Institute of Japan, pp.1815-1816 September 2022, Ken Ikai, Jun Shinoda, <b><u>Kan Shindo</u></b> , Shin-ichi Tanabe.
Conference paper	Environmental Performance Verification at Open-air ZEB Airport Terminal Part.5 Comparison of Environmental Satisfaction Models by Opening and Closing Windows, Annual meeting of Society of Heating, Air-Conditioning and Sanitary Engineers of Japan, pp.233-236, September 2022, Ryosuke Onoda, Yutaro Ogawa, Yuki Saito, Miku Tazaki, Kazuya Matsuo, <b><u>Kan Shindo</u></b> , Takuya Asagawa, Osamu Nagase, Naoyuki Harada, Kikka Uchida, Shin-ichi Tanabe.
Conference paper	Environmental Performance Verification at Open-air ZEB Airport Terminal Part.6 Effects of Opening and Closing Windows on Thermal Environment and Comfort, Annual meeting of Society of Heating, Air-Conditioning and Sanitary Engineers of Japan, pp.237-240, September 2022, Yutaro Ogawa, Ryosuke Onoda, Miku Tazaki, Yuki Saito, Kazuya Matsuo, <b><u>Kan Shindo</u></b> , Takuya Asagawa, Osamu Nagase, Naoyuki Harada, Kikka Uchida, Shin-ichi Tanabe.
Conference paper	Environmental Performance Verification at Open-air ZEB Airport Terminal Part.7 The Effect of Opening and Closing Windows on How Biophilia Feels, Annual meeting of Society of Heating, Air-Conditioning and Sanitary Engineers of Japan, pp.241-244, September 2022, Miku Tazaki, Yutaro Ogawa, Ryosuke Onoda, Yuki Saito, Kazuya Matsuo, <b><u>Kan Shindo</u></b> , Takuya Asagawa, Osamu Nagase, Naoyuki Harada, Kikka Uchida, Shin-ichi Tanabe.
Conference paper	Using CityGML to Estimate Photovoltaic Potential in Urban Districts, Annual meeting of Society of Heating, Air-Conditioning and Sanitary Engineers of Japan, pp.493-496, September 2022, Ryota Matsumura, <b><u>Kan Shindo</u></b> , Ken Ikai, Yutaro Ogawa, Yuki Saito, Miku Tazaki, Shin-ichi Tanabe.
Conference paper	Evaluation of an Open-air Sub-tropical Airport for Energy and Comfort Part 1: Outline of Building, Annual meeting of Architectural Institute of Japan, pp.907-908, September 2021, Erika Tsuchida, Takuya Asagawa, Osamu Nagase, Naoyuki Harada, Kikka Uchida, Kwan Shin-Wi, Shin-ichi Tanabe, Soma Sugano, <b><u>Kan Shindo</u></b> , Marina Inasaka, Mayumi Ohba, Ryo Ochiai, Ryo Nitta.

## List of research achievements for application of Doctor of Engineering, Waseda University

Full Name : 新藤 幹

seal or signature

Date Submitted(yyyy/mm/dd): 2023/12/07

種別 (By Type)	題名、発表・発行掲載誌名、 (theme, journal name, date & year of publication, name of authors inc. yourself)
Conference paper	Evaluation of an Open-air Sub-tropical Airport for Energy and Comfort Part 2: Usage of energy results and heat source and air conditioning, Annual meeting of Architectural Institute of Japan, pp.909-910, September 2021, Takuya Asagawa, Osamu Nagase, Erika Tsuchida, Naoyuki Harada, Kikka Uchida, Kwan Shin-Wi, Shin-ichi Tanabe, Soma Sugano, <b><u>Kan Shindo</u></b> , Marina Inasaka, Mayumi Ohba, Ryo
Conference paper	Evaluation of an Open-air Sub-tropical Airport for Energy and Comfort Part 3: Outline of Questionnaire Survey and Result of Environmental Satisfaction, Annual meeting of Architectural Institute of Japan, pp.911-912, September 2021, Marina Inasaka, Soma Sugano <b><u>Kan Shindo</u></b> , Ryo Nitta, Mayumi Ohba, Ryo Ochiai, Takuya Asagawa, Osamu Nagase, Naoyuki Harada, Erika Tsuchida, Kikka Uchida, Kwan Shin-Wi, Shin-ichi Tanabe.
Conference paper	Evaluation of an Open-air Sub-tropical Airport for Energy and Comfort Part 4: Environmental Measurement and Thermal Comfort Vote, Annual meeting of Architectural Institute of Japan, pp.913-914, September 2021, <b><u>Kan Shindo</u></b> , Marina Inasaka, Ryo Nitta, Soma Sugano, Ryo Ochiai, Mayumi Ohba, Takuya Asagawa, Osamu Nagase, Naoyuki Harada, Erika Tsuchida, Kikka Uchida, Kwan Shin-Wi, Shin-ichi Tanabe
Conference paper	Evaluation of an Open-air Sub-tropical Airport for Energy and Comfort Part 5: Survey on Biophilia, Annual meeting of Architectural Institute of Japan, pp.915-916, September 2021, Ryo Nitta, Soma Sugano, <b><u>Kan Shindo</u></b> , Marina Inasaka, Ryo Ochiai, Mayumi Ohba, Takuya Asagawa, Osamu Nagase, Naoyuki Harada, Erika Tsuchida, Kikka Uchida, Kwan Shin-Wi, Shin-ichi Tanabe
Conference paper	Evaluation of an Open-air Sub-tropical Airport for Energy and Comfort Part 6 : Behavioral analysis and visualization by LiDAR, Annual meeting of Architectural Institute of Japan, pp.917-918, September 2021, Osamu Nagase, Yuji Yokota, Takuya Asagawa, Msamichi Oura, Erika Tsuchida, Naoyuki Harada, Kikka Uchida, Kwan Shin-Wi, Shin-ichi Tanabe, Soma Sugano, <b><u>Kan Shindo</u></b> , Marina Inasaka, Ryo Ochiai, Ryo Nitta, Mayumi Ohba.
Conference paper	Evaluation of an Open-air Sub-tropical Airport for Energy and Comfort Part 7: Wind Environment Digital Twin, Annual meeting of Architectural Institute of Japan, pp.919-920, September 2021, Kikka Uchida, Takuya Asagawa, Osamu Nagase, Erika Tsuchida, Naoyuki Harada, Kwan Shin-Wi, Shin-ichi Tanabe, Soma Sugano, <b><u>Kan Shindo</u></b> , Marina Inasaka, Mayumi Ohba, Ryo Ochiai, Ryo Nitta.
Conference paper	Design Method of Ceiling Slit Capable of Both Daylight Harvesting and Solar Heat Removal (Part 1) Outline of Building and Thermal Environmental Measurement, Annual meeting of Architectural Institute of Japan, pp.951-952, September 2021, Takeshi Takenaka, Shuichi Tamura, Ken Ikai, Jun Shinoda, <b><u>Kan Shindo</u></b> , Ryo Nitta, Tsubura Watanabe, Tetsuo Kobori, Shin-ichi Tanabe.
Conference paper	Design Method of Ceiling Slit Capable of Both Daylight Harvesting and Solar Heat Removal (Part 2) Study of Heat Balance Model for Ceiling Slit, Annual meeting of Architectural Institute of Japan, pp.953-954, September 2021, Ken Ikai, Jun Shinoda, <b><u>Kan Shindo</u></b> , Ryo Nitta, Takeshi Takenaka, Shuichi Tamura, Tetsuo Kobori, Shin-ichi Tanabe.
Conference paper	Numerical Comfort Simulator for Thermal Environment Part 71: Development of Coupled Method of Thermoregulation Model JOS-3 and Thermal Environment Simulations on 3D-CAD, Annual meeting of Architectural Institute of Japan, pp.1043-1044, September 2021, Yutaro Ogawa, Shu Yoda, Ryo Hisayama, Akihisa Nomoto, Mizuho Akimoto, Kanako Fujii, <b><u>Kan Shindo</u></b> , Jun Nakagawa, Shin-ichi
Conference paper	その他国内学会25報、国際学会11報発表済み